CHEMISTRY OF MATERIALS

pubs.acs.org/cm

Perspective

# Materials Design of Highly Branched Bottlebrush Polymers at the Intersection of Modeling, Synthesis, Processing, and Characterization

Tianyuan Pan,[§] Sarit Dutta,[§] Yash Kamble,[§] Bijal B. Patel,[§] Matthew A. Wade,[§] Simon A. Rogers, Ying Diao, Damien Guironnet, and Charles E. Sing*

Cite This: *Chem. Mater.* 2022, 34, 1990−2024

Read Online

ACCESS | Metrics & More | Article Recommendations



**ABSTRACT:** Highly branched "bottlebrush" polymers are a class of macromolecules characterized by side chains that are densely grafted from a backbone that is typically linear. Their unique and often-desirable properties stem from steric repulsion between side chains, which stiffens the molecular contour and increases interchain spacing. There has been a renaissance in both our fundamental understanding, practical synthesis, and application of these materials, due to synergistic advances in all branches of polymer science. In this perspective, we outline how a wide variety of new functional bottlebrush materials have emerged from the convergence of insights from the entire materials design process; the integration of synthesis, characterization, processing, and modeling has demonstrated the promise of these branched macromolecules as a versatile platform for molecular engineering. We discuss how this platform may be further developed to exhibit novel material properties in and out of equilibrium and put into practice due to the next generation of synthetic, analytical, processing, and computational tools in materials chemistry.

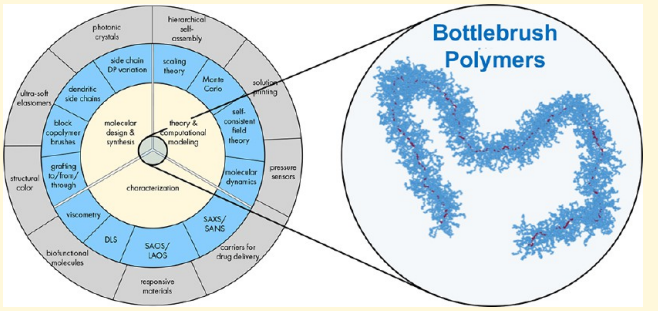


## 1. INTRODUCTION

Polymers are extremely versatile, finding use in applications ranging from commodity plastics to advanced functional materials, and are the foundation of entire classes of biological macromolecules such as proteins or DNA. This versatility stems from key physicochemical features of long-chain molecules; for example, the ability to form copolymers with multiple chemical building blocks distributed along the backbone is a powerful tool for modulating macroscopic properties. Synthetic polymers use this chemical variation to either combine the properties of two separate chemical monomers or to imbue the material with nanoscale structure.[1,2] Biological polymers can be even more precise, storing genetic information in monomer sequence. This chemical variation has been extensively explored, revealing emergent properties of copolymerization such as microphase separation or information storage.[3−5]

Analogous to advances in the chemical features of polymers, there has been a longstanding appreciation of the role physical features play in dictating material properties. One physical attribute that is central to polymer science is *polymer architecture*.[6] *Polymer architecture* is a broad term that refers to the many ways that monomers are connected together, such as the presence of branch points or cross-links, which can result in a rich array of macromolecular structures such as rings, branched chains, networks, star polymers, or telechelic polymers. This plays a role in all polymer applications, for example, giving rise to the dramatic range of properties exhibited by commodity polymers such as polyethylene and also being a defining feature in a number of biological macromolecules.[7−12]

Similar to chemical copolymerization, architectural modifications exhibit a range with respect to their precision, ranging from random branching to precisely defined networks or regular branches. One major goal of polymer science is to capitalize on architecture as a tool to engineer materials at the molecular level, by utilizing the emergent properties associated with branching or network formation. In this perspective, we lay out the significant progress made by the materials chemistry community in pursuit of this goal for a class of branched macromolecules known as *bottlebrush polymers*. These bottlebrush polymers are characterized by a linear backbone that has been densely grafted with long side chains. These branches interact strongly, leading

Received: November 22, 2021
Revised: February 8, 2022
Published: February 23, 2022

to dramatically different properties compared with bare linear counterparts.

The key feature that makes bottlebrushes so useful is the introduction of another *dimension* in polymer design, where the branches impart a molecular "width" that can be tuned essentially independently from molecular "length". The ability to simultaneously control both the bottlebrush linear backbone as well as the side chain lengths introduces a new parameter that can affect polymer properties, both in terms of equilibrium structure via the steric nature of bottlebrush−bottlebrush repulsion[13,14] as well as the dynamics via the suppression of molecular entanglement.[15] While we will discuss these points in detail in this perspective, we note that this molecular "width" makes these polymers a conceptually straightforward extension of traditional linear chains, inspiring the adaptation of traditional (linear) polymer physics and chemistries to this more elaborate molecular structural motif.

This perspective will showcase the extent to which the development and future innovation in bottlebrush polymers relies on the synergistic efforts of the wide array of disciplines in and adjacent to polymer science. We first note that several reviews in the field of bottlebrush polymers have outlined this literature, including older reviews that inspired the ongoing flurry of research,[16,17] and more recent efforts specifically focusing on subdisciplines such as bottlebrush synthesis[18] or modeling.[19] In this perspective, our goal is to highlight some of the most recent emerging areas in this very dynamic field and to articulate how our understanding of bottlebrush polymers benefits from a convergence of advances in polymer synthesis, molecular modeling, and materials characterization (Figure 1). These advances provide the tools necessary to bring bottlebrush polymers from a synthetic curiosity to a material that has found use in disparate applications such as photonic materials,[20−22] tunable elastomers,[23−26] pressure-sensitive adhesives,[27] hydrophobic surfaces,[28,29] responsive materials,[30] and drug delivery vehicles.[31,32] The structure of this perspective is as follows; first, we will provide a brief glimpse into the foundational concepts underlying bottlebrush polymer synthesis, characterization, modeling, and application. We will then discuss how recent efforts in these same areas have led to significant advances in molecular engineering these materials. Finally, we highlight a number of promising future areas that are just now starting to bear scientific fruit.

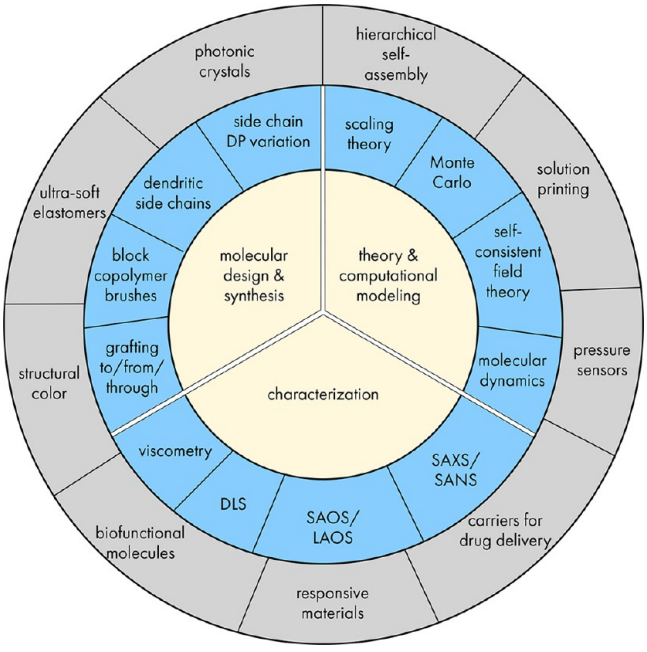


**Figure 1.** Visual outline of this perspective, highlighting the core subdisciplines of molecular design and synthesis, theory and computational modeling, and computation (central circle) that must work synergistically to realize promising bottlebrush applications (gray circle). This is enabled by an increasing array of methods (blue circle) that measure, tune, and model bottlebrush polymers at the molecular level.

## 2. THE BASICS OF BOTTLEBRUSH POLYMERS—A HISTORICAL VIEW

The emergence of bottlebrush polymers as an interesting class of soft materials relies on the interplay between polymer physics and synthetic polymer chemistry. Advances in bottlebrush physics are motivated by the need to understand the properties of new chemical structures, while new bottlebrush chemistries are conversely motivated by these same properties and the promise of molecular-level control enabled by physical models. Therefore, progress in engineering these macromolecules is contingent on a broad understanding of concepts across both fields, and recent efforts have built on foundational concepts decades in the making. We start with this context, describing both the synthesis and the physics enabling modern advances in bottlebrush polymers.

**2.1. Fundamentals of Bottlebrush Synthesis.** Nonlinear polymer architectures, such as bottlebrush polymers, have been synthesized for decades going back to the 1950s.[33−38] Synthesis of these highly grafted polymers have evolved from using naturally obtained macromolecules as backbones[34,36,37,39−43] or incorporating oligosaccharide side chains,[44−47] to using synthetic monomers entirely.[17] Synthetic advances in controlled/living polymerization techniques have simplified the synthesis of advanced architectures like bottlebrush polymers. Indeed, living/controlled polymerizations enable the synthesis of end-functionalized (i.e., semitelechelic) polymers that are essential in the synthesis of branched polymers and enable grafting techniques. Furthermore, the molecular weight control offered by controlled/living polymerization provides a predictable and precise control over polymer architecture. Strategies for synthesis of bottlebrush polymers can be categorized into one of three general methodologies: graft-onto, graft-from, and graft-through processes (Figure 2).[18,48,49] Each methodology offers certain strengths and limitations, leading to a need for a variety of techniques to enable versatile control over composition and architecture of bottlebrush polymers.

The **grafting-onto method** relies on the separate synthesis of polymeric backbones and semitelechelic side chains (Figure 2A). Complementary functional groups are embedded in both the backbone and the side chains and can undergo grafting reactions to form the bottlebrush architecture.[50−52] The reported graft-onto approaches rely on the implementation of highly effective, robust, and high-yielding coupling reactions, such as click chemistry,[50,53,54] nucleophilic substitutions,[55,56] Diels−Alder cycloaddition,[57] or thiol−ene/yne reactions.[58] Uniquely, this methodology allows for the precise characterization of the backbone and side chains prior to the synthesis of bottlebrush polymers. While this method is very effective for the synthesis of polymers with low grafting density (e.g., comb-polymers), it is limited in accessing polymers with high grafting


https://doi.org/10.1021/acs.chemmater.1c04030
Chem. Mater. 2022, 34, 1990−2024

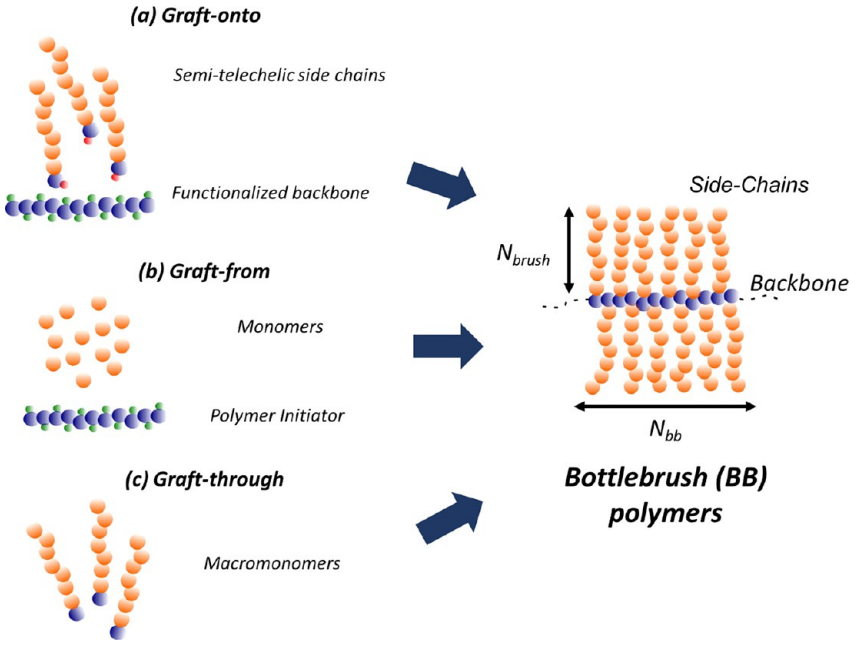


**Figure 2.** Schematic of the three general methods for synthesizing bottlebrushes. (A) Graft-onto synthesis couples side chains directly to the backbone, with each species synthesized separately. (B) Graft-from synthesis initiates side chain polymerization directly from a linear polymer backbone. (C) Graft-through synthesis polymerizes existing side chains to form a linear backbone. Each method has advantages and disadvantages for the final structural dispersity and precision, overall molecular weight, and ability to explore a range of different chemistries.

density due to the steric hindrance caused by the newly added side chains on the backbone.[48,59]

The **grafting-from method** also relies on synthesizing the backbone first (Figure 2B). In this technique, side chains are polymerized directly from the functionalized backbone (containing initiating groups or chain transfer agents) using controlled/living polymerizations.[60−64] The use of atom transfer radical polymerization (ATRP) to polymerize the side chains has become extremely popular.[65] This success is in part due to the simplicity of synthesizing a backbone decorated with ATRP initiating groups and the vast number of vinyl monomers compatible with these polymerization methods.[66] The use of reversible addition−fragmentation chain-transfer (RAFT) polymerization is less common due to the complexity of synthesizing a polymer backbone decorated with RAFT agents.[67,68] Finally the use of ring-opening polymerization (ROP) is rare due to the difficulty of identifying a solvent for the polymeric backbone (polyol) that is compatible with the polymerization. All in all, the graft-from approach is a powerful technique to synthesize a large variety of BB polymers. Unique to this method is its ability to access a polymer with high grafting density and high degree of polymerization (DP) backbones and side chains.[48,59] The use of controlled radical polymerization methods, however, sets limitations on the synthetic precision; lower-than-expected grafting density and dispersity in side chain molecular weight distribution are difficult to prevent and assess.[69]

The **graft-through method** has emerged as an effective way to synthesize BB polymers with "perfect" grafting density, as it relies on the polymerization of macromonomer (i.e., a side chain-first approach, Figure 2C).[70−74] This methodology is compatible to only limited types of polymerization methods.[48,75−88] The low reactivity of the macromonomer (caused by the steric hindrance of the polymer chain), the low concentration of reactive end-groups (resulting from the high molecular weight of the macromonomer and the increased viscosity of the reaction), and the need for high macromonomer conversion (resulting from the difficulty in separating residual macromonomer from the targeted BB polymers) requires the use of highly reactive polymerization methods.[48] Over the years, ring opening metathesis polymerization (ROMP) of norbornenyl functionalized macromonomers initiated by Grubbs' third generation catalyst (G3) has emerged as one of the most effective graft-though polymerization methods.[72,89] This dominance is in part motivated by its excellent chemical compatibility and molecular weight control at high macromonomer conversion. The drawback of this polymerization, however, is the sensitivity of the catalyst. Slow catalyst decomposition results in a broadening of the molecular weight distribution and potentially incomplete macromonomer conversion. This limitation has in part been addressed through the implementation of a highly reactive norbornenyl linker,[90−92] but limitations on the degree of polymerization remain.

These techniques offer the opportunity to access a variety of branched polymers, yet each methodology offers certain strengths and limitations in comparison with the others. The grafting-onto approach enables the precise characterization of the backbones and the side chains; however, it is difficult to achieve high grafting densities. The grafting-from approach is compatible with a high degree of polymerizations for backbones and side chains but suffers from deviation from target side chain dispersity and graft density. The graft-through approach enables high graft densities; however, it is limited in the achievable degree of polymerizations. These limitations highlight how a variety of synthetic routes must be considered to achieve the chemical and structural features desired for a specific bottlebrush application.

### 2.2. Foundational Theories of Bottlebrush Structure.

Concomitant with advances in bottlebrush synthesis, there have been extensive efforts to understand the physical properties of bottlebrush polymers. These efforts can be traced back to theoretical studies on conformations of dense comb polymers from the late 1980s.[93,94] The principal focus of these works was


https://doi.org/10.1021/acs.chemmater.1c04030
Chem. Mater. 2022, 34, 1990−2024

to relate the overall molecular size and flexibility to the architectural parameters as well as environmental variables like solvent quality and concentration. Physical predictions of these branched molecules quickly converged on a standard set of three architectural parameters for homopolymer bottlebrush molecules—(i) the number of backbone segments $N_{bb}$, (ii) the number of segments on each side chain $N_{sc}$, and (iii) the grafting density $f$, as shown in Figure 1. Derived quantities such as the number of segments between two graft points along the backbone $1/f$ and the overall degree of polymerization $N = N_{bb}(1 + fN_{sc})$ may also be considered as architectural parameters (Figure 3).

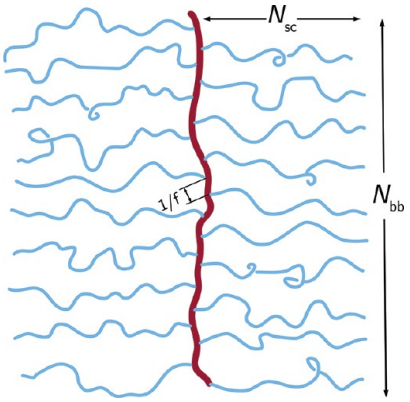


**Figure 3.** Schematic of a bottlebrush polymer, with the key variables used in the simulation and theory literature to describe the bottlebrush architecture.

Most initial theoretical predictions focused on *scaling arguments*,[95] which seek to identify key length scales that govern polymer conformations and structure. Two historic results are still widely used to understand bottlebrushes in equilibrium; the work of Birshtein et al.[93] and the work of Fredrickson et al.[96] establish key theoretical ideas that play a central role in the theory of bottlebrush structure.

*2.2.1. Birshtein Superblob Theory.* For sufficiently long and dense combs in solution, such that $N_{bb} \gg N_{sc} \gg 1/f$, Birshtein et al.[93] proposed that the *local* molecular structure, governed by the repulsion between the densely grafted side chains, sets a molecular thickness $D$ and Kuhn length $\lambda^{-1}$ (a measure of flexibility, notation adapted from Yamakawa),[97] and the large scale *global* structure is similar to that of a uniform chain with contour length $L'$, thickness $D$, and Kuhn length $\lambda^{-1}$. For individual bottlebrush molecules (i.e., dilute chains), *conformational* features are related to *architectural* parameters (i.e., $N_{bb}$, $N_{sc}$, and $f$) in one of three regimes in the state space spanned by a normalized temperature $\tau = (T - \theta)/T$ (where $T$ is the temperature and $\theta$ is the $\theta$-temperature) and per-backbone monomer side chain length $N_{sc}f$:[93] (i) unstretched backbone/unstretched side chains, (ii) unstretched backbone/stretched side chains, and (iii) stretched backbone/stretched side chains. For most realistic bottlebrush conditions,[17] the second regime dominates the phase space due to the significantly higher concentration of side chain monomers compared to those of the backbone within a cylindrical region of thickness $D$ surrounding the backbone. This thickness is predicted to be related to the chain architecture and thickness by the relationship $D \sim N_{sc}^{5/7} f^{2/21} \tau^{5/21}$,[93] which is notably described in this paper as related to a structure called a *superblob* due to the prediction that the Kuhn segment size $\lambda^{-1} \sim D$. This is the key physical result of this paper, which is that the bottlebrush could be considered as a

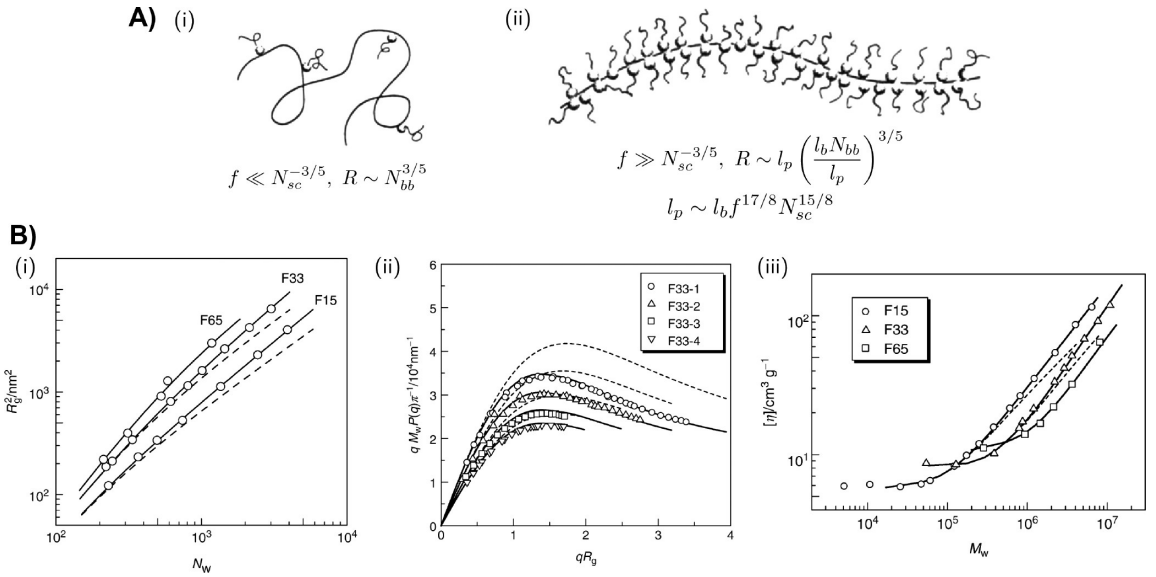


**Figure 4.** (A) (i) Graft polymers in the low grafting density limit, $f \ll N_{sc}^{3/5}$.[96] Each polymer remains in a coiled, swollen conformation. (ii) High grafting density limit, forming the so-called *bottlebrush* polymers, $f \gg N_{sc}^{3/5}$. In this case a transformation to a wormlike conformation with persistence length $l_p$ has occurred. Reprinted (adapted) with permission from Fredrickson, G. H. Surfactant-induced lyotropic behavior of flexible polymer solutions. *Macromolecules* **1993**, *26*, 2825. Copyright 1993 American Chemical Society. (B). Comparison between experimental data for polystyrene-*g*-polystyrene bottlebrushes in toluene at 15 °C with fits from wormlike cylinder models. (i) Backbone length dependence of mean squared radius of gyration for $N_{sc}$ = 15, 33, and 65.[103−105] (ii) Holtzer plots for four samples with $N_{sc}$ = 33.[104] (iii) Molecular-weight dependence of intrinsic viscosity $[\eta]$.[105,106] The solid and dashed lines in all three panels show fits to theoretical predictions for a wormlike cylinder with and without excluded-volume effect, respectively. Reprinted with permission from Nakamura, Y.; Norisuye, T. Brush-like polymers. In *Soft Matter Characterization*; Borsali, R., Pecora, R., Eds.; 2008; pp 236−286. Copyright 2008 Springer Nature Customer Service Centre GmbH.


https://doi.org/10.1021/acs.chemmater.1c04030
Chem. Mater. 2022, 34, 1990−2024

self-avoiding flexible chain of impenetrable spherical segments of size $D$, giving rise to the prediction that the bottlebrush "size" is given by the relationship $R \sim N^{3/5}(N_{sc}f)^{-6/25}\tau^{1/5}$.[93]

These results were subsequently extended to semidilute solutions by Borisov et al.[94] In the phase space spanned by $\tau$ and concentration $c$, four regimes were identified based on the extent that backbone or side chains are stretched.[94] A dilute solution regime is simply the single-chain case and is a swollen linear chain of impenetrable superblobs.[93,94] The second regime appears as $c$ is increased above the overlap concentration, where linear chains of unperturbed superblobs begin to interpenetrate to form a standard semidilute polymer solution.[94] The third higher-$c$ regime appears when interpenetration of bottlebrushes leads to the perturbation of superblob structures, resulting in a solution structure akin to a melt of linear superblob chains.[94] Finally, excluded volume screening increases until, at very high $c$, a fourth regime appears where both backbone and side chains behave as independent linear chains under semidilute conditions.[94] The molecular size for all nondilute regimes shows a leading order scaling behavior $R \sim N^{1/2}$, with additional power law dependence on $N_{sc}$, $f$, $\tau$, and $c$.[94]

*2.2.2. Fredrickson Theory.* Fredrickson developed an alternative theory,[96] originally in the context of surfactant-induced stiffening of linear flexible polymers, whose predictions differ from those of Birshtein et al.[93] by not invoking the "superblob" concept that $\lambda^{-1} \sim D$. This theory instead used a free energy argument that predicted the conformational perturbations that arise as the grafting density $f$ increases. This work started from a low-$f$ ($f \ll N_{sc}^{-3/5}$) limit, with a backbone that behaves as a flexible coil ($R \sim N_{bb}^{3/5}$) (Figure 4A.i).[96] Salient for bottlebrush polymers, this work predicted the presence of a wormlike conformation at the high-$f$ ($f \ll N_{sc}^{-3/5}$) limit, with a persistence length $l_p = \lambda^{-1}/2 \sim l_b f^{17/8} N_{sc}^{15/8}$ and overall size $R \sim l_b f^{17/20} N_{sc}^{3/4} N_{bb}^{3/5}$ that is related to the bond length $l_b$.[96] In direct contrast with the Birshtein "superblob" model,[93] the ratio of the Kuhn segment to the molecular thickness $\lambda^{-1}/D \sim f^{15/8} N_{sc}^{9/8}$ is much larger than unity and can even be sufficiently rigid to induce rigid-rod conformations (Figure 4A.ii).[96] The above prediction allows the possibility that bottlebrush solutions may exhibit lyotropic nematic ordering,[98] as demonstrated in later experimental works on synthetic[99−101] and DNA bottlebrushes.[102]

*2.2.3. Finite Chain-Length Effects.* Both the original Birshtein and Fredrickson theories considered long backbone systems;[93,96] however, some of the most common synthetic approaches (e.g., graft-through) create polymers that are far from this long-chain limit. In an early example of addressing this limitation, Shiokawa[107] applied a Flory-type mean-field theory to predict the existence of three conformational states for bottlebrush polymers in good solvents—star, rod, and coil. The rod and star conformations occur when the backbone and side chains are similar in length ($N_{sc} \approx N_{bb}$, rod) or the backbone is much shorter ($N_{sc} \gg N_{bb}$, star).[107] The latter case is limited to the classical Daoud−Cotton model for star polymers with $N_{bb}$ arms.[108] In the coiled state, when the backbone size $R_{bb}$ is much larger than the size of the side chains $R_{sc}$, $R_{bb} \sim \nu^{1/5} N_{bb}^{3/5} N_{sc}^{2/5}$, where $\nu$ is the excluded volume of a segment.[107] A similar conclusion was reached by Denesyuk using a combination of renormalized perturbation theory and scaling analysis,[109,110] who demonstrated a similar set of transitions from a star-like molecule (short $N_{bb}$) to a rod-like molecule ($N_{sc} \approx N_{bb}$) to a coil-like molecule (large $N_{bb}$). They determined a series of scaling results[109,110] for the molecular diameter $D \sim N_{sc}^{3/4}$, persistence length $l_p \sim N_{sc}^{5/4}$, and end-to-end distance $R \sim D^{1/5} l_p^{1/5} L^{3/5}$ that places the model as an intermediate between the Birshtein[93] and the Fredrickson results.[96]

**2.3. Early Advances in the Solution Characterization of the Bottlebrush Structure.** Historical synthetic and theoretical results were followed by a flurry of experimental research characterizing the dilute solution structure of bottlebrush polymer molecules.[104−106,111−119] A number of structural and transport properties in dilute solutions, such as radius of gyration (Figure 4B.i), hydrodynamic radius, form factor (Figure 4B.ii), center-of-mass diffusivity, intrinsic viscosity (Figure 4B.iii), Kuhn length, and molecular diameter, were extracted from experimental data to the predictions from the Kratky−Porod[120] wormlike chain (WLC) model and its finite width extension, the wormlike cylinder (WLCy) model.[121] The fits to the theoretical predictions are very good across a variety of monomer chemistries and solvents and provided insights into several key geometric parameters as follows.

*2.3.1. Kuhn/Persistence Length.* A large set of early experimental observations have shown that the stiffness of bottlebrush polymer molecules, as reflected in the Kuhn length $\lambda^{-1}$ or persistence length $l_p$, is several times more than that of the bare backbone.[104,111,122−128] Early work by Wintermantel[100,122,123] found the ratio $\lambda^{-1}/D$ to be 10 or more, consistent with lyotropic ordering in nondilute solutions.[99,100] Concomitantly, Nemoto et al.[124] reported $\lambda^{-1}$ = 90 nm for poly(methyl methacrylate)-*g*-poly(styrene) bottlebrushes in benzene, which is much higher than $\lambda^{-1}$ = 3.2 nm for bare poly(methyl methacrylate); Gerle et al.[125] reported $\lambda^{-1}$ = 120 nm for poly(methyl methacrylate)-*g*-poly(methyl methacrylate), and Lecommandoux et al.[126] reported $l_p$ = 11 nm for poly(chlorovinyl ether)-*g*-poly(styrene), in contrast to $l_p$ = 1.2 nm for the bare backbone.

These observations motivated Nakamura and Norisuye[103,129] to develop a framework for improving the scaling picture of bottlebrush rigidity and refining predictions for the molecular origins of bottlebrush Kuhn lengths. They separated the overall Kuhn length into two contributions, $\lambda^{-1} = \lambda_0^{-1} + \lambda_b^{-1}$, where $\lambda_0^{-1}$ is the Kuhn length of the bare backbone and $\lambda_b^{-1}$ is induced by the presence of the side chains. Denoting the size of each backbone unit as $l_b$ and each side chain unit as $l_{sc}$, first-order perturbation theory assuming Gaussian side chains led to $\lambda_b^{-1} = 0.02334(N_{sc}/l_{sc})^2\beta_3/l_b^3$ in $\theta$ solvent and $\lambda_b^{-1} = (N_{sc}/l_{sc})^2(\beta_2/8\pi)$ in good solvents, where $\beta_2$ and $\beta_3$ are the binary and ternary cluster integrals, respectively. These predictions agree with a limited set of experimental data on polystyrene bottlebrushes in cyclohexane ($\theta$ solvent) and toluene (good solvent) from Terao et al.[104−106,112,113,117] Later self-consistent field theory predictions by Subbotin et al.[130] give $\lambda_b^{-1} = 0.047\nu N_{sc}^2/h^2$ for good solvents, in agreement with Nakamura and Norisuye's good-solvent prediction, where $\nu$ is the excluded volume of each side chain unit and $h$ is the distance between two graft points.

*2.3.2. Bottlebrush Contour.* The contour length of bottlebrushes, obtained from fitting to WLCy formulas[131,132] or measured in SFM experiments,[125,133] was found to be shorter than that of the fully stretched bare backbone and explained as arising out of local crumpling of the backbone. Thus, the contour length per backbone monomer was considered as a measure of the side chain induced stretching of the backbone. It was found to increase with increase of side chain length as well as solvent quality, ultimately approaching the value corresponding to the bare backbone for a fully stretched bottlebrush.[131,134,135] Later


https://doi.org/10.1021/acs.chemmater.1c04030
Chem. Mater. 2022, 34, 1990−2024

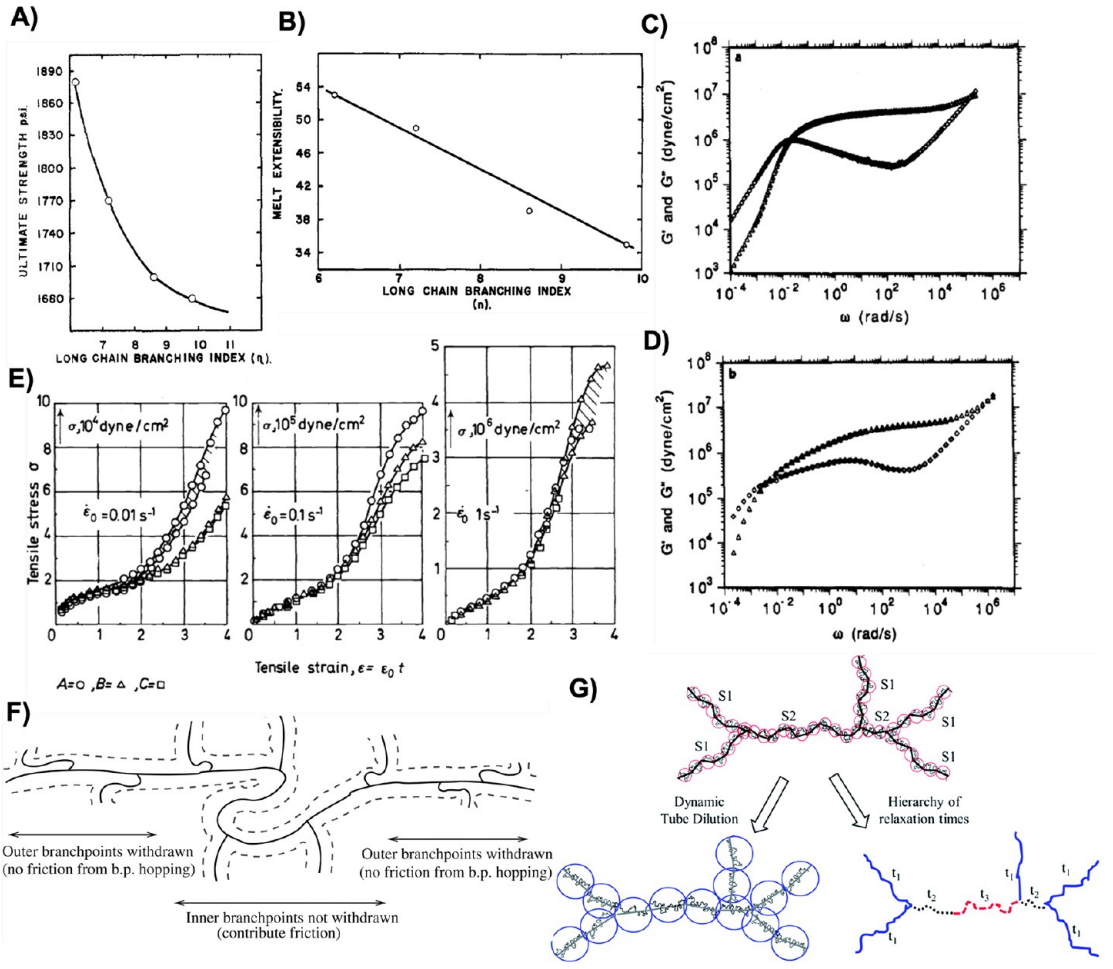


**Figure 5.** Effect of long-chain branching on (A) the fracture point and (B) the extensibility of an LDPE system.[148] Reprinted (adapted) with permission from Sperati et al. The molecular structure of polythylene. V. The effect of chain branching and molecular weight on physical properties. *J. Am. Chem. Soc.* **1953**, *75*, 6127−6133. Copyright 1953 American Chemical Society. Frequency dependent $G'$, $G''$ master curves for (C) linear polyisoprene ($M_w = 5 \times 10^5$ Da) and (D) 4-arm star polyisoprene ($M_w = 3.8 \times 10^5$ Da), two polymers with similar zero shear viscosities ($\eta_0 = 10^8$ P and $\eta_0 = 1.8 \times 10^8$ P, respectively) that demonstrate the impact of branching on the relaxation spectra of a material.[155] Reprinted (adapted) with permission from Fetters et al. Rheological behavior of star-shaped polymers. *Macromolecules* **1993**, *26*, 647−654. Copyright 1993 American Chemical Society. (E) Stress vs strain responses during tensile deformation of three different branched LDPE materials at 150 °C at three different shear rates, highlighting the impact of branching on nonlinear deformations.[146] Republished with permission from Meissner, J. Basic parameters, melt rheology, processing and end-use properties of three similar low density polyethylene samples. *Pure Appl. Chem.* **1975**, *42*, 553. Copyright 1975 Walter de Gruyter and Company; permission conveyed through Copyright Clearance Center, Inc. (F) A diagram depicting the withdrawing of outer branches during flow, leading to sections of the molecule not contributing to the overall friction and viscosity of the material.[160] Reprinted with permission from Lentzakis et al. Pom-pom-like constitutive equations for comb polymers. *J. Rheol.* **2014**, *58*, 1855−1875. Copyright 2014 The Society of Rheology. (G) Schematic representing the hierarchical relaxation of a branched polymer. The outer branches will relax first at time $t_1$, followed by the shorter inner segments at time $t_2$, followed by the longer inner segment at time $t_3$.[164] Republished with permission from van Ruymbeke et al. Molecular rheology of branched polymers: Decoding and exploring the role of architectural dispersity through a synergy of anionic synthesis, interaction chromatography, rheometry and modeling, *Soft Matter* **2014**, *10*, 4762. Copyright 2014 Royal Society of Chemistry; permission conveyed through Copyright Clearance Center, Inc.

simulation work[136] has also shown that to fit to the WLC formula, the bottlebrush contour length must be shortened.

**2.4. Early Computational Studies into Bottlebrush Polymers.** Synthesis and characterization are useful in understanding the physical features of bottlebrushes but are largely reliant on models to interpret these measurements and provide context with respect to the backbone and side chain features. While theory has a key role in these efforts, simulation also emerged as an early way to provide this same insight; assumptions that are convenient choices needed to make progress in theory (e.g., invoking superblobs, the assumption of asymptotic scaling regimes) are no longer necessary, leaving only assumptions standard in computation (e.g., the use of coarse-grained potentials).[19]

Initial computational efforts focused on chain stiffness, typically determining $\lambda^{-1}$ from the backbone bond−bond autocorrelation function. Key results include the observation that $\lambda^{-1}$ increases with both $N_{bb}$ and $N_{sc}$.[136,137] Saariaho et al.[138] further showed that a bond−bond autocorrelation function in simulation revealed the existence of two levels of stiffness—the backbone remains flexible on smaller length scales comparable to the size of the spacers but exhibits enhanced stiffness on longer length scales, an idea originally put forward in the scaling analysis of Birshtein et al.[93] Computational efforts are further capable of considering nonflexible bottlebrush components, and


https://doi.org/10.1021/acs.chemmater.1c04030
Chem. Mater. 2022, 34, 1990−2024

rigid rod-like side chains result in a higher persistence length for bottlebrushes.[118,138,139] This is consistent with static light and X-ray scattering on bottlebrushes with a flexible polystyrene main chain and poly(*n*-hexyl isocyanate) rod side chains,[118] which have shown that the Kuhn length $\lambda^{-1} \sim N_{sc}^{1}$ is larger than those of brushes with flexible polystyrene side chains.

Chain stiffness is typically determined in the context of the overall molecular size. In good solvent, several computational studies[136,137,140,141] predicted that the main chain extension on $R \sim N_{bb}^{\nu}$ follows a power-law with a scaling exponent of $\nu = 0.6-0.7$ as long as $N_{sc}$ is sufficiently smaller than $N_{bb}$, suggesting that its conformation is close to or slightly enlarged compared to self-avoiding linear chain, though when $N_{sc} \approx N_{bb}$ the exponent can be close to $\nu = 2$,[140] indicating an extended rod-like conformation. Scaling exponents from the form factor over the intermediate scattering vector, $q$, range have not conclusively shown a rod-like regime.[136,137]

While the abundance of early computational research focused on a single-bottlebrush structure in good solvents, a few studies considered the prospect of intramolecular bottlebrush assembly due to solvophobic blocks or segments. For example, bottlebrush side chains with attractive units were predicted to exhibit an intramolecular microphase transition[142] and could lead to a first-order coil−globule transition induced by side chain attraction as a function of $N_{bb}$, $N_{sc}$, and $f$.[142] For low $N_{bb}$, this leads to a spherical globule with a side chain-enriched core surrounded by a shell consisting primarily of the backbone monomers. For high $N_{bb}$, several spherical micellar aggregates can be formed with side chain monomers bridged by the backbone units. The resulting globule shape depends on the position of the attractive units along the side chains,[139,143] and the solvent quality $\chi_{AB}$ needed to induce this transition is due to the overall side chain length $N_{sc}$.[144,145]

**2.5. Traditional Role of Polymer Branching in Polymer Engineering.** The impact of polymer architecture on a material's physical properties has historically been an important area of focus for the polymer community. Motivated by applications in industry, early investigations into branched polymers focused on the impact of long-chain branching in low density polyethylene (LDPE) and the effects it has on the dynamics and structure of the polymer.[146−148] Sperati et al.[148] demonstrated that the degree of branching in LDPE leads to a decrease in the overall strength (Figure 5A) and melt extensibility (Figure 5B) of the material under tensile conditions. Meissner further demonstrated that branching in LDPE can also lead to vastly different melt fracture points, swelling ratios, and stress responses during nonequilibrium processing conditions.[146] This was despite similarities in the measured shear modulus and viscosity in the linear regime as well as the intrinsic viscosity and molecular weight.[146] Long-chain polymer branching also results in a reduction of the bulk moduli (Figure 5C,D) and an increase in melt strength and strain hardening (Figure 5E),[146] two properties that are integral to manufacturing techniques such as thermoforming, blow molding, and foaming.[149] On the other hand, the presence of short-chain branching can lead to a slight increase in the tensile strength of the polymer when compared to a linear polymer of equivalent molecular weight.[150] This type of branching does not exhibit the same level of strain hardening and melt strength observed in long-chain branching systems.[151]

The ability to suppress and control the moduli, viscosities, and relaxation times by adjusting branching has led to widespread interest in characterizing and modeling the size and shape of various branched polymers, including h-polymers,[152,153] star polymers,[108,154−158] and comb polymers;[158−160] all of these architectures provide insights important for bottlebrush polymers.[23,101] The combination of theoretical work, scattering, and intrinsic viscosity measurements to determine the structure of these complex molecules with rheological techniques such as small amplitude oscillatory shear, steady shear, and time temperature superposition to determine the frequency-dependent shear moduli, zero shear viscosity, steady shear viscosity, and relaxation spectrum has allowed for property−process relations to be established between the architecture of a polymer and its physical properties.[23,101,108,152−160] This concept of branching and its impact on physical properties such as elasticity and extensibility has been taken to what could be considered an extreme limit in the form of highly functionalized star polymers and dendritic polymers.[161,162] The architecture of these polymers results in core−shell structures and dynamics reminiscent of micelles and soft particles and gives rise to bulk polymers that have poor mechanical strength and a Newtonian-like response during flow.[162] As a result, this has prompted a discussion on the distinction between branched polymers and particles.[163]

To better understand how branching and polymer topology affect the dynamics and physical properties of a material, several groups have worked to understand the relaxation mechanisms of branched polymer systems that capture their rheological behavior. Early studies applied modified versions of the Doi−Edwards tube model that accounted for the retraction and movement of branches in a confining tube to explain the relaxation dynamics of simple branched polymers.[152,153,155,157] In work from 1988 on modeling H-polymers, McLeish notes that the points where the polymer branches constrain the motion of the polymer and require the branch to retrace its contour back toward the branching point in order for the molecule to fully relax.[152] This phenomenon results in a slowing down of the dynamics, with larger deformations appearing to accelerate this process and thus the relaxation of the polymer.[152] The relaxation of more complicated architectures such as star polymers involves arms undergoing a breathing motion as they retract toward a central branching point, resulting in a broader relaxation spectrum than observed in equivalent linear polymers.[155] More recently, Lentzakis et al. presented a modified version of the pom-pom model in which they incorporate equations to describe the stretching of interbranch backbone segments and side arm retraction to capture the dynamics of comb polymers (Figure 5F).[160] Upon arm retraction, the backbone is able to move with greater freedom, which in turn can lead to a cascade effect as an arm's outer segments relax first, followed by inner segments.[160] This work is corroborated by van Ruymbeke et al.'s proposal of a hierarchical relaxation scheme for branched polymers in which the polymer segments furthest away from the center or backbone of a complex branched polymer are the first to relax (Figure 5G).[164] As external segments relax, constraints on the internal segments are released, allowing those portions of the molecule to move and relax and eventually resulting in the relaxation of the entire molecule.[164] This mechanism of hierarchical relaxation gives rise to the broad spectrum of relaxation times observed in early studies of branched systems.

In general, branching in polymers allows for the design and control over the relaxation time and moduli simply by changing the topology of the material. In the case of long-chain branching, this can lead to a softening of the material while also increasing


https://doi.org/10.1021/acs.chemmater.1c04030
Chem. Mater. 2022, 34, 1990−2024

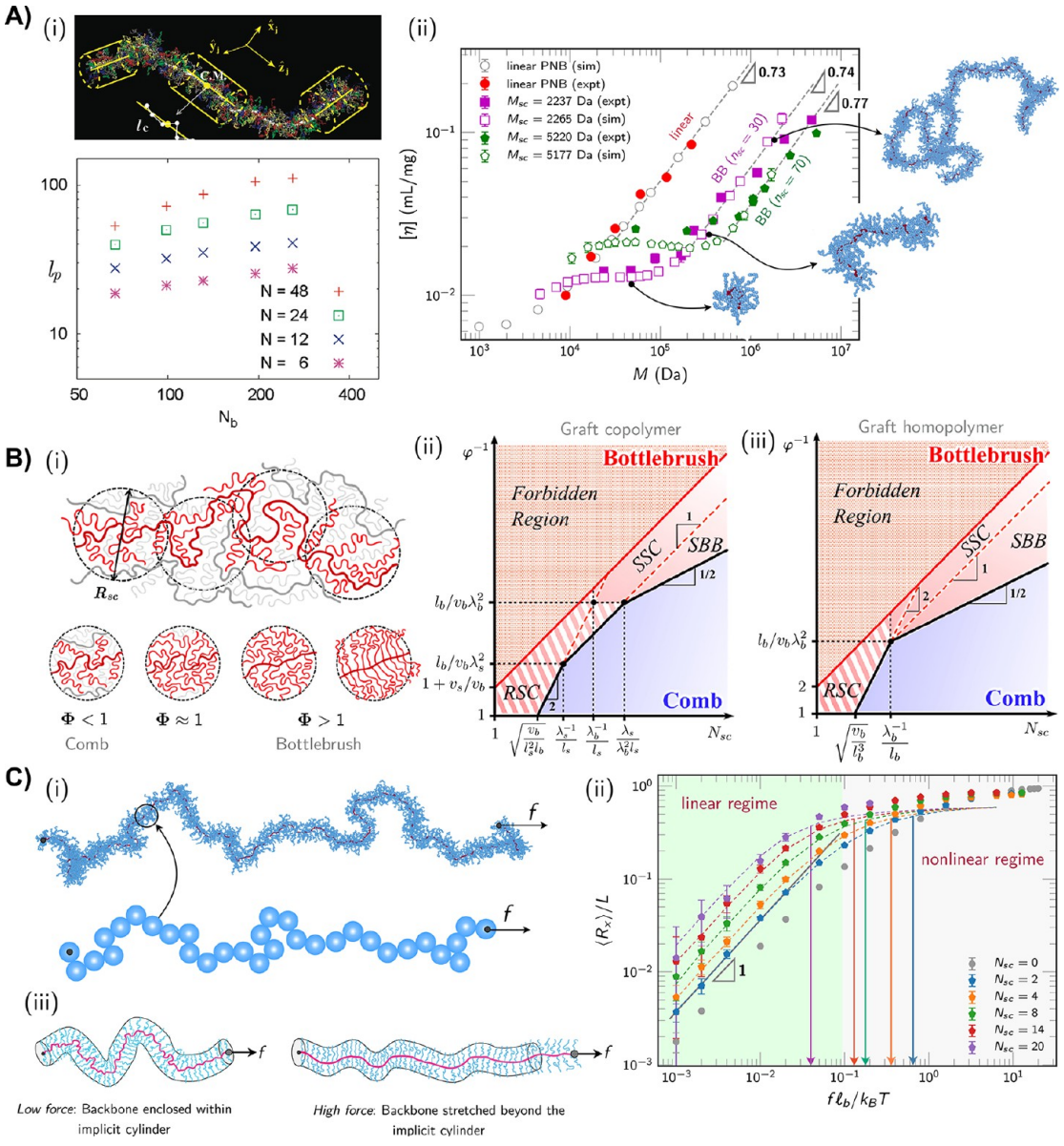


**Figure 6.** (A) (i) (top) Simulation snapshot of a bottlebrush polymer with $N_{bb}$ = 387, $N_{sc}$ = 48, and $f$ = 1, plotted adjacent one segment of the backbone consisting of $l_c$ bonds.[174] (bottom) Persistence length $l_P$ of bottlebrush polymers increases with increase in backbone length $N_{bb}$ and side chain length $N_{sc}$.[174] Reprinted (adapted) with permission from Hsu et al. Characteristic length scales and radial monomer density profiles of molecular bottlebrushes: Simulation and Experiment. *Macromolecules* **2010**, *43*, 1592−1601. Copyright 2010 American Chemical Society. (ii) Intrinsic viscosity [$\eta$] as a function of bottlebrush molecular weight.[175] Filled symbols denote experimental measurements on poly(norbornene)-*g*-poly(lactic acid) in chlorobenzene at 30 °C and unfilled symbols denote simulation results.[175] Republished with permission from Dutta et al. Dilute solution structure of bottlebrush polymers. *Soft Matter* **2019**, *15*, 2928−2941. Copyright 2019 Royal Society of Chemistry; permission conveyed through Copyright Clearance Center, Inc. (B) (i) (top) Schematic representation of a test graft polymer (red) as a chain of blobs of size $R_{sc}$, surrounded by other macromolecules in the melt state (gray).[13] (bottom) Schematic illustrating the value Φ that quantifies bottlebrush behavior as situations where side chains cannot "fit" into the blobs of size $R_{sc}$ and thus must stretch.[13] Reprinted (adapted) with permission from Liang et al. Combs and bottlebrushes in a melt, *Macromolecules* **2017**, *50*, 3430−3437. Copyright 2017 American Chemical Society. (ii) Diagram of states of comb and bottlebrush polymers in a melt with $\lambda_b^{-1} > \lambda_s^{-1}$, where $\lambda_b^{-1}$ and $\lambda_s^{-1}$ are the Kuhn lengths of the bare backbone and side chain, respectively.[176] Black solid lines are boundaries between comb and bottlebrush regimes, and red dashed lines show boundaries of different bottlebrush subregimes: (a) stretched backbone (SBB) regime, (b) stretched side chain (SSC) regime, and (c) rod-like side chain (RSC) regime. The upper boundary of the accessible region is given by $\varphi^{-1} \leq \varphi_{max}^{-1} = 1 + N_{sc} f_{max} v_s / v_b$, which is shown as the red solid line for $f_{max}$ = 1. (iii) Diagram of states for graft homopolymers with chemically identical backbones and side chains.[176] Reprinted (adapted) with permission from Liang et al. Combs and bottlebrushes graft copolymers in a melt, *Macromolecules* **2019**, *52*, 3942−3950. Copyright 2019 American Chemical Society. (C) (i) Simulation snapshot of a stretched explicit side chain (*top*) and an implicit side chain (*bottom*) bottlebrush under a pulling force $f$.[177] (ii) Force−extension curves for bottlebrush polymers for different values of side chain lengths, $N_{sc}$.[177] Markers denote results determined using an explicit side chain model, while dashed lines indicate data obtained using an implicit side chain model. For all side chain lengths, the implicit and explicit model predictions deviate beyond a certain force $f^{**}$, with estimates denoted by vertical arrows. (iii) Schematic showing backbone conformations under low and high pulling forces relative to the implicit cylinder.[177] Reprinted (adapted) with permission from Dutta, S.; Sing, C .E. Two stretching regimes in the elasticity of bottlebrush polymers, *Macromolecules* **2020**, *53*, 6946−6955. Copyright 2020 American Chemical Society.


https://doi.org/10.1021/acs.chemmater.1c04030
Chem. Mater. 2022, 34, 1990−2024

the melt strength of the system.[146,149] To overcome the strength limitations that arise from long-chain branching, these polymers are often mixed with linear or short-chain branched polymers, resulting in an increase in the moduli while retaining the high melt strength and strain hardening characteristics of long-chain branched polymers,[151,165] thus making these blends ideal for the manufacturing of blown films. Higher degrees of repeated, dense branching can also lead to brittle systems with low elasticity, physical characteristics typically not associated with linear polymers, as the branches inhibit the formation of entanglements.[161,162,166] Bottlebrush polymers represent a natural extension of these studies carried out on branched polymer systems; these materials similarly exhibit the softening effect that results from branches inhibiting backbone interactions while simultaneously exhibiting a broad spectrum of relaxation dynamics due to the hierarchical arm-backbone structure.[23]

**2.6. Questions Left Open in Early Work on Bottlebrush Polymers.** Extensive work on bottlebrush polymers had already been performed by the mid-2000s, spanning synthesis, modeling, theory, and characterization. Our brief review of these prior efforts should highlight the extent to which there was a broad understanding of the physicochemical attributes of these molecules and the promise they held in engineering new materials. Nevertheless, this body of work spurred a new wave of research into bottlebrush polymers, due to some clear open questions and opportunities that emerged from these original efforts and foundational concepts:

- In what ways can synthesis further functionalize or vary the base bottlebrush architecture, in order to develop more advanced materials? Advances in controlled polymer synthesis, flow chemistry, computer-guided synthesis, and new monomer chemistries provide opportunities to explore the vast chemical diversity offered by bottlebrush polymers.
- How far can we push the precision and characterization of bottlebrush synthesis? Advances in controlled synthesis are continuously pushing toward atomistic precision, but concomitant advances in characterization methods are needed to accurately assess this synthetic precision. Tools and techniques developed to characterize linear polymers will need to be reevaluated or modified to account for bottlebrush architectures.
- Is it possible to resolve disparities in the predictions made by bottlebrush theories and leverage these predictions for material design? There are a number of notable differences between even the most foundational theories (i.e., Birshtein versus Fredrickson),[93,96] which limits their utility as tools to predict material structure and function.
- Can computation and characterization move beyond individual bottlebrushes in dilute solution, to model properties in bulk melts or concentrated solutions? Early computational models were unable to simulate more than a single bottlebrush of any length, and dilute solution was the focus of early characterization anyway. However, this is far from application in real functional materials.
- What are the molecular origins of bottlebrush material properties? More specifically, the dynamics of bottlebrushes is also integral to their practical use in materials, and only a few early papers studied these dynamical properties.

All these fundamental questions boil down to a single need in the field, immediately prior to the most recent set of investigations (starting roughly 2010); advances in synthesis, modeling, and characterization had yet to make a substantive impact on the practical engineering of bottlebrush materials and realize the promise of molecular design in this highly tunable class of materials.

## 3. RECENT ADVANCES IN BOTTLEBRUSH ENGINEERING

In the past decade, there has been a renaissance in our understanding of bottlebrush materials, starting to bridge this gap in the field between fundamental studies and practical polymer engineering. This has been spurred by several synthetic, theoretical, and characterization advances, which have benefitted from efforts that combine expertise and insights in these areas and thus make progress toward an increasingly sophisticated view of this class of macromolecules. We highlight a few notable areas of progress in the areas of bottlebrush polymer science, ranging from a broader array of fundamental tools in synthesis and modeling, to advances in bottlebrush characterization, and to recent progress in bottlebrush materials engineering.

**3.1. New Fundamental Insights into Bottlebrush Structure and Dynamics.** Despite the development of theories to understand the behavior of bottlebrush polymers over the previous decades, starting in the late 2000s the advent of more powerful computational tools has enabled these theories to be both tested and then extended beyond the single-bottlebrush scaling models that originally prevailed.

*3.1.1. Simulation Insights into Single-Bottlebrush Structure.* Computation has enabled many of the scaling arguments developed by Birshtein,[93] Fredrickson,[96] and follow-up papers to be directly tested in coarse-grained models; this includes models designed to access values of $N_{sc}$ and $N_{bb}$ typical in synthesized bottlebrushes and even approach long-chain scales. For example, Hsu et al.[167,168] considered a simpler variant of bottlebrush molecules consisting of an entirely rigid backbone and flexible side chains. Using extensive Monte Carlo simulations for molecules with varying side chain lengths under good solvent condition, they found the side chains extend only weakly beyond that of a 3D self-avoiding walk, even for $N_{sc} = 2000$ at grafting density $f = 1$, in contrast to a scaling prediction of $R_{sc} \sim N_{sc}^{\nu}$, $\nu \approx 0.75$.[93,107,109] They reported that the side chain stretching as a function of $N_{sc}$ is inconsistent with the assumption of radial stretching of side chains, again in contrast with scaling theories. Instead, they invoke the unconventional notion of anisotropic blobs to maintain qualitative consistency with observed trends.

They subsequently considered the persistence length from simulation data (Figure 6A.i), using the backbone bond−bond autocorrelation function; however, by simulating longer bottlebrushes they revealed ambiguities in the calculation of $l_p$ due to a strong dependence on $N_{bb}$. Hsu et al.[169−171] traced this issue back to the fundamental deficiency of the autocorrelation method for topologically stiff molecules. They instead proposed extracting $l_p$ either from the $q^{-1}$ that marks the onset of the plateau appearing in a Holtzer plot, i.e., a plot of $qP_{bb}$ *vs* $q$, where $P_{bb}$ is the form factor, or more simply from the relation $R_{bb}^2 = 2l_p l_b N_{bb}^{2\nu}$, where $\nu$ depends on the solvent quality.[169−171] To further probe the effect of side chains on persistence length, brush molecules with multiple side chains at each grafting point[172] and dendritic side chains[173] were also studied computationally and theoretically. This led to the insight that $l_p$ is independent of the specific side chain topology; rather, the


https://doi.org/10.1021/acs.chemmater.1c04030
Chem. Mater. 2022, 34, 1990−2024

overall mass (or volume) corresponding to the grafted chain governs the backbone stretching and persistence length.

In addition to providing fundamental insights into bottlebrush structure, the relationship of these computational models to synthesized bottlebrush molecules in experiment was considered by Dutta et al.[175,178] Extensive simulations on long bottlebrushes were performed, varying $N_{bb}$, $N_{sc}$, and $f$ within experimentally accessible values assuming an athermal solvent using a bead−spring model parametrized for poly(norbornene)-*g*-poly(styrene) bottlebrushes. Excellent agreement was observed with experimental measurements of intrinsic viscosity (Figure 6A.ii), highlighting the transition from a star-like spherically symmetric conformation at low $N_{bb}$ to a coil-like conformation at high $N_{bb}$. The transition from sphere to coil was also noted in asphericity data for the overall molecule as a function of $N_{bb}$. Based on scaling exponents of molecular size and form factor data,[178] they concluded that, in the range of $N_{sc}$ and $f$ that can be synthesized, bottlebrush polymer molecules remain considerably swollen but do not show a discernible rod-like scaling. However, such a scaling was observed for extremely high grafting density, $f = 5$, which is beyond what is currently accessible to synthesis.

*3.1.2. Models of Bottlebrush Melts.* Recent studies of bottlebrush structure extend beyond the single-bottlebrush limit, with particular attention on the opposite limit of bottlebrush melts. Key insights into bottlebrush melt structure have emerged from the computational and theoretical work by Dobrynin and co-workers,[13,15,176,179−183] in close collaboration with experiments by Sheiko et al.[23,24,184−186] These papers used scaling arguments to establish a theoretical basis for the distinction between combs and bottlebrushes in a melt,[13] comparing the pervaded volume of a chain of blobs with a side chain random walk $R_{sc}$ ($V = N_{bb}R_{sc}^3/N_{sc}$) and the overall volume of monomers $V_m$. The resulting crowding parameter $\Phi = \frac{V_m}{V} \approx \frac{\nu}{(l_b)^{3/2}} \frac{N_{sc}/N_g + 1}{N_{sc}^{1/2}}$ ($N_g = 1/f$ is the number of monomers between grafting points) quantifies the extent that side chains must distort (Figure 6B.i); when $\Phi < 1$, the monomers can "fit" within the pervaded volume, maintain random walk statistics, and thus exhibit comb-like behavior.[13] Conversely, for $\Phi > 1$, side chains must stretch because they cannot fit within the pervaded volume at a melt density $\rho \approx \nu^{-1}$.[179] The authors further introduced a composition parameter $\varphi^{-1} = \frac{N_g}{N_{sc} + N_g}$, therefore transforming the crossover condition to $\varphi^{-1} \approx (l_b)^{3/2}N_{sc}^{1/2}$ for flexible side chains ($N_{sc} \geq b/l$) and $\varphi^{-1} \approx l^3N_{sc}^2$ for rigid side chains.[13] The diagram of states can be mapped out as a function of $\varphi^{-1}$ and $N_{sc}$ (Figure 6B.ii).[13,181] In the bottlebrush regime denoted by the boundary $\varphi^{-1} \sim N_{sc}^{1/2}$, three subregimes were further identified. Below the boundary of $\varphi^{-1} \sim N_{sc}$ is the stretched backbone (SBB) regime; between $\varphi^{-1} \sim N_{sc}$ and $\varphi^{-1} \sim N_{sc}^2$ is the stretched side chain (SSC) regime; and above $\varphi^{-1} \sim N_{sc}^2$ is the rod-like side chain (RSC) regime.[13]

This framework has been useful for understanding bottlebrush properties. One straightforward application is determining bottlebrush molecular conformation. The scaling results indicate that the effective Kuhn length of the bottlebrush should be a function of $N_{bb}$, $N_{sc}$, and $N_g$, based on the subregime that the macromolecule is in. Liang et al. showed that these predictions are confirmed by MD simulations[13,176] and experiments,[181] and the crossover criteria $\Phi \approx 1$ delineates the two scaling regimes of the graft polymer.

Bottlebrush surfaces have also been a topic of intense study, with several recent efforts to understand the partitioning and orientation of bottlebrushes to the surface.[187−190] The large number of per-molecule free ends has been shown to strongly partition bottlebrushes to free surfaces, where it is more entropically favorable to have free-ends than central chain segments.[187] This picture can be complicated, however, by disparities between the relative length of linear chains when they are blended with bottlebrush polymers as well as short-ranged $\chi$ interactions.[189] Comprehensive mapping of these surface properties has been developed in integrated experimental and theoretical investigations, providing useful design rules for bottlebrush films and coatings.[187,189,190]

*3.1.3. Bottlebrush Mechanical Properties.* Advances in models for both melt and dilute bottlebrushes has prompted the study of the consequent material properties, in particular mechanical properties such as the modulus or the molecular elasticity analogues at the single-bottlebrush level. For the former, Liang et al.[179] used a generalized expression of entanglement plateau modulus $G_{e,gr} \cong \frac{\rho k_B T}{n_{e,bb}\varphi^{-1}}$ to account for the swelling effect that comes from the compositional parameter $\varphi^{-1}$ and the total number densities of monomers $\rho$ and DP of polymer strands between entanglements $n_{e,bb}$.[179] They found two entanglement regimes, where one has only entangled backbones and the other has both side chains and backbones entangled. In the first regime, they found the relative entanglement plateau modulus with respect to the linear counterpart to be $G_{e,gr}/(\varphi^3 G_{e,lin}) \cong \Phi^3$, while in the second regime the scaling becomes $G_{e,gr}/(\varphi^3 G_{e,lin}) \cong \sqrt{(N_{sc})}\Phi$.[15,179] The universality of entanglement plateau modulus in bottlebrush systems is confirmed with experiments.[15] Similar approaches are adopted toward bottlebrush network systems, and the scaling analysis is also in agreement with MD simulations and experimental data in terms of nonlinear elasticity.[180,183]

Molecular elasticity is the counterpart to bulk elasticity at the single-bottlebrush level and is determined via the molecular extension in response to an applied force. For linear chains, this is a well-understood, fundamental polymer physics concept;[191] however, side chains play a major role in determining bottlebrush elasticity. Experimental studies[192] on force—extension of dsDNA bottlebrushes showed evidence of at scale dependent stiffness—at low pulling force the extension was well described by the Marko−Siggia model[193] for a WLC, but the persistence length $l_p$ required for a similar description at high forces required a drastically smaller $l_p$. Molecular manipulation with magnetic tweezers on ssDNA-*g*-poly(ethylene glycol)[194] and hyaluronan-*g*-aggrecan[10] bottlebrushes provides further evidence that a single value of $l_p$ is not sufficient to describe the molecular extension over the entire range of pulling forces. It was hypothesized[10,194] that the side chains induce internal tension within the molecule, which disappears as the backbone gets extended at high forces, leading to reduction of stiffness. Scaling theory based on the *superblob* argument[93,195] predicts that, beyond the linear regime, two nonlinear regimes exist: (i) At low force, $f \sim D^{-1}(R_x/L^*)^{3/2}$, where $R_x$ is the extension and $L^*$ is an effective contour length, showing a Pincus-like regime[196] similar to self-avoiding linear chains. (ii) At high force, $f \sim (R_x/L)^{\nu/1-\nu}$, where $L$ is the actual contour length of the backbone and $\nu$ depends on solvent quality. Simulation studies by Dutta and Sing[177] using both explicit side chain and *implicit* side chain models (Figure 6C.i) could resolve a low force linear regime


https://doi.org/10.1021/acs.chemmater.1c04030
Chem. Mater. 2022, 34, 1990−2024

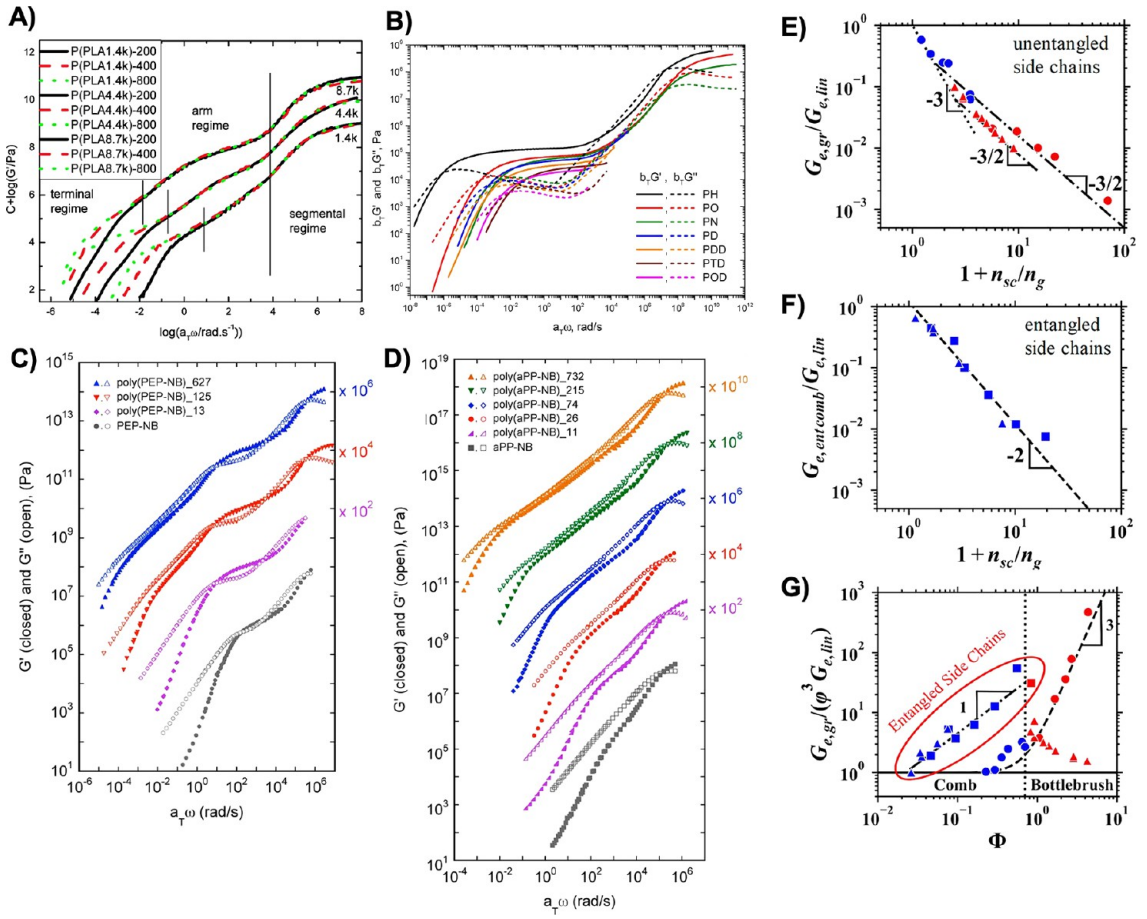


**Figure 7.** (A) Frequency dependent storage modulus master curves highlighting the segmental, arm, and terminal regimes for PLA bottlebrush polymers with different arm and backbone lengths.[200] Reprinted (adapted) with permission from Hu et al. Linear rheological response of a series of densely branched brush polymers. *Macromolecules* **2011**, *44*, 6935−6943. Copyright 2011 American Chemical Society. The presence of plateaus (B) at frequencies immediately above the terminal regime[85] (reprinted (adapted) with permission from López-Barrón et al. Highly entangled $\alpha$-olefin molecular bottlebrushes: Melt structure, linear rheology, and interchain friction mechanism. *Macromolecules* **2018**, *51*, 6958−6966; copyright 2018 American Chemical Society) and (C) in the arm regime[199] indicates the possibility of entanglements at those length scales when backbone and arm molecular weights, respectively, are sufficiently large, while (D) short arms and backbones lead to master curves without plateaus and indicate a lack of entanglement.[199] Reprinted (adapted) with permission from Dalsin et al. Linear rheology of polyolefin-based bottlebrush polymers. *Macromolecules* **2015**, *48*, 4680−4691. Copyright 2015 American Chemical Society. Scaling behaviors can be identified between the entanglement molecular weight of the polymer and a graft polymer composition parameter $\varphi = N_g/(Ng + N_{sc})$, where $N_g$ is the length between grafts along the backbone and $N_{sc}$ is the length of a side chain for (E) graft polymers with unentangled side chains, (F) graft polymers with entangled side chains, and (G) as a function of the crowding parameter ($\Phi$).[15] Reprinted (adapted) with permission from Liang et al. Universality of the entanglement plateau modulus of comb and bottlebrush polymer melts. *Macromolecules* **2018**, *51*, 10028−10039. Copyright 2018 American Chemical Society.

described by WLC-type behavior and a nonlinear regime where the WLC behavior breaks down (Figure 6C.ii); no Pincus-like scaling was observed.[177] Backbone bond−bond autocorrelation functions exhibit significant deviation from WLC-type behavior,[177] which was attributed to a stretching of the cylindrical bottlebrush geometry itself that supports the existence of multiple "levels" of bottlebrush stiffness (Figure 6C.iii).

*3.1.4. Bottlebrush Rheology and Dynamics.* Steric repulsions between side chains along the backbone are also known to affect the dynamics and rheology of bottlebrush materials and have been shown to inhibit the formation of topological entanglements along the backbone contour. In bottlebrush melts and solutions, entangled dynamics thus only emerge at molecular weights well beyond where entanglements are observed in linear chains of the same chemistry.[101,175,176,180,197−200] The extent of this steric repulsive effect is highly dependent on the length of the arms relative to their spacing.[85,201−203] As a result, rheological properties of a bottlebrush polymers can be adjusted and manipulated simply by varying key parameters, such as the length of the side chains, length of the polymer backbone, and grafting density of side chains along the backbone.

Extensive work has been carried out to classify the impact of these molecular parameters on shear moduli determined through small amplitude oscillatory measurements. Hu et al. demonstrated the impact of both backbone length and side chain length on the dynamic moduli master curves as a function of frequency for a series of polylactic acid-*g*-norbornene polymers.[200] In this work, segmental, arm, and terminal regimes are identified in the master curves of the dynamic moduli (Figure 7A). Plateaus in the dynamic moduli as a function of frequency are observed in the segmental and arm regime for bottlebrushes with 4.4 and 8.7 kDa side chains. The separation of these plateaus in frequency, corresponding to a hierarchical relaxation of the arms at short time scales, followed by the polymer backbone at longer time scales. Iwawaki et al.


https://doi.org/10.1021/acs.chemmater.1c04030
Chem. Mater. 2022, 34, 1990−2024

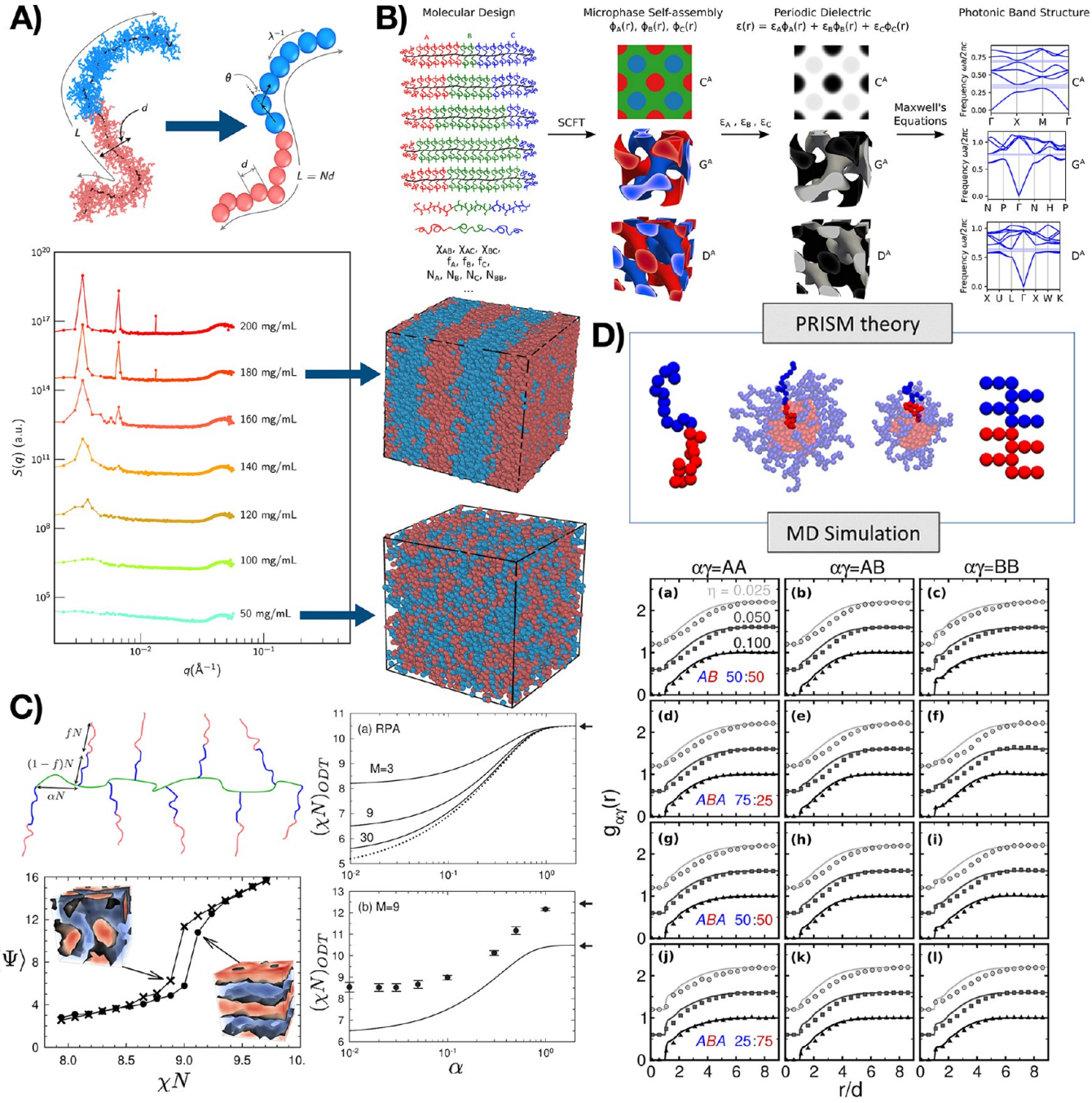


**Figure 8.** (A) (Top) Coarse-grained representation of the bottlebrush with an implicit side chain model. (Bottom) Structure factor from coarse-grained simulations.[14] (Right) Simulation snapshots show a disordered phase in the low concentration regime and an ordered, lamellar phase in the concentrated regime.[14] Reprinted (adapted) with permission from Pan et al. Implicit side chain model and experimental characterization of bottlebrush block copolymer solution assembly. *Macromolecules* **2021**, *54*, 3620−3633. Copyright 2021 American Chemical Society. (B) Computational workflow to compute photonic band structures for bottlebrush block polymers. Self-consistent field theory is used to capture phase behaviors of a given bottlebrush architecture.[222] Reprinted (adapted) with permission from Lequieu et al. Complete photonic band gaps with nonfrustrated ABC bottlebrush block polymers. *ACS Macro Lett.* **2020**, *9*, 1074−1080. Copyright 2020 American Chemical Society. (C) (Top-left) Schematic of a bottlebrush with diblock copolymer grafts. (Bottom-left) Order parameter obtained from a pair of parallel tempering runs in field-theoretic simulations, with snapshots showing disordered and lamellar morphologies.[218] (Right) Order−disorder transition result from field-theoretic simulations in comparison with that from random phase approximation.[218] Reprinted from Spencer, R. K. W.; Matsen, M. W. Field-theoretic simulations of bottlebrush copolymers. *J. Chem. Phys.* **2018**, *149*, 184901, with permission of AIP Publishing. (D) (Top) Schematic of solution assembly of amphiphilic bottlebrush block copolymers. (Bottom) Intermolecular pair correlation function at differently volume fractions.[209] The results from PRISM theory (lines) are in quantitative agreement with those from molecular dynamic simulations (symbols).[209] Reprinted (adapted) with permission from Lyubimov et al. Molecular dynamics simulation and PRISM theory study of assembly in solutions of amphiphilic bottlebrush block copolymers. *Macromolecules* **2018**, *51*, 7586−7599. Copyright 2018 American Chemical Society.

corroborated these results with a series of rheo-optical studies that were carried out on polystyrene polymacromonomers with varying backbone and arm lengths.[204,205] This hierarchical relaxation is similar to the phenomenon observed in other


https://doi.org/10.1021/acs.chemmater.1c04030
Chem. Mater. 2022, 34, 1990−2024

branched architectures in which outer branches of the molecule relax first, followed by inner portions of the molecule.[164]

The impact of longer side chains on dynamic moduli has been studied by Dalsin et al. in which a series of atactic polypropylene (aPP) and poly(ethylene-*alt*-propylene) (PEP) bottlebrush polymers were rheologically characterized.[199] The molecular weight of the side chains for the aPP bottlebrushes was approximately half the linear entanglement molecular weight, while the molecular weight of the side chains for the PEP bottlebrush was 3.5 times the linear entanglement molecular weight. In the arm regime of the dynamic moduli master curve, a plateau in the dynamic moduli was observed for the PEP bottlebrushes (Figure 7C) while no plateau was observed for the aPP bottlebrushes (Figure 7D). The presence of a rubbery plateau indicated an entanglement of the side chains for the PEP bottlebrushes.[199] At lower frequencies, neither aPP nor PEP bottlebrushes exhibited a rubbery plateau, indicating a lack of entanglements between backbones despite the very high molecular weights of the polymers.[199] On the opposite end of the spectrum, Lopez-Barron et al. characterized the linear rheology of a series of bottlebrush polymers with very short side chains ranging from 4 to 16 carbons in length.[85] The dynamic moduli master curves for these $\alpha$-olefin bottlebrush polymers exhibited well-defined rubbery plateaus at low frequency (Figure 7B). These plateaus were attributed to the entanglement of the bottlebrush backbone as the side chains were far too short to entangle themselves. The entanglement molecular weight for each of these polymers was determined based on the observed plateau modulus. This calculation allowed for scaling parameters to be determined, relating the entanglement molecular weight to the length of the side chains for short arm bottlebrushes.[85]

The density of the bottlebrush polymer arms along the backbone has been shown to play a key role in the dynamics of the polymer. Liang et al. characterized the scaling of the entanglement modulus as a function of both the graft polymer composition parameter $\varphi = N_g/(N_g + N_{sc})$ (Figure 7E,F, where $n_g$ is the length between grafts along the backbone and $n_{sc}$ is the length of a side chain) and the crowding parameter (Figure 7G), which is defined as the ratio between the volume fraction of monomers of the graft polymer in the pervaded volume of the side chains along the backbone.[15] The resulting model provided insight into how the rubbery plateau modulus can be affected by the relative crowding of the side chains along the backbone and thus helped define the key difference between comb and bottlebrush polymers.[15] Haugan et al. carried out an extensive linear rheological characterization of a series of poly(norbornene)-*graft*-poly(lactide) bottlebrush polymers with varying backbone length, side chain length, and density.[201] The resulting dynamic moduli master curves demonstrated the impact of all three of these physical parameters on the linear rheological properties of the polymer. By comparing the side chain grafting density to the normalized plateau modulus, key scaling regimes are identified, highlighting key differences between comb and brush-like polymers.[201] A loose brush regime is not observed in the work carried out by Haugan et al.[201] This is attributed to the transition between barely overlapping and densely overlapping arms occurring over a very narrow range of grafting densities, resulting in the loose brushes not appearing in the experimental results.[201] Haugan et al. also considered the impact of these molecular parameters on additional rheological parameters such as the zero-shear viscosity. Bottlebrush polymers that exceed the entanglement molecular weight exhibited zero-shear viscosity scaling as a function of molecular weight with a power-law scaling $\eta_0 \sim N_{bb}^3$. Unentangled bottlebrush polymers had a Rouse-like scaling for the zero-shear viscosity with molecular weight exhibiting a power-law scaling of $\eta_0 \sim N_{bb}^1$. Departure from Rouse scaling for dense bottlebrush polymers is interpreted as entanglement of these polymers.[201]

**3.2. Computational Modeling of Bottlebrushes.** Concomitant with advances in the theory and experimental studies of fundamental bottlebrush polymer physics, there have been significant advances in computational modeling of bottlebrush polymers. While we discussed key simulation results in the context of theory and experiment in the previous section, there have been several advances in the modeling methods themselves that have made computational tools more viable for studying bottlebrush polymers. The principal challenge is that a bottlebrush molecule consisting of a backbone $N_{bb} \sim O(10^2 - 10^3)$ and a side chain $N_{sc} \sim O(10 - 10^2)$ would result in a total degree of polymerization of $N \sim O(10^3 - 10^5)$. Particle-based simulation methods such as Monte Carlo (MC),[168,169] molecular dynamics (MD),[171,206−208] and Brownian Dynamics (BD)[175] have been used to study the effect of molecular parameters ($N_{bb}$, $N_{sc}$, grafting density $f$, etc.) on single bottlebrush conformation. These methods can easily handle $O(10^3 - 10^5)$ number of particles,[168,169,171,206,208] yet bottlebrush multichain systems are much more computationally expensive to simulate if the number of particles per chain remains $O(10^3 - 10^5)$. To this end, state-of-the-art particle-based simulations are limited to a modest $O(10^2)$ number of particles per chain.[176,181,182,186,209,209−214] However, there remains a strong need for modeling large bottlebrush molecules to match synthetic polymers. There have been two general approaches to address this problem. Following the framework of particle-based simulations, one can develop advanced coarse-grained models to reduce the computational cost. Alternatively, one may choose to perform field-based simulations which are often not sensitive to the molecular size.

*3.2.1. Bottlebrush Coarse-Graining.* To access larger length and time scales, Dutta et al. further adopted the wormlike cylinder model to develop an *implicit side chain* representation of bottlebrush molecules by mapping them to a discretized version of the continuous wormlike cylinder model.[175,177,178] The parameters were obtained by fitting the explicit side chain structural and transport property data to theoretical expressions for a perturbed wormlike cylinder.[121] This model has four parameters—(i) Kuhn length $\lambda^{-1}$, (ii) contour length $L$, assumed proportional to $N_{bb}$, (iii) diameter $D$, and (iv) excluded volume parameter $B$. Comparison with independent simulations with explicit side chains showed excellent agreement for the large-scale molecular properties,[177,178] albeit at the expense of losing intramolecular details, the latter being less important for large scale self-assembly calculations.

Based on this initial effort, Pan et al. further investigated the interbottlebrush interactions in solutions and extended the implicit side chain model to study bottlebrush block copolymer self-assembly (Figure 8A).[14] The key ingredient of the implicit side chain model is the pairwise potential between the coarse-grained segments. Scaling arguments were invoked, where key length scales associated with side chain packing are represented as a series of thermal blobs around a straight backbone.[108,215,216] A potential of mean force was determined by interpolating between the free energy of two nonoverlapping chains and that of two chains with backbones that are immediately adjacent,


https://doi.org/10.1021/acs.chemmater.1c04030
Chem. Mater. 2022, 34, 1990−2024

yielding the potential of mean force $W(r)/k_BT \sim hN_{sc}^{3/4}l_G^{-13/8}b^{5/8}[(r/d)^m - 1]$.[14] This interaction informed pairwise potentials in MD simulations, using a phenomenological parameter $\epsilon = N_{sc}^{3/4}l_G^{-13/8}b^{5/8}$ to tune the interaction strength between different blocks. With this additional ingredient, the implicit side chain model such as lamellar spacing and phase transition concentrations is described.[14] This coarse-graining strategy features a reduction of the number of particles per chain from $O(10^3 - 10^5)$ to $O(10^1)$, while still maintaining enough molecular details such that self-assembly properties can be reproduced and matched with experiments (Figure 8A).

*3.2.2. Field-Based Simulations.* Field-based simulations are attractive as an alternative to particle-based simulations because they use a particle-to-field transformation to replace the many-chain interactions with the behavior of a single chain within a field of its neighbors. This dramatically decreases the number of degrees of freedom that must be modeled, especially (1) in melts, where the large number of polymer−polymer interactions simplifies the calculation because mean-field arguments can be invoked, and (2) when side chains can be treated as identical, because they can all be modeled with essentially a single calculation (Figure 8B). Matsen and co-workers used self-consistent field theory (SCFT)[217] and field-theoretic simulations (FTS)[218] to investigate bottlebrush copolymer systems (Figure 8C). SCFT has been widely used for modeling block copolymer systems.[219] SCFT invokes a number of approximations, such as a mean-field approximation for the polymer field theory and an assumption that chains have Gaussian conformational statistics;[219] however, it is possible to predict assembly of bottlebrush diblock copolymers of different lengths $L$, showing that a lamellar structure is formed with lamellar spacing $d_0 \sim L^{\gamma}$.[217,218] The exponent in this scaling relation ranges from $\gamma < 0.3$ at small $L$ to $\gamma = 1$ at large $L$, which can be attributed to the transition from starlike to brushlike molecules as the backbone becomes long relative to the length of the side chains.[217,218,220] These observations are also in line with experiments that have corresponding bottlebrush molecular parameters. SCFT has also been used to understand the behavior of bottlebrush polymers at surfaces, accompanying and contextualizing experimental studies of surface assembly and partitioning.[189,190]

Spencer et al.[218] demonstrated via a FTS approach that high grafting densities also affect the order−disorder transition when the side chains themselves are copolymers. FTS approaches have the advantage that they relax the mean-field approximation, however, at the cost of a more complicated calculation. Panagiotou et al.[221] also used FTS to study the isotropic to nematic phase transition in bottlebrush homopolymer melts. Their results suggested that, even for fully flexible chains, an isotropic to nematic phase transition can still occur.[221] SCFT was also used to confirm experimental observations by Macfarlane et al. that linear polymer additives can improve the ordering in self-assembled morphology of bottlebrush block copolymers.[20] Overall, SCFT and FTS methods can overcome the computational expense of simulating bottlebrush polymers with large length scale and time scale.

An alternative theoretical formalism that has been used to understand bottlebrush self-assembly is the Polymer Reference Interaction Site Model (PRISM).[209,223−225] PRISM relates intermolecular pair correlations, intramolecular pair correlations, and direct pair correlations in liquid state systems through the Ornstein−Zernike equation and judiciously chosen closure relationships.[225] In general, the molecules within the system would be modeled as a series of interaction sites. Lyubimov et al. applied this theory in bottlebrush block copolymer solution assembly.[209] They consider two types of interaction sites representing solvophilic and solvophobic blocks.[209] The self-assembly properties (e.g., structure factor, pair correlations) they found with PRISM were in agreement with MD simulations in the disordered state, upon approach to the order−disorder transition (Figure 8D).[209,212] The advantage of PRISM is that it significantly reduces the computational cost, thus enabling an early stage exploration of a larger design space; however, this is at the expense of only being able to simulate nonhomogeneous morphologies. This information can guide more computationally expensive approaches such as MD simulations, to expedite the study of ordered morphologies.

**3.3. Advances in Bottlebrush Synthesis.** Progress in understanding bottlebrush physical properties has relied on—and inspired—further development of bottlebrush synthesis. We broadly classify these developments into four categories: simplification of synthetic procedures, accessing bottlebrush polymers with unique compositions or architectures, and formation of bottlebrush polymer networks.

*3.3.1. Synthetic Simplification.* Grafting-to, grafting-from, or grafting-through methods rely on at least two polymerizations performed consecutively and isolation of the intermediate polymers (backbone for grafting-to/grafting-from and macromonomer for grafting-through). New one-pot polymerization protocols have been developed to bypass the need for isolation of the intermediate polymers.[67,226−228] Two key requirements for the implementation of a one-pot synthesis are the orthogonality and compatibility of the two polymerization methods employed:

> *Orthogonality:* The reactive functionality involved in one polymerization should be inert toward the other polymerization.
>
> *Compatibility:* The chemical components used to perform one polymerization should not negatively react with the components of the other polymerization.[67,226−228]

For example, the cascade ring opening polymerization (ROP, of cyclic esters and siloxanes), ROMP of norbornenyl macromonomer initiated with Grubbs 3rd generation catalyst in a graftthrough manner and the cascade ROMP/ATRP in a graft-from manner have been successfully performed.[226−231] Most recently, a tandem ROP and ROMP was reported where the macromonomers and the backbones were synthesized simultaneously.[229] Such tandem synthesis protocols require the simultaneous compatibility of the two polymerizations employed.

*3.3.2. Accessing New Bottlebrush Architectures.* Several methodologies have been developed for accessing more refined control over bottlebrush compositions and architectures. Bottlebrushes with extremely high grafting density have been reported with polymeric brushes on every backbone atom.[232,233] Programmable control over the branching density (including gradation of densities along the backbone) was achieved by copolymerizing macromonomers and short monomers with unique copolymerization parameters.[90,234−236] Such a technique has allowed the synthesis of copolymers with identical bulk composition but different architectures. This concept of controlling the polymer architecture through the use of copolymerization parameters has been further expanded to the synthesis of bottlebrush block copolymers.[237,238] The (stereo)-


https://doi.org/10.1021/acs.chemmater.1c04030
Chem. Mater. 2022, 34, 1990−2024

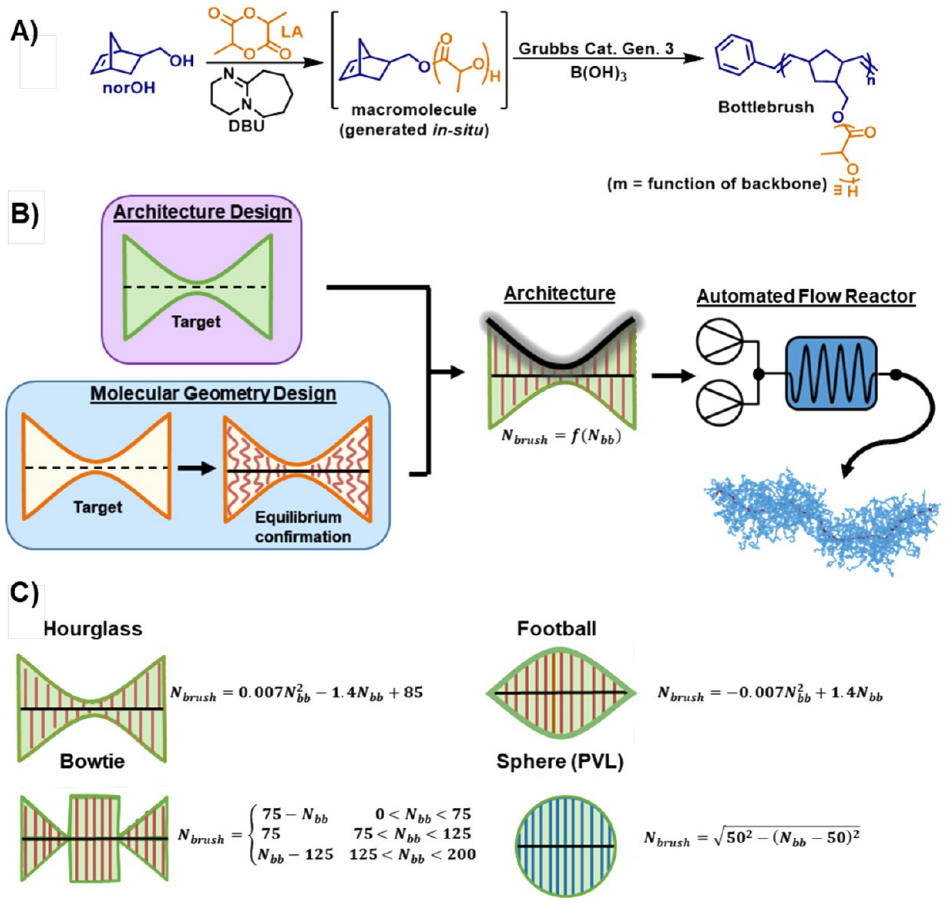


**Figure 9.** (A) Graft-through synthesis of architecture-controlled bottlebrush polymers utilizing ring opening polymerization of lactide to produce the macromonomers which are subsequently polymerized by G3 via ring opening metathesis polymerization.[229,231] (B) Design workflow for the synthesis of the bottlebrush. The upper route implements the targeted design directly to the architecture, while the bottom route implements an inverse design protocol to determine the architecture needed to produce a targeted molecular geometry.[231] (C) Targeted bottlebrush architectures with corresponding mathematical functions describing the architectures synthesized in the work of Walsh et al.[231] Reprinted (adapted) with permission from Walsh et al. Engineering of molecular geometry in bottlebrush polymers. *Macromolecules* **2019**, *52* (13), 4847−4857. Copyright 2019 American Chemical Society.

chemical structure of norbornene linkers (Figure 9A) has been demonstrated to greatly impact the rates of grafting-through ROMP,[91,92,234] so fast-reacting PS macromonomers have been copolymerized with slow-reacting PLA macromonomers to yield a blocky bottlebrush copolymer.[237,238]

Sequential graft-through techniques have the drawback that they are tedious due to the synthesis of multiple batches of macromonomers, and this limits architectural control to blocky structures.[239−241] Walsh et al. have pioneered an alternative protocol to synthesize bottlebrush polymers with programmable and tunable architecture.[229,231] This methodology consists of performing the synthesis of macromonomers in a flow reactor and slow feeding the macromonomer of a specific length into a second vessel where graft-through polymerization occurs. By ensuring that the rate of macromonomer addition remains slower than the rate of graft-through polymerizations, instantaneous incorporation of the macromonomers along the bottlebrush backbone results in sequence-controlled bottlebrush synthesis. A model considering both polymerization kinetics and reactor design equations was developed to predictably convert any architectural design into a flow rate of the macromonomers (Figure 9B), enabling the synthesis of polymeric architectures inaccessible to traditional sequential polymerization (Figure 9C). The success of the synthesis was confirmed by quantifying the instantaneous conversion of macromonomers and the narrow dispersity of the bottlebrush polymers ($Đ$ < 1.1) and from microscopic imaging (AFM). Furthermore, predictions from coarse-grained simulation were consistent with intrinsic viscosity measurements of different architectures,[231] which also allowed us to develop a computer guided synthesis with simulations protocol for predicting the architecture required to yield a desired bottlebrush molecular shape.

*3.3.3. Accessing New Bottlebrush Compositions.* Advances in bottlebrush polymer synthesis have expanded the palette of chemical features that can be incorporated into the brush structure in several different ways beyond just the architectural attributes. A broad synthetic parameter space facilitates the molecular design of bottlebrush chemistry with specific applications in mind. For example, bottlebrush polymers have been considered for several biomedical applications such as drug delivery carriers,[31,242−246] *in vivo* imaging,[247,248] antimicrobial polymers,[249] and antifouling agents.[249] In these applications, a key synthetic challenge for the implementation of bottlebrush polymers is the need for water solubility and biocompatibility.[250] A remaining hurdle is the nontrivial synthesis of PEG-based bottlebrush polymers, due to the ubiquity of PEG as a water-soluble polymer. So far, this direction relies on a select few


https://doi.org/10.1021/acs.chemmater.1c04030
Chem. Mater. 2022, 34, 1990−2024

commercial semitelechelic PEG precursors, limiting the chemical diversity of the corresponding bottlebrush polymers.[250] Alternative water-soluble polymers are being investigated, but their synthesis is often tedious and/or insufficiently precise for functional bottlebrush materials.[30,32,251]

This expanded design space for bottlebrush chemistry also allows for copolymers where the side chains and/or backbone are composed of more than one monomer species. Recent work in bottlebrush copolymers is motivated by their tendency to undergo molecular self-assembly into large microphase separated domains and enabled by advances in bottlebrush synthetic methods.[252−254] Grafting-through and grafting-from techniques provide orthogonal advantages when synthesizing bottlebrush copolymers. For compositional variation along the side chains (core−shell type BB copolymer (Figure 10A),

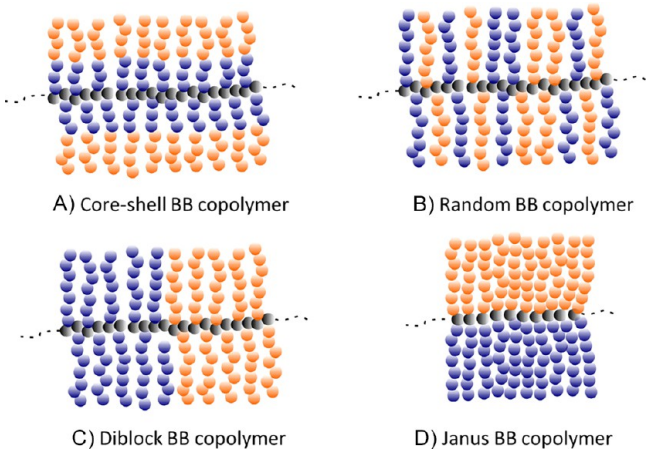


**Figure 10.** Various types of bottlebrush copolymers: (A) core−shell, (B) random, (C) diblock, and (D) Janus BB copolymers.

sequential grafting-from polymerization of different monomers is advantageous.[255−260] For compositional variation along the backbone (random (Figure 10B),[254] block (Figure 10C),[261−267] or Janus BB copolymers (Figure 10D)[268]), the sequential grafting-through method proves to be more useful. In contrast to random or block BB copolymer where each repeat unit consists of distinct side chains, Janus BB copolymers consist of a repeating unit of the backbone with two different macromonomers.[268−272] This "A-branch-B" type macromonomer results in phase separation along the backbone (instead of across) of the bottlebrush polymers which has been shown to yield extremely small domain sizes of ∼7 nm.[269,270] The increasing robustness of these polymerizations and consequent chemical versatility that enables functionalization with, for example, cross-linkable[183,186,273] or liquid crystalline units,[271,274] opens up bottlebrush polymers to new applications beyond widely established nanomedicine and block copolymer self-assembly.

*3.3.4. Chemical Cross-Linking of Bottlebrush Polymers.* In the past decade, there has been an increasing interest in cross-linking bottlebrush polymers into networks. This interest stems from the extremely high entanglement molecular weight of bottlebrush polymers, which imbues material with unique elastomeric properties.[275] Similar to linear polymers, three synthetic methodologies have emerged to cross-link bottlebrush polymers into networks: (1) thermal curing of the system and the addition of a cross-linking agent that reacts with the bottlebrush polymer directly,[276−280] (2) incorporating light-triggered cross-linking reactions that can be spatially or temporally controlled,[25,273,274,281−285] and (3) incorporating dynamic covalent cross-linking units that can be thermally reprocessable.[27,286−288] Each of these routes has advantages and disadvantages and for the latter two can be designed with an application in mind where spatial, temporal, or dynamic control of the cross-linking behavior is desired.

**3.4. Advanced Bottlebrush Materials.** *3.4.1. Bottlebrush Elastomers.* Recent advances in bottlebrush synthesis and the theory of bottlebrush elasticity and entanglement have motivated the development of elastomers—one way in which the community has begun to bridge the previous gap between fundamental study and practical materials. Cross-linked bottlebrush polymer elastomers have received significant attention due to the elastomer's low modulus ($G \sim 1$ to 10 kPa) and ability to undergo large deformations relative to linear polymers of equivalent molecular weight.[26,289−292] These unique characteristics, along with the ability to tune the physical properties by adjusting the molecular parameters such as side chain length, side chain density, and backbone length between cross-links, has prompted consideration of bottlebrush networks in a wide range of applications such as mimicking biological systems,[24,291,293−296] supersoft actuators,[291,293] self-healing polymers,[297−300] and 3D printing.[301,302] The suppression of entanglements by side chains is the central feature of these networks, with the side chains conceptualized as a "solvent" that dilutes the backbone of the bottlebrush.[289] The ability to artificially swell a network by increasing the side chain length in addition to the inhibition of entanglements allows for the physical properties of bottlebrush elastomers to be tuned over a broader range than their linear counterparts.[289]

Various polymer architectures have been explored as an avenue to tune the bulk properties of bottlebrush polymer elastomers. Specifically, linear-brush-linear triblock copolymers with linear segments that cross-link to one another (Figure 11A) have garnered significant interest due to the relative elongation of the bottlebrush polymer between the densely cross-linked linear polymers.[294−296,303,304] The inherent elongation of the bottlebrush leads to unique stress−strain behavior that has been taken advantage of by Keith et al. and Vatankhah-Varnosfaderani et al. to replicate the characteristics of various biological materials, such as with structural color (Figure 11B) or biomechanical properties (Figure 11C).[294,295] The unique hierarchical structure that results from these bottlebrush elastomers leads to an initial unfolding of the bottlebrush at very small strains, followed by a stretching of the backbone at larger strains.[294] As a result, these bottlebrush elastomers exhibited a low modulus at small deformation, followed by a rapid strain stiffening with increasing strain (Figure 11D).[294] The impact of changing molecular parameters on the physical properties of these bottlebrush elastomers was explored by Daniel et al.[184] In their study, the ratio of side chain length to block length was varied to identify the impact of the aspect ratio on the assembly, and the resulting bulk characteristics of these linear-brush-linear copolymer elastomers.[303] When the side chain lengths were well below the backbone length, percolated crystals form from the linear blocks. Increasing the backbone length inhibited the formation of these crystalline structures, resulting in supersoft elastomeric properties. Increasing the side chain length such that it is comparable to the backbone length prevented the cross-linking of linear blocks, resulting in a bottlebrush melt.[303]


https://doi.org/10.1021/acs.chemmater.1c04030
Chem. Mater. 2022, 34, 1990−2024

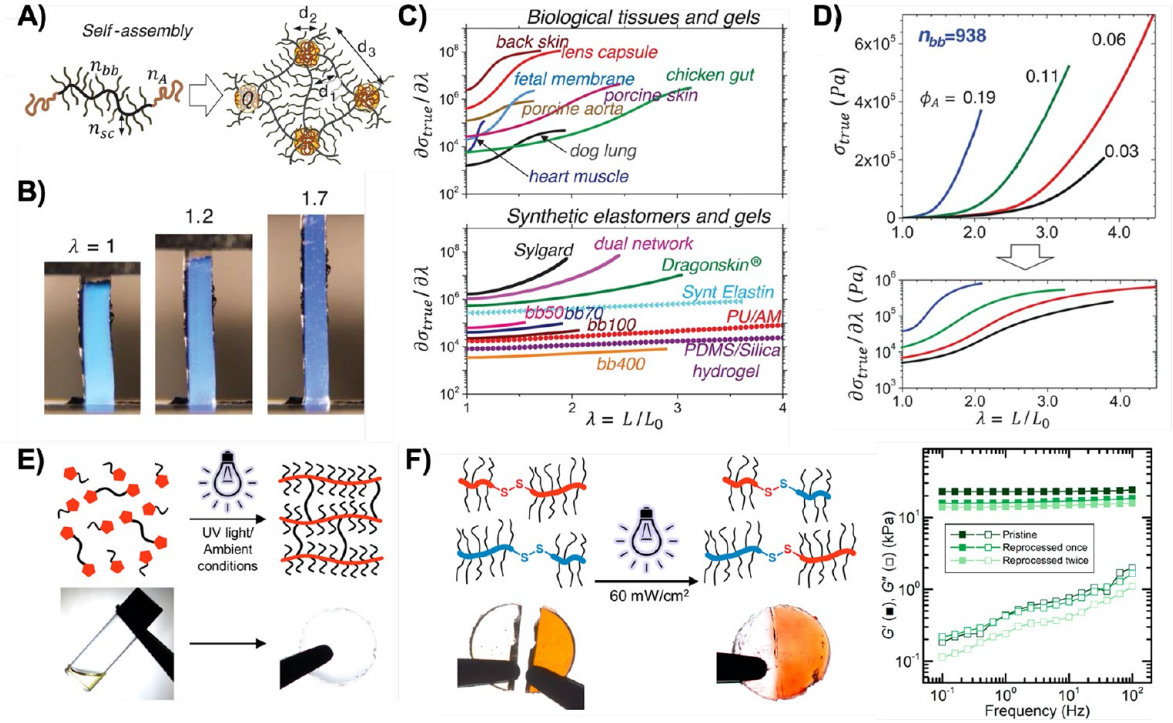


**Figure 11.** (A) Schematic of linear−bottlebrush−linear (PMMA−bbPDMS−PMMA) triblock copolymers and their self-assembly into physically cross-linked networks that exhibit (B) strain-adaptive coloration upon uniaxial stretching.[295] (C) Differential modulus of various biological and conventional and pure-bottlebrush synthetic materials, where bb represents bottlebrush and PU/AM represents polyurethane/acrylamide hydrogel.[295] The comparison highlights the sigmoidal strain-stiffening response of biological tissue that is difficult to capture with synthetic elastomers. (D) Stress−strain and differential modulus−strain curves showing strain-stiffening behavior in linear−bottlebrush−linear triblock copolymer networks with fixed bottlebrush size and varying linear block fraction, $\phi_A$.[295] Reprinted with permission from Vatankhah-Varnosfaderani et al. Chameleon-like elastomers with molecularly encoded strain-adaptive stiffening and coloration. *Science* **2018**, *359*, 1509. Copyright 2018 AAAS. (E) Schematic of the light-mediated synthesis of bottlebrush networks from PDMS-$\alpha$-lipoic acid and bis-PDMS-$\alpha$-lipoic acid monomers to form a transparent elastomer.[273] (F) Self-healing upon exposure to ultraviolet light allows for full recovery of elastic properties.[273] Reprinted (adapted) with permission from Choi et al. Light-mediated synthesis and reprocessing of dynamic bottlebrush elastomers under ambient conditions. *J. Am. Chem. Soc.* **2021**, *143*, 9866−9871. Copyright 2021 American Chemical Society.

Bottlebrush polymers have also been identified for applications in self-healing networks (Figure 11E). By selecting specific cross-linkers, bottlebrush polymers have been cross-linked to form covalent adaptable networks (CANs), self-healing networks that can reform form after mechanical failure.[299] These bottlebrush networks broadened the spectrum of physical properties exhibited by CANS to include supersoft elastomers. Self et al. demonstrated the ability to synthesize these cross-linked bottlebrush networks and the impact backbone and side chain length have on the elastic properties of the elastomer.[299] Upon failure, the material was reconstructed and reprocessed by heating and hot pressing it at 180 °C for 5 h. The resulting recycled sample exhibited nearly identical stress−strain behavior during tensile testing (Figure 11F).[299] Choi et al. demonstrated similar reprocessability with PDMS-$\alpha$-lipoic acid and bis-PDMS-$\alpha$-lipoic acid macromonomers.[300] When exposed to UV light, these macromonomers reacted to form a bottlebrush network. Upon mechanical failure, the sample was once again exposed to UV-light, resulting in the macromonomers re-cross-linking and forming a network with near identical elastic properties.[300] Noncovalent systems have also been investigated for self-healing bottlebrush elastomers by Chen and Guan.[297] In their work, they synthesized bottlebrushes with a PMMA backbone and polyacrylate-amide (PA-amide) side chains that formed temporary cross-links through hydrogen bonding interactions between the side chains.[297] The stress−strain behavior was measured through tensile testing for both pristine samples and samples that were cut and allowed to heal for varying lengths of time at room temperature. As the healing time increased, the stress−strain behavior approached the initial tensile response of the pristine material, demonstrating self-healing behavior.[297]

*3.4.2. Photonic Crystals.* The same suppression of entanglements that makes elastomers viable applications of bottlebrush polymers, combined with advances in copolymerization chemistries, have prompted interest in using bottlebrush self-assembly for photonic materials. Bottlebrush copolymers are known to assemble into lamellae, which act as one-dimensional photonic crystals known as Bragg stacks. These assemblies are composed of alternating layers of material with two different indices of refraction, resulting in a photonic band gap within the material.[305−308] This band gap prevents the propagation of select wavelengths of light, constructively reflecting them and leading to the material appearing to have a specific "structural color" (Figure 12A).[21,305−307,309] Rapid self-assembly is observed due to the lack of entangled dynamics, leading to highly ordered structures with few defects. Furthermore, the increased stiffness of bottlebrush molecules gives rise to large structural length scales that are on the order of the wavelength of light. These features result in rapid dynamics, leading to bottlebrush copolymers having a distinct advantage over ultrahigh molecular weight linear polymers that have also been


https://doi.org/10.1021/acs.chemmater.1c04030
Chem. Mater. 2022, 34, 1990−2024

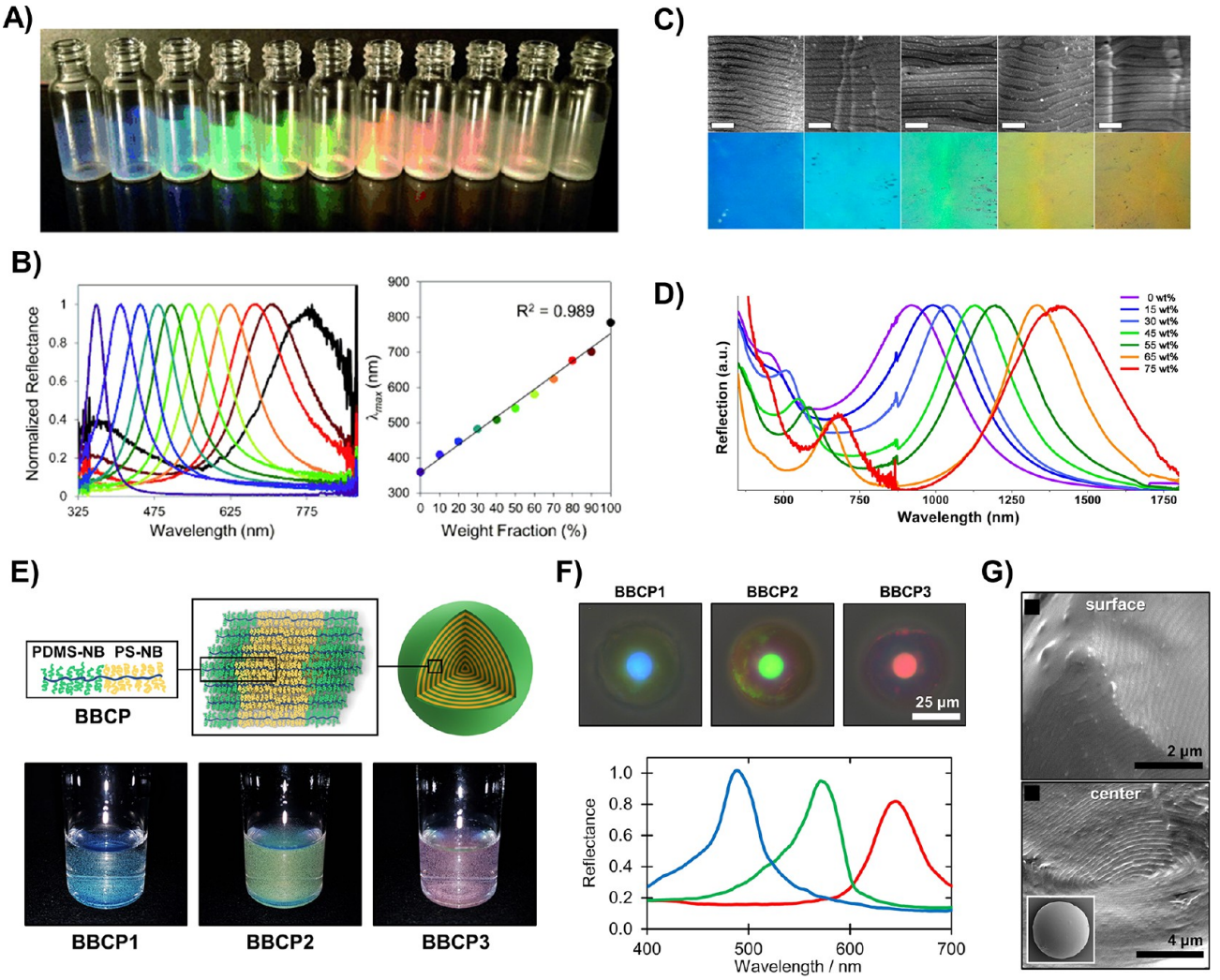


**Figure 12.** (A) Photographs and (B) UV−visible reflection spectra for a series of lamellar bottlebrush block copolymer photonic crystal films prepared by blending of low and high molecular weight polymers at different weight fractions.[22] Reprinted (adapted) with permission from Miyake et al. Precisely tunable photonic crystals from rapidly self-assembling brush block copolymer blends. *Angew. Chem., Int. Ed.* **2012**, *51*, 11246−11248. Copyright 2012 John Wiley and Sons. (C) Cross-sectional scanning electron micrographs, corresponding photographs, and (D) UV−vis−NIR reflection spectra of photonic crystal films prepared by blending bottlebrush block copolymers with linear homopolymer at varying weight percents.[20] Reprinted (adapted) with permission from Macfarlane et al. Improving brush polymer infrared one-dimensional photonic crystals via linear polymer additives. *J. Am. Chem. Soc.* **2014**, *136*, 17374−17377. Copyright 2014 American Chemical Society. (E) Schematic of the confined self-assembly of lamellar-forming bottlebrush block copolymers within spherical microdroplets along with photographs of suspensions of three polymers with increasing molecular weight from BBCP1 to BBCP3.[318] (F) Microscope images and reflection spectra from single assembled microspheres.[318] (G) Cross-sectional SEM images taken at the surface and center of the sphere showing lamellar ordering throughout. Reprinted (adapted) with permission from Song et al. Hierarchical photonic pigments via the confined self-assembly of bottlebrush block copolymers. *ACS Nano* **2019**, *13*, 1764−1771. Copyright 2019 American Chemical Society.

shown to assemble into lamellae with sufficiently large characteristic length scales.[20] The ultrahigh molecular weight of linear polymers required for similar spacings leads to significant entanglement and an associated slowing of dynamics, making processing difficult.[1,310]

A number of recent studies have focused on the impact of various molecular parameters on the self-assembly of diblock bottlebrush copolymers into uniform lamellae that act as one-dimensional photonic crystals.[20−22,311−314] Most of these studies consider self-assembled diblock bottlebrush copolymers in dried thin films. For example, Miyake et al. characterized the effects of molecular weight on the reflected color and concluded that increasing the backbone length without changing the arm length caused an increase in the lamellar spacing, resulting in the peak reflected wavelength shifting toward longer wavelengths (Figure 12B).[313] The impact of additives on the self-assembly of a single bottlebrush copolymer has been characterized by Macfarlane et al. and Miyake et al.[20,22] The addition of linear polymers and higher molecular weight diblock bottlebrush copolymers (Figure 12C) both resulted in an increase in lamellar domain spacing and a red-shift in the reflected wavelength (Figure 12D).[20,22] These observations allowed for the properties of the self-assembled photonic crystal to be adjusted simply by varying the molecular parameters of the bottlebrush block copolymer as well as the composition of the solution used to make the polymer thin film.

Additional factors such as processing conditions have been shown to play a significant role in the reflected color of a block bottlebrush photonic crystal. The polymers within thin films formed through solvent casting may not be at equilibrium due to


https://doi.org/10.1021/acs.chemmater.1c04030
Chem. Mater. 2022, 34, 1990−2024

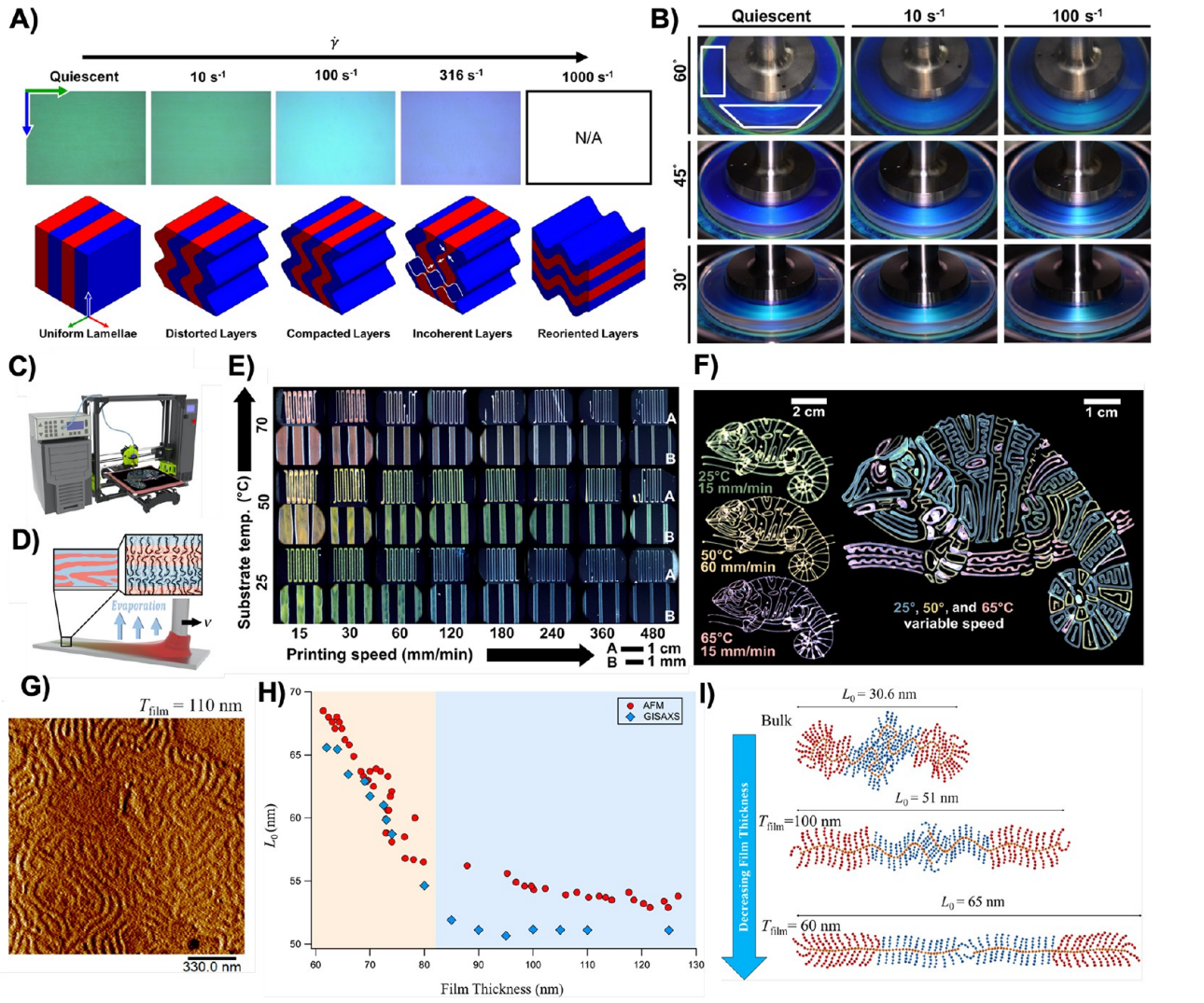


**Figure 13.** (A) Impact of shear rate on observed photonic properties and the corresponding microstructure as determined through rheo-microscopy and rheo-SANS, respectively.[319] (B) Color of the sample when viewed at an off angle as a function of shear rate.[319] Key regions of change are highlighted with white boxes. Republished with permission from Wade et al. Color, structure, and rheology of a diblock bottlebrush copolymer solution. *Soft Matter* **2020**, *16*, 4919−4931. Copyright 2020 Royal Society of Chemistry; permission conveyed through Copyright Clearance Center, Inc. (C, D) Schematic of the solution casting approach used by Patel et al. to control domain size in lamella-forming PDMS-*b*-PLA bottlebrush block copolymer films via kinetic trapping of metastable chain conformations from a single ink.[317] (E) Photonic properties (reflected wavelength) were modulated across the visible spectrum by systematically varying printing speed and substrate temperature to modulate drying rate and polymer dynamics, respectively.[317] (F) Demonstration of simultaneous spatial and functional patterning of BBCP photonic crystals.[317] From Patel et al. Tunable structural color of bottlebrush block copolymers through direct-write 3D printing from solution. *Sci. Adv.* **2020**, *6*, eaaz7202. Copyright The Authors, some rights reserved; exclusive licensee AAAS. Distributed under a CC BY-NC 4.0 license http://creativecommons.org/licenses/by-nc/4.0/. Reprinted with permission from AAAS. (G) Atomic force microscopy (AFM) phase image of vertically oriented lamellae studied by Sunday et al. after annealing of PS-*b*-PLA bottlebrush block copolymer films prepared by blade coating.[332] (H) Lamellar domain size ($L_0$) was found to be strongly modified by confinement effects.[332] (I) Schematic of the inferred planarization of the molecular backbone with increasing confinement (decreasing film thickness).[332] Reprinted (adapted) with permission from Sunday et al. Confinement and processing can alter the morphology and periodicity of bottlebrush block copolymers in thin films. *ACS Nano* **2020**, *14*, 17476−17486. Copyright 2020 American Chemical Society.

the rate of solvent evaporation, leaving the self-assembled polymers in a kinetically trapped state. Annealing the thin film at elevated temperatures allowed the material to explore a larger potential energy landscape and progress toward thermodynamic equilibrium.[311,312,315,316] This kinetic trapping process has been exploited by Patel et al. to obtain multiple colors from a single diblock bottlebrush copolymer during direct-ink writing.[317] Patel et al. demonstrated control over the rate of evaporation and polymer relaxation by varying both the print speed and the substrate temperature. The resulting thin films exhibited a wide accessible wavelength range from 403 to 626 nm, spanning a significant portion of the visible spectrum with a single bottlebrush sample.[317]

Prior to drying, the self-assembled microstructure of a diblock bottlebrush can also be affected by the flow conditions the material experiences prior to being deposited onto a substrate. Work carried out by Wade et al. explored the impact of steady shear on the microstructure and resulting photonic characteristics.[319] Under quiescent conditions, the polymer assembled into uniform lamellae that was gradually compressed and disrupted with increasing shear rate. At lower shear rates, a color transition from green to cyan was observed and related to the


https://doi.org/10.1021/acs.chemmater.1c04030
Chem. Mater. 2022, 34, 1990−2024

compression of the lamellae. Higher shear rates resulted in the lamellae destabilizing, warping, and pinching, which leads to a cyan to indigo color transition. Very high shear rates caused the lamellae to rotate perpendicular to the viewing angle, causing the sample to appear colorless due to an effectively infinite path length through the photonic crystal.[319]

Additional methods are also being explored to control the self-assembly of bottlebrush polymers and their resulting photonic properties. The inclusion of metallic nanoparticles in a bottlebrush copolymer allowed for the modulation of domain spacing and refractive index contrast.[320−323] By carefully selecting the composition of the polymer such that hydrogen bonding drove the nanoparticles toward one of the layers, it was possible to tune the reflected wavelength of the various samples from visible light to near IR.[320] Highly confined self-assembly of diblock bottlebrush copolymers has been shown to be a possible alternative to achieve well-defined structures and color.[318] When confined within microscale droplets, PDMS-PS diblock bottlebrush polymers assembled into layered microspheres during solvent evaporation (Figure 12E). The resulting spheres exhibited vibrant colors across the visible spectrum depending on the backbone length of the bottlebrush polymer (Figure 12F). The resulting spheres demonstrated long-range ordering which in turn enhances the reflectivity of the photonic crystal (Figure 12G).[318]

**3.5. Processing Bottlebrush Materials.** In the final stage of the hierarchy of the engineering and design of bottlebrush materials, there has been considerable effort in understanding how to use processing to guide the material properties of bottlebrush polymers. The practical application of these bottlebrush polymers in advanced processing and additive manufacturing is the culmination of the fundamental synthesis, theory, modeling, and material mechanics that were discussed in the previous sections and highlight the incredible progress in this field over the past decade or so.

The importance of processing conditions on the self-assembled microstructures and the resulting macroscopic properties has already been demonstrated for soft materials such as gels and linear polymeric systems.[324−329] However, these systems require large forces, and the induced structure shear can be stymied by kinetic traps. The rapid dynamics and inhibition of entanglement resulting from the bottlebrush polymer architecture represent an ideal alternative platform for process-driven control over microstructure as demonstrated in the work carried out by Wade et al.[319] and Patel et al.[317] Applications for these materials in additive manufacturing have been particularly appealing due to the possibility of direct patterning of functional materials exhibiting optoelectric, stimuli-responsive, and/or biological properties. Inks containing bottlebrush polymers have particular promise due to enhanced synthetic flexibility, rapid self-assembly into well-ordered hierarchical structures with unique mechanical and photonic properties, and the potential for tuning of the microstructure via direct nanopatterning and on-the-fly variation of mechanical and optical properties. These possibilities represent the range of control and tunability offered by the unique bottlebrush architecture for applications in out-of-equilibrium and additive manufacturing techniques.

Three recent reports highlight the sensitivity of the bottlebrush block copolymer microstructure, in terms of both domain size and orientation, to three distinct phenomena that arise during processing: (1) flow-driven structural reconfiguration;[319] (2) kinetic trapping of metastable chain conformations during solution casting;[330,331] and (3) confinement effects in annealed thin films.[332] Two more recent works also reveal a promising new approach for additive manufacturing that involves exploiting shear-induced disordering for tailored design of thixotropic inks for freeform fabrication of supersoft bottlebrush elastomers.[25,333]

Structural reconfiguration with steady shear was recently demonstrated with diblock bottlebrush copolymers in the work of Wade et al.[319] In this work, in situ SANS and microscopy measurements were carried out on a concentrated diblock bottlebrush copolymer solution under quiescent and steady shear conditions to determine the impact of processing on the self-assembled morphology and the resulting structural color, respectively. At quiescence and low shear rates, a light green color was observed along with highly uniform lamellae oriented parallel to the walls of the geometry (Figure 13A). When shear rates above a critical shear rate were applied to the sample, the principal peak of the lamellae, observed through neutron scattering, shifted toward higher $q$, suggesting a compression of the lamellae and resulting in a green to cyan color shift. Smearing of the scattering features in the azimuthal direction with increasing steady shear rate indicated a distortion and warping of the self-assembled lamellae, which further blue-shifted the observed color of the sample. Shear rates above a second, higher critical shear rate led to an increase in the full width at half-maximum of the lamellae peaks, which corresponded to an increase in the dispersity of the lamellae spacings and a cyan to indigo color shift. An eventual reorientation of the lamellae parallel to the vorticity direction was observed at very high shear rates, resulting in a colorless sample when viewed along the shear gradient direction.[319] These structural and corresponding color changes demonstrated the impact of steady flow on the self-assembled structure and physical properties of the sample (Figure 13B).[319]

Patel et al.[330,331] have recently used a modified 3D printer to achieve wide tunability of domain size and photonic band gap (reflected color) in lamella-forming poly(dimethylsiloxane)-*b*-poly(lactic acid) (PDMS−PLA) bottlebrush block copolymers during solution casting (Figure 13C). An ink solution was made by dissolving the bottlebrush block copolymer in a weakly selective good solvent, allowing for only weak lamellar ordering in the reservoir (domain spacing ∼ 160 nm). Upon evaporation of the solvent during solution printing, the segregation strength increases and the $d$-spacing increases toward the larger values of ∼200 nm (obtained from drop casting) or 212 nm (thermally annealed). By precisely controlling printing speed and substrate temperature, Patel et al. demonstrated the ability to control both evaporation rate and molecular mobility and thus arrest the self-assembly process at intermediate domain sizes (Figure 13D). This allowed for tuning of domain $d$-spacing over a range of >70 nm for a single material system, corresponding to a change in the peak reflected wavelength across the visible spectrum (Figure 13E). Simultaneous spatial and functional patterning was demonstrated through printing complex chameleon patterns (Figure 13F). Solvent annealing experiments clarified that the observed domain spacings were metastable (kinetically trapped) and not the result of confinement effects.

While the preceding work focused on nonequilibrium processing of relatively thick films (15−250 layers), Sunday et al.[332] have performed a systematic investigation of confinement effects in thin films of PS-*b*-PLA prepared by solution coating followed by extended annealing well above $T_g$ of both blocks. Unlike the well-studied case for linear block copolymers under


https://doi.org/10.1021/acs.chemmater.1c04030
Chem. Mater. 2022, 34, 1990−2024

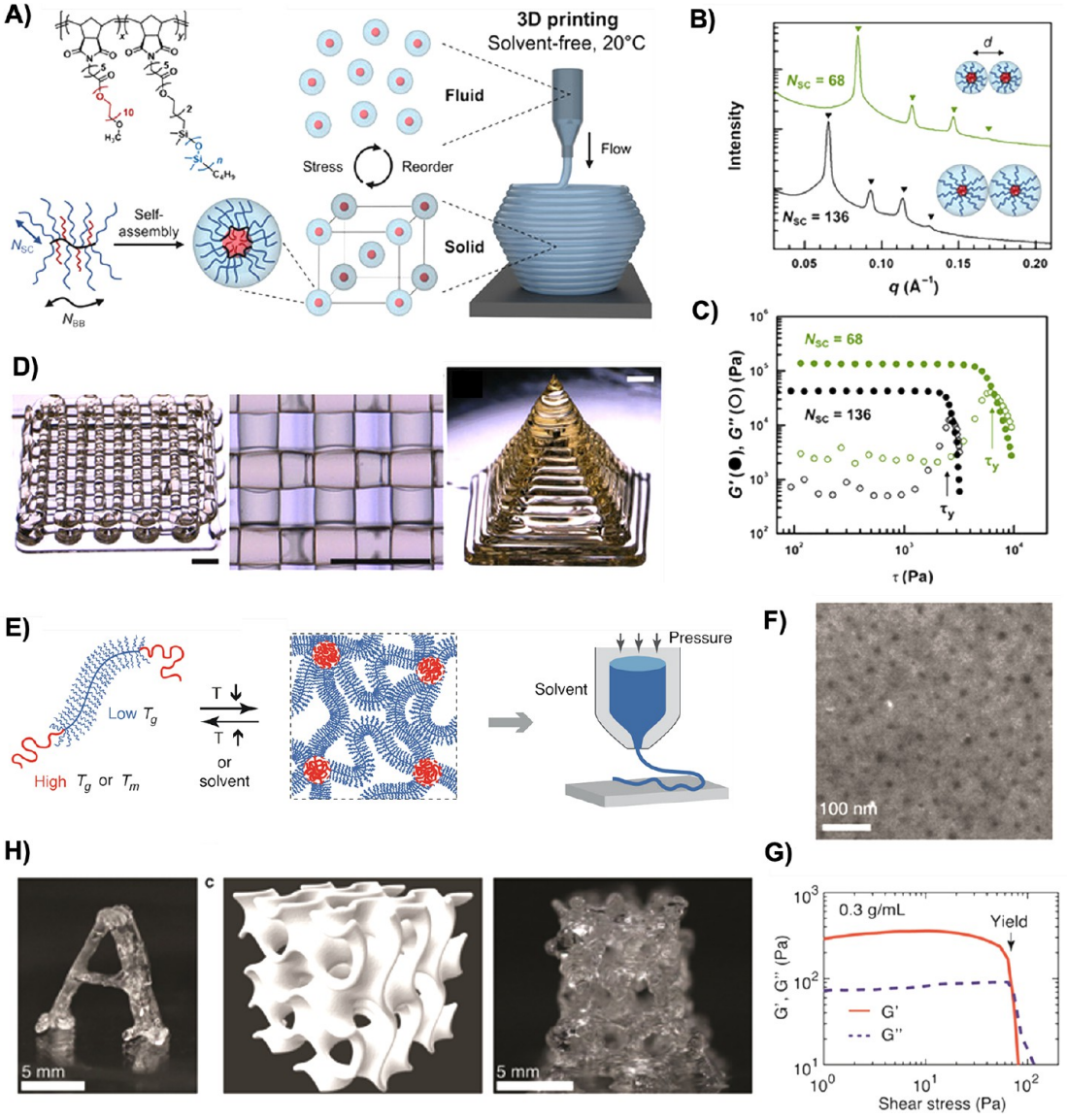


**Figure 14.** (A) Schematic diagram of the solvent-free direct ink writing approach for additive manufacturing of sphere-forming PDMS-*stat*-PEO statistical bottlebrush block copolymers developed by Xie, Bates, et al.[25] During extrusion, shear forces in the nozzle disrupt BCC packing of spherical PEO domains before the structure reforms after exiting the nozzle. (B) Domain spacing and (C) yield stress, as defined by the $G'$, $G''$ crossover, can be tuned by varying the lengths of the PDMS side chains ($N_{sc}$). (D) A range of structures printed by direct ink writing of the solvent-free ink without chemical cross-linking.[25] From Xie et al. Room temperature 3D printing of supersoft and solvent-free elastomers. *Sci. Adv.* **2020**, *6*, eabc6900. Copyright The Authors, some rights reserved; exclusive licensee AAAS. Distributed under a CC BY-NC 4.0 license http://creativecommons.org/licenses/by-nc/4.0/. Reprinted with permission from AAAS. (E) Schematic diagram of the self-assembly behavior of the linear−bottlebrush−linear (PBnMA−PDMS−PBnMA) ink used by Nian et al. as a directly 3D-printable elastomer.[333] (F) Transmission electron micrograph of the spherical PBnMA domains (dark spots) surrounded by a PDMS matrix (white region). (G) The addition of solvent as a plasticizer results in the material exhibiting features typically associated with yield-stress fluids. (H) Examples of a 3D printed block "A" and gyroid structure.[333] Reprinted (adapted) with permission from Nian et al. Three-dimensional printable, extremely soft, stretchable, and reversible elastomers from molecular architecture-directed assembly. *Chem. Mater.* **2021**, *33*, 2436−2445. Copyright 2021 American Chemical Society.

soft confinement,[334] no island/hole morphology was found at the free interface. Instead, bottlebrush block copolymers cast from tetrahydrofuran (THF) formed a mix of lamellae oriented parallel and perpendicular to the substrate (Figure 13G) which was persistent and did not converge upon further annealing.[332] Using a combination of atomic force microscopy (AFM) and grazing incidence small-angle X-ray scattering (Figure 13H),[332] the authors demonstrate that, below a critical film thickness, the lamellar *d*-spacing of the vertical (substrate-perpendicular) domains increased substantially to a value approaching the maximum possible domain spacing for the fully extended molecule in an end-to-end bilayer conformation.[332] This observed *d*-spacing under strong confinement was greater than double the bulk value and was explained by increased stretching of the bottlebrush backbone (Figure 13I).[332] Coating from a less selective solvent (propylene glycol methyl ether acetate, PGMEA) revealed more complex phase behavior, with the presence of a smaller cylinder phase, although domain spacing in vertically oriented regions scaled similarly to the THF case.[332] Differences in assembled morphology were rationalized based on the decrease in PGMEA selectivity which accentuated the


https://doi.org/10.1021/acs.chemmater.1c04030
*Chem. Mater.* 2022, 34, 1990−2024

volume asymmetry between the two blocks, leading to stabilization of the cylinder phase.[332]

Bottlebrush-containing elastomers are receiving substantial and increasing attention; due to their semiflexible nature and decreased entanglement density, they exhibit remarkable softness, with moduli on the order of 100 Pa—a full 3 orders of magnitude lower than those of conventional elastomers[335] and similar to that of the softest biological tissue.[336] In recent work, two independent groups of researchers[333,337] demonstrated two distinct approaches toward support-free direct-write 3D printing of bottlebrush elastomers—in each case designing the self-assembled microstructure to enable shear-induced disordering at a yield stress easily achieved in the printing nozzle. Xie et al.[337] prepared a biocompatible, solvent-free ink of highly asymmetric statistical bottlebrushes comprising primarily PDMS arms with a minor fraction of poly(ethylene oxide) ($\phi_{PEO}$ = 0.04−0.06). Due to their extremely low glass transition temperatures and large Flory−Huggins interaction parameter, these BBCPs rapidly assemble at room temperature to form a well-ordered body-centered cubic phase with PEO spheres embedded in a PDMS medium (Figure 14A). Domain spacing (Figure 14B) and yielding behavior (Figure 14C) were controlled by the length of PDMS side chains and during printing materials exhibit fast and reversible yielding, allowing for printing of the viscoelastic ink into self-supporting structures (Figure 14D). Incorporation of a telechelic PDMS additive with benzophenone end groups was found to allow for cross-linking under UV light after printing, with resulting elastomers exhibiting network moduli <50 kPa and withstanding over 300% elongation at break.

Nian and Cai et al.[333] have reported an alternate approach which enables direct-write 3D printing of a viscoelastic linear−bottlebrush−linear (LBBL) triblock copolymer solution which dries to form an elastomer without the use of post-treatment. They formulate an ink containing a 1:2 volume ratio of polymer in dichloromethane (a highly volatile solvent), where the triblock comprises a bottlebrush with PDMS (rubbery) side chains and a small fraction ($\phi$ = 0.06) of poly(benzyl methacrylate) linear end groups (Figure 14E).[333] Due to the strong chemical incompatibility between the blocks, the material spontaneously microphase separates to form a network structure comprising spherical microdomains of glassy linear end chains which act as physical cross-linking points that are bridged by rubbery bottlebrush blocks (Figure 14F). By appropriately tuning the solvent fraction, the microphase structure is preserved at quiescence but dissociates after reaching a certain yield stress (Figure 14G), before rapidly reforming after exiting the nozzle. The structure is preserved upon solvent drying, allowing for printing of self-supporting structures (Figure 14H). The prepared elastomers exhibited Young's moduli as low as 102 Pa, were thermostable up to 180 °C, and were fully solvent reprocessable.[333]

## 4. OUTLOOK: BOTTLEBRUSH POLYMERS AS A MATERIALS DESIGN PLATFORM

The study of bottlebrush polymers has matured into a large research effort spanning multiple subcommunities in polymer science and materials engineering, and significant progress over the past decade has stemmed from a convergence of synthesis, theory, modeling, characterization, and materials processing. Much of this progress has been the output of interdisciplinary research teams, due to the wide range of skills needed to combine molecular-level design with material applications. The future of bottlebrush polymers as highly tunable and versatile materials will likely continue this trend by further integrating expertise across the field of polymer science while continuing to add other areas of expertise. This is in addition to further development in each subdiscipline, which will further feed into new ideas and concepts that can be incorporated into the overall interdisciplinary approach for engineering bottlebrush polymers. We highlight several areas of particular promise, that we anticipate will be very dynamic areas in the next few years and beyond.

**4.1. Automation and Machine Learning for Material Design and Characterization.** Design of novel materials for targeted applications largely depends on establishing a reliable correlation between structure and function within the tunable parameter space. In the case of bottlebrush polymers, synthetic, characterization, and theoretical advances made over the past decade are broadly motivated by the goal of establishing these structure−function relationships.[48] As the variety of applications proliferates, however, there is an increasing need to navigate the broad bottlebrush design space efficiently to facilitate their efficient use as advanced materials. One emerging area of bottlebrush polymer materials to supplement physics- and chemistry-informed molecular design with automation and machine learning approaches that are specifically designed to create large databases and contend with large design spaces, respectively.

Accelerating the polymer synthesis and characterization of the synthesized polymers using computer-aided automation techniques is of emerging interest, and there has been some recent advances that will play a role in expediting material design. Examples include—but are not limited to—advanced flow polymerization processes[338−340] with high-throughput synthesis and screening with material characterization[341]/testing.[342] The combination of automated synthesis and characterization is crucial for advancing materials design for specific applications and could be particularly powerful as a tool to assess the wide domain space offered by the bottlebrush polymers and to establish structure−function relationships for targeted applications.

One major limitation for developing robust automation methodologies is the need for precise characterization of bottlebrush synthesis. An intrinsic requirement for the establishment of an accurate and general molecular structure−function relationship is precise characterization of the molecular structure of the copolymer. While there have been recent advances in directly visualizing bottlebrush polymers,[343] the characterization of the chemical composition of a polymer remains primarily done through the combination of gel permeation chromatography (GPC) and nuclear magnetic resonance (NMR) spectroscopy.[344] Both techniques, while ubiquitous in polymer synthesis, suffer from limitations that challenge the precision of the derived structure−function relationships. For example, in the case of grafting-from polymerization, the determination of branch density or dispersity is not trivial as neither NMR nor GPC of the final BB give direct access to these values. The types of architecture−property relationships needed to make this characterization quantitative are not general or well established, stemming from the particularly complicated physics of bottlebrush conformations in solution. Indeed, ATRP based grafting-from polymerization has been reported to yield bottlebrushes with grafting density up to 40% lower than the theoretical value.[62,64] In graft-through polymerization, the determination of the composition of a block polymer


https://doi.org/10.1021/acs.chemmater.1c04030
Chem. Mater. 2022, 34, 1990−2024

synthesized through sequential addition is not trivial due the minor differences in hydrodynamic radius between the intermediate homopolymer bottlebrush and the block copolymer, thereby leading to negligible differences in molecular weights reported using GPCs. Indeed, as much as 20 wt % of a homopolymer can remain undetected when using GPC as the method of analysis.[344] Protocols to determine these fundamental chemical features have been developed; however, they remain sparingly implemented.

Automated materials synthesis and characterization provides the basis for techniques such as machine learning that benefit from large data sets and can be used to establish nontrivial relationships between molecular and processing-based parameters and targeted outcomes such as properties related to structural color or mechanical properties.[345] The advantage of machine learning as an approach is that it can efficiently contend with the large and highly correlated parameter spaces that have been the subject of prior theoretical and computational predictions.[345] There has not been significant exploration of this approach, though Bayesian approaches have been used to interpret structural parameters obtained from molecular scattering over a large number of measurements in the literature.[346] However, this largely untapped approach holds significant promise for bridging the gap between bottlebrush polymer molecular structure and material applications.

**4.2. Bottlebrush Molecules Out-of-Equilibrium.** One major disconnect between the physical understanding of bottlebrush molecules and their application in advanced materials processing is the focus on equilibrium structure and dynamics in fundamental studies, while applications frequently rely on the out-of-equilibrium behavior of bottlebrushes for their function. There are examples where these two behaviors are bridged, such as in the work by Wade et al. that provided a fundamental characterization of shear-driven lamellar reordering and distortion.[319] However, most computational, theoretical, and characterization approaches rely on equilibrium or near-equilibrium concepts to make progress; this may not reflect real processing conditions, which can be significantly out-of-equilibrium. In practice, this means that engineers are often forced to rely on Edisonian parameter sweeps to design for a target application. We point to two areas of bottlebrush science well-positioned to bridge this gap: nonlinear rheology and dynamic bonds. Nonlinear rheology promises to characterize more complicated aspects of bottlebrush mechanical response, reflecting changes in material structure. Dynamic bonds complement this approach, providing a means to modify these material responses in a way that is orthogonal to the underlying bottlebrush architecture.

Nonlinear rheology is an inherently out-of-equilibrium characterization approach that seeks to understand the response of materials to the strong flows and stresses frequently encountered in material processing. To contrast, *linear* rheology deals with small deformations such as those in commonly used tools such as small-amplitude oscillatory shear (SAOS) experiments;[347] this approach probes the equilibrium molecular structure and characterizes the linear response with quantities such as the storage and loss moduli.[347] These quantities are associated with elastic and dissipative processes, respectively. Several tools have been developed to move beyond this paradigm in recent years. Weakly nonlinear large-amplitude oscillatory shear (LAOS) experiments systematically increase sinusoidal deformations, characterizing the emergence of nonsinusoidal mechanical responses in a series of higher-order harmonic responses.[348−350] The advantage of these methods is the direct connection to SAOS experiments and the ability to characterize the transition from linear (i.e., equilibrium) to nonlinear (i.e., out-of-equilibrium) responses.[348] However, there are weaknesses in this approach due to the challenge of interpreting the physical meaning of these higher-order harmonics in the context of molecular deformations. Recently, a class of methods known as "recovery rheology" approaches have sought to specifically overcome this limitation.[351−354] Here, oscillatory shear is abruptly "stopped" mid-deformation, and the relaxation of the material to the applied shear is also measured. This enables the extraction of molecular relaxation processes and has been applied to a number of material classes including linear polymer solutions and melts[351,352] and colloidal yield-stress fluids.[355] A related idea, intended to characterize the instantaneous material response, is called the *sequence of physical processes* (SPP).[356−359] This formalism provides a geometric interpretation of the instantaneous material response in shear rate, strain, and stress space that removes the reliance on the standard assumption of a form for the response trajectory.

The use of these new methods will be crucial for establishing a processing-relevant physical picture of bottlebrush dynamics. The hierarchical relaxation of bottlebrush polymers is considered one of the most important aspects of their utility as a material design platform,[155,164] and new SPP and recovery rheology approaches will be critical for resolving these various molecular relaxation phenomena and their importance for mechanical properties. As with any rheological tools that may supply properties under process-relevant conditions, complementary molecular-level information will be required to create links to the structure. Time-resolved scattering of X-rays and neutrons while performing out-of-equilibrium rheological testing may provide such information, as both techniques have already been used to characterize equilibrium structures successfully. This is especially intriguing in the context of bottlebrush polymers, where we expect that hierarchical dynamics will couple with out-of-equilibrium structure via the highly branched architecture.

The other tool that will be useful in this effort will be the incorporation of dynamic bonds, which can be used to directly modulate relaxation in ways connected to chemical functionality or stimuli, rather than architectural relaxation modes.[360−362] This will allow the tuning of polymer relaxation and driven mechanical response, by functionalizing the bottlebrush polymers with bonds chosen to exhibit specific kinetics or response to stimuli.

**4.3. Frontiers in Bottlebrush Modeling—Moving toward Processing Predictions.** There has been tremendous progress in modeling bottlebrush polymers,[19] with a proliferation of methods that can account for the multiscale structure of these complicated architectures using a combination of polymer field theory,[218,220,222] particle-based simulation,[136,167−171,175,177,178,209,212,213,231,363] liquid-state theory,[209] scaling arguments,[93,94,96,195] and a number of coarse-graining approaches.[14,178,364] It is now possible to span from the molecular to assembly length scales in bottlebrush materials. Nevertheless, we still lack the ability to predict these materials at the level of material processing, with no ability to simultaneously resolve the polymer structure at the assembly and subassembly length scales as well as the dynamics and large-scale morphological structures that give rise to the complicated structures apparent in out-of-equilibrium assembly. While current modeling approaches provide key insights that aid


https://doi.org/10.1021/acs.chemmater.1c04030
Chem. Mater. 2022, 34, 1990−2024

material development, it is desirable to have tools that more predictably connect with macroscopic length scales when there are strong flows or material deformations. This is of practical importance for applications in advanced additive manufacturing, where the properties inherent to bottlebrush polymers have already been demonstrated to be of significant use.

The next major step is to develop physical models that can capture material dynamics. This will depend in part on the system of interest, whether there is a need to model bottlebrush solutions, melts, and/or assembled structures. Bottlebrush melts will likely rely on dynamic field representations, building on Cahn−Hilliard continuum arguments,[365−369] dynamic field theory,[370−372] or other particle-based or particle−field hybrid representations.[373−376] There are several challenges in implementing these types of models, the most important being the choice of models for the bottlebrush diffusion constant. This is simplified somewhat by the suppression of entanglements;[199] however, it is unclear that the standard Rouse dynamics[377] used for linear, unentangled polymers will be relevant in these systems. It is likely that diffusion is highly anisotropic with relation to bottlebrush polymers oriented by self-assembly or liquid crystalline order. More generally, we anticipate nontrivial coupling between bottlebrush architecture, out-of-equilibrium conformations, and molecular diffusion that will represent a significant and persistent open question in modeling bottlebrush material dynamics. The other challenge for bottlebrush melts and self-assembled structures will be the further coarse-graining or molecular interactions to large length scales; for example, the values of both homogeneous and square gradient terms in standard Cahn−Hilliard free energy functionals will depend nontrivially on molecular architecture.[365,366] This level of coarse-graining has, to our knowledge, not been performed.

Bottlebrush solutions are even more challenging; many of the same difficulties will apply as in melts; however, hydrodynamics will be possibly important to molecular relaxation at both the molecular and branch levels. Recent work on branched[194,378−380] and ring polymers[381−389] has demonstrated the key role that hydrodynamics plays in polymer solutions, even at relatively high concentrations where screening has often been thought to be dominant.[384,390] Indeed, driven polymer systems can move significantly outside the typical equilibrium framework where scaling arguments are used; this can lead to marked conformational fluctuations that are dictated by the local hydrodynamic environment, even in situations well above the overlap concentration.[383,384] Modeling these hydrodynamic interactions remains a key challenge in polymer simulations, due to the expense of satisfying fluctuation dissipation in implicit solvent representations and the long-range nature of these interactions that complicates periodic simulation boxes.[391] Some standard methods, however, show promise. For dense systems, quasi-explicit solvent methods like lattice Boltzmann[392] simulations or multiparticle collision dynamics methods[393] scale favorably as they are not strongly dependent on the number of particles but rather the size of the simulation box. A number of other numerical/algorithmic[394,395] or physically motivated[390,396,397] approaches have also shown success enabling massive implicit solvent simulations. Further challenges arise when considering specific solution processing methods, with coating and solution printing being also affected significantly by solvent evaporation. Modeling of evaporation is an ongoing challenge[398] and drives flows that can significantly affect structure.

For both bottlebrush solutions and melts, the connection between molecular structure and strong flows will ultimately affect mechanical properties, reflecting the largest length-scale effects and the other key component of any prediction of bottlebrush processing. In soft materials, this connection is typically encoded in some sort of mechanical constitutive model,[399−401] which establishes a material-dependent response to an applied deformation and can be both directly compared with rheological data and used to predict flows and stresses in processing scenarios. Constitutive models are developed both empirically and with knowledge of molecular dynamics and represent a large area of research that has yet to consider the specific challenges of bottlebrush polymers; however, standard models for soft materials such as linear polymers[401−403] and wormlike micelles[404,405] may provide useful starting points for polymer melts and solutions, respectively.

## 5. CONCLUSION

In this perspective we have outlined both the historic and the recent developments in bottlebrush polymers, framing this narrative with the primary challenges in this rich area of soft materials research; namely, there has been an increasing trend toward more integration between efforts in polymer synthesis, theory, computation, characterization, and processing, moving the field from fundamental developments to practical application. This has been commensurate with developments in the polymer science field, with improvements in these areas all converging to contribute to our understanding of bottlebrush polymers. We note a few directions that represent what we think are the natural "next steps" in realizing the promise of bottlebrush polymers as a versatile macromolecular platform for material design, which focus on bridging the gap between fundamental molecular understanding and practical materials processing. This will require advances at the forefront of our understanding of material dynamics and polymer synthesis, as well as advances in tools for materials exploration and process/characterization automation. Like recent and historic developments, we look to the broader field of polymer science for inspiration in the next stages of bottlebrush polymer development.

## AUTHOR INFORMATION


### Corresponding Author

**Charles E. Sing** − *Department Chemical and Biomolecular Engineering, University of Illinois at Urbana−Champaign, Urbana, Illinois 61801, United States;* orcid.org/0000-0001-7231-2685; Email: cesing@illinois.edu

### Authors

**Tianyuan Pan** − *Department of Materials Science and Engineering, University of Illinois at Urbana−Champaign, Urbana, Illinois 61801, United States;* orcid.org/0000-0002-8837-1230

**Sarit Dutta** − *Department Chemical and Biomolecular Engineering, University of Illinois at Urbana−Champaign, Urbana, Illinois 61801, United States;* orcid.org/0000-0002-6197-7881

**Yash Kamble** − *Department Chemical and Biomolecular Engineering, University of Illinois at Urbana−Champaign, Urbana, Illinois 61801, United States*

**Bijal B. Patel** − *Department Chemical and Biomolecular Engineering, University of Illinois at Urbana−Champaign,*




https://doi.org/10.1021/acs.chemmater.1c04030
Chem. Mater. 2022, 34, 1990−2024

*Urbana, Illinois 61801, United States;* orcid.org/0000-0002-8015-9075

**Matthew A. Wade** − *Department Chemical and Biomolecular Engineering, University of Illinois at Urbana−Champaign, Urbana, Illinois 61801, United States*

**Simon A. Rogers** − *Department Chemical and Biomolecular Engineering, University of Illinois at Urbana−Champaign, Urbana, Illinois 61801, United States*

**Ying Diao** − *Department Chemical and Biomolecular Engineering, University of Illinois at Urbana−Champaign, Urbana, Illinois 61801, United States;* orcid.org/0000-0002-8984-0051

**Damien Guironnet** − *Department Chemical and Biomolecular Engineering, University of Illinois at Urbana−Champaign, Urbana, Illinois 61801, United States;* orcid.org/0000-0002-0356-6697

Complete contact information is available at: https://pubs.acs.org/10.1021/acs.chemmater.1c04030

### Author Contributions

[§]T.P., S.D., Y.K., B.B.P, and M.A.W. contributed equally. The manuscript was written through contributions of all authors. All authors have given approval to the final version of the manuscript.

### Notes

The authors declare no competing financial interest.

### Biographies

Tianyuan Pan is currently a Ph.D. candidate in the Department of Materials Science and Engineering at the University of Illinois at Urbana−Champaign, under the supervision of Prof. Charles Sing. He received his B.S. degree in Materials Science and Engineering from Tsinghua University, China, in 2018. His current research is to understand the physics of polymers with complex architectures and develop coarse-grained molecular models and simulation tools to study these macromolecules.

Sarit Dutta is currently a research scientist in Laboratoire de Chimie at École Normale Supérieure de Lyon. He received his Ph.D. in Chemical Engineering from the University of Minnesota in 2014 and pursued postdoctoral research at the University of Wisconsin and the University of Illinois. Recent research interests include the nonequilibrium dynamics of wormlike micelles and the modeling of bottlebrush polymers. Current research interests include understanding scattering patterns and mechanical instabilities in colloidal semiconductor nanocrystals.

Yash L. Kamble is currently a Ph.D. student in the Department of Chemical and Biomolecular Engineering at the University of Illinois at Urbana−Champaign, under the supervision of Prof. Damien Guironnet. He received his B.S. degree in Chemical Engineering from the Institute of Chemical Technology, Mumbai, India, in 2019. His current research is on the synthesis of bottlebrush polymers, with an emphasis on advancing the chemical versatility for shape-controlled bottlebrush polymers.

Bijal B. Patel is currently an NRC Postdoctoral Fellow at the National Institute of Standards and Technology. He received his B.S. in Chemical Engineering at the University of Texas at Austin and his Ph.D. in Chemical and Biomolecular Engineering at the University of Illinois at Urbana−Champaign. His graduate research was under the supervision of Prof. Ying Diao, studying the additive manufacturing and self-assembly of bottlebrush block copolymers. His current research is on resonant soft X-ray scattering.

Matthew A. Wade is currently a Ph.D. student in the Department of Chemical and Biomolecular Engineering at the University of Illinois at Urbana−Champaign, under the supervision of Prof. Simon Rogers. He received his B.S. degree in Chemical Engineering from Case Western Reserve University in 2017. His current research is on characterizing the viscoelastic behavior of bottlebrush polymers using transient and out-of-equilibrium rheological techniques.

Simon A. Rogers is currently an Assistant Professor in the Department of Chemical and Biomolecular Engineering at the University of Illinois at Urbana−Champaign. He received his B.S. Ph.D. in 2011 from Victoria University of Wellington in New Zealand and joined the University of Illinois at Urbana−Champaign in 2015. His current research is focused on understanding the fundamental physics behind time-dependent phenomena in advanced colloidal, polymeric, and self-assembled materials. He received the NSF CAREER and ACS PRF Doctoral New Investigator Awards.

Ying Diao is an Associate Professor and Gunsalus Scholar in the Department of Chemical and Biomolecular Engineering at the University of Illinois at Urbana−Champaign. She received her Ph.D. in 2012 from MIT and joined the University of Illinois at Urbana−Champaign in 2015. Her research focuses on the assembly of organic functional materials and innovating printing approaches that enable structural control down to the nanoscale. She received the MIT TR35 Award, Sloan Research Fellowship, and NSF CAREER Award.

Damien S. Guironnet is an Associate Professor in the Departments of Chemical and Biomolecular Engineering and Chemistry at the University of Illinois at Urbana−Champaign. He joined the University of Illinois at Urbana−Champaign in 2014 from BASF and received his Ph.D. in Chemistry from Universität Konstanz. His research focuses on developing polymerization techniques, along with reactor engineering and automation strategies, to achieve precise control over polymer composition and architecture. He was recognized as an ACS PMSE Young Investigator in 2019.

Charles E. Sing is currently an Associate Professor in the Department of Chemical and Biomolecular Engineering at the University of Illinois at Urbana−Champaign. He received his Ph.D. in 2012 from MIT and joined the University of Illinois at Urbana−Champaign in 2014. His research interests are using polymer physics, statistical mechanics, and coarse-grained simulations to understand the molecular origin of material properties of soft materials. He received the NSF CAREER Award and was an ACS PMSE Young Investigator in 2020.

## ■ ACKNOWLEDGMENTS

The authors acknowledge support from the National Science Foundation under DMREF Award Number DMR-1727605 and DMREF Award number DMR-2119172. T.P. also acknowledges support from the ACS Petroleum Research Fund under Award Number 61500-ND7.

## ■ REFERENCES

(1) Bates, C. M.; Bates, F. S. 50th Anniversary Perspective: Block Polymers-Pure Potential. *Macromolecules* **2017**, *50* (1), 3−22.

(2) Bates, F. S.; Fredrickson, G. H. Block Copolymer Thermodynamics: Theory and Experiment. *Annu. Rev. Phys. Chem.* **1990**, *41*, 525−557.

(3) Lutz, J.-F. Coding Macromolecules: Inputting Information in Polymers Using Monomer-Based Alphabets. *Macromolecules* **2015**, *48* (14), 4759−4767.

(4) Lutz, J. F.; Ouchi, M.; Liu, D. R.; Sawamoto, M. Sequence-Controlled Polymers. *Science* **2013**, *341*, 1238149.

(5) Lutz, J. F.; Lehn, J. M.; Meijer, E. W.; Matyjaszewski, K. From Precision Polymers to Complex Materials and Systems. *Nat. Rev. Mater.* **2016**, *1*, 16024.
(6) Polymeropoulos, G.; Zapsas, G.; Ntetsikas, K.; Bilalis, P.; Gnanou, Y.; Hadjichristidis, N. *50th Anniversary Perspective*: Polymers with Complex Architectures. *Macromolecules* **2017**, *50* (4), 1253−1290.
(7) Lee, Y.; Choi, J.; Hwang, N. S. Regulation of Lubricin for Functional Cartilage Tissue Regeneration: A Review. *Biomater. Res.* **2018**, *22* (1), 9.
(8) Chandran, P. L.; Horkay, F. Aggrecan, an Unusual Polyelectrolyte: Review of Solution Behavior and Physiological Implications. *Acta Biomater.* **2012**, *8* (1), 3−12.
(9) Kiani, C.; Chen, L.; Wu, Y. J.; Yee, A. J.; Yang, B. B. Structure and Function of Aggrecan. *Cell Res.* **2002**, *12* (1), 19−32.
(10) Innes-Gold, S.; Berezney, J.; Saleh, O. Single-Molecule Stretching Shows Glycosylation Sets Tension in the Hyaluronan-Aggrecan Bottlebrush. *Biophys. J.* **2020**, *119* (7), 1351−1358.
(11) McGuckin, M. A.; Lindén, S. K.; Sutton, P.; Florin, T. H. Mucin Dynamics and Enteric Pathogens. *Nat. Rev. Microbiol.* **2011**, *9* (4), 265−278.
(12) Button, B.; Cai, L.; Ehre, C.; Kesimer, M.; Hill, D. B.; Sheehan, J. K.; Boucher, R. C.; Rubinstein, M. A Periciliary Brush Promotes the Lung Health by Separation the Mucus Layer from Airway Epithelia. *Science* **2012**, *337*, 937−941.
(13) Liang, H.; Cao, Z.; Wang, Z.; Sheiko, S. S.; Dobrynin, A. V. Combs and Bottlebrushes in a Melt. *Macromolecules* **2017**, *50* (8), 3430−3437.
(14) Pan, T.; Patel, B. B.; Walsh, D. J.; Dutta, S.; Guironnet, D.; Diao, Y.; Sing, C. E. Implicit Side-Chain Model and Experimental Characterization of Bottlebrush Block Copolymer Solution Assembly. *Macromolecules* **2021**, *54* (8), 3620−3633.
(15) Liang, H.; Morgan, B. J.; Xie, G.; Martinez, M. R.; Zhulina, E. B.; Matyjaszewski, K.; Sheiko, S. S.; Dobrynin, A. V. Universality of the Entanglement Plateau Modulus of Comb and Bottlebrush Polymer Melts. *Macromolecules* **2018**, *51* (23), 10028−10039.
(16) Rzayev, J. Molecular Bottlebrushes: New Opportunities in Nanomaterials Fabrication. *ACS Macro Lett.* **2012**, *1* (9), 1146−1149.
(17) Verduzco, R.; Li, X.; Pesek, S. L.; Stein, G. E. Structure, Function, Self-Assembly, and Applications of Bottlebrush Copolymers. *Chem. Soc. Rev.* **2015**, *44* (8), 2405−2420.
(18) Xie, G.; Martinez, M. R.; Olszewski, M.; Sheiko, S. S.; Matyjaszewski, K. Molecular Bottlebrushes as Novel Materials. *Biomacromolecules* **2019**, *20*, 27−54.
(19) Mohammadi, E.; Joshi, S. Y.; Deshmukh, S. A. A Review of Computational Studies of Bottlebrush Polymers. *Comput. Mater. Sci.* **2021**, *199*, 110720.
(20) Macfarlane, R. J.; Kim, B.; Lee, B.; Weitekamp, R. A.; Bates, C. M.; Lee, S. F.; Chang, A. B.; Delaney, K. T.; Fredrickson, G. H.; Atwater, H. A.; Grubbs, R. H. Improving Brush Polymer Infrared One-Dimensional Photonic Crystals via Linear Polymer Additives. *J. Am. Chem. Soc.* **2014**, *136* (50), 17374−17377.
(21) Liberman-Martin, A. L.; Chu, C. K.; Grubbs, R. H. Application of Bottlebrush Block Copolymers as Photonic Crystals. *Macromol. Rapid Commun.* **2017**, *38* (13), 1700058.
(22) Miyake, G. M.; Piunova, V. A.; Weitekamp, R. A.; Grubbs, R. H. Precisely Tunable Photonic Crystals from Rapidly Self-Assembling Brush Block Copolymer Blends. *Angew. Chem. - Int. Ed.* **2012**, *51* (45), 11246−11248.
(23) Vatankhah-Varnoosfaderani, M.; Daniel, W. F. M.; Zhushma, A. P.; Li, Q.; Morgan, B. J.; Matyjaszewski, K.; Armstrong, D. P.; Spontak, R. J.; Dobrynin, A. V.; Sheiko, S. S. Bottlebrush Elastomers: A New Platform for Freestanding Electroactuation. *Adv. Mater.* **2017**, *29* (2), 1604209−7.
(24) Vatankhah-Varnosfaderani, M.; Daniel, W. F. M.; Everhart, M. H.; Pandya, A. A.; Liang, H.; Matyjaszewski, K.; Dobrynin, A. V.; Sheiko, S. S. Mimicking Biological Stress−Strain Behaviour with Synthetic Elastomers. *Nature* **2017**, *549* (7673), 497−501.
(25) Xie, R.; Mukherjee, S.; Levi, A. E.; Reynolds, V. G.; Wang, H.; Chabinyc, M. L.; Bates, C. M. Room Temperature 3D Printing of Super-Soft and Solvent-Free Elastomers. *Sci. Adv.* **2020**, *6*, eabc6900.
(26) Reynolds, V. G.; Mukherjee, S.; Xie, R.; Levi, A. E.; Atassi, A.; Uchiyama, T.; Wang, H.; Chabinyc, M. L.; Bates, C. M. Super-Soft Solvent-Free Bottlebrush Elastomers for Touch Sensing. *Mater. Horiz.* **2020**, *7* (1), 181−187.
(27) Arrington, K. J.; Radzinski, S. C.; Drummey, K. J.; Long, T. E.; Matson, J. B. *Reversibly Cross-Linkable Bottlebrush Polymers as Pressure-Sensitive Adhesives* **2018**, *10*, 26662.
(28) Li, X.; Prukop, S. L.; Biswal, S. L.; Verduzco, R. Surface Properties of Bottlebrush Polymer Thin Films. *Macromolecules* **2012**, *45* (17), 7118−7127.
(29) Pesek, S. L.; Lin, Y. H.; Mah, H. Z.; Kasper, W.; Chen, B.; Rohde, B. J.; Robertson, M. L.; Stein, G. E.; Verduzco, R. Synthesis of Bottlebrush Copolymers Based on Poly(Dimethylsiloxane) for Surface Active Additives. *Polymer* **2016**, *98*, 495−504.
(30) Li, X.; Shamsijazeyi, H.; Pesek, S. L.; Agrawal, A.; Hammouda, B.; Verduzco, R. Thermoresponsive PNIPAAM Bottlebrush Polymers with Tailored Side-Chain Length and End-Group Structure. *Soft Matter* **2014**, *10* (12), 2008−2015.
(31) Johnson, J. A.; Lu, Y. Y.; Burts, A. O.; Xia, Y.; Durrell, A. C.; Tirrell, D. A.; Grubbs, R. H. Drug-Loaded, Bivalent-Bottle-Brush Polymers by Graft-through ROMP. *Macromolecules* **2010**, *43* (24), 10326−10335.
(32) Huang, Y. S.; Chen, J. K.; Kuo, S. W.; Hsieh, Y. A.; Yamamoto, S.; Nakanishi, J.; Huang, C. F. Synthesis of Poly(N-Vinylpyrrolidone)-Based Polymer Bottlebrushes by ATRPA and RAFT Polymerization: Toward Drug Delivery Application. *Polymers* **2019**, *11* (6), 1079.
(33) Weiss, P.; Gerecht, J. F.; Krems, I. J. Graft Copolymers from Poly(Styrene Co Dimethyl Maleate) and Poly(Styrene Co Allyl Acetate). *J. Polym. Sci.* **1959**, *35* (129), 343−354.
(34) Oster, G.; Shibata, O. Graft Copolymer of Polyacrylamide and Natural Rubber Produced by Means of Ultraviolet Light. *J. Polym. Sci.* **1957**, *26* (113), 233−234.
(35) Chen, W. K. W.; Mesrobian, R. B.; Ballantine, D. S.; Metz, D. J.; Glines, A. Studies on Graft Copolymers Derived by Ionizing Radiation. *J. Polym. Sci.* **1957**, *23* (104), 903−913.
(36) Faraone, G.; Parasacco, G.; Cogrossi, C. Grafting on Cellulose Acetate. *J. Appl. Polym. Sci.* **1961**, *5*, 16−22.
(37) Cooper, W.; Vaughan, G. The Graft Polymerization of Methyl Methacrylate to Natural Rubber. *J. Appl. Polym. Sci.* **1959**, *1* (2), 254−254.
(38) Rempp, P. F.; Franta, E. Macromonomers: Synthesis, Characterization and Applications. In *Polymerization Reactions*; Advances in Polymer Science; Cantow, H.-J., Dall'Asta, G., Dušek, K., Ferry, J. D., Fujita, H., Gordon, M., Henrici-Olivé, G., Kennedy, J. P., Kern, W., Okamura, S., Olivé, S., Oveberger, C. G., Saegusa, T., Schulz, G. V., Slichter, W. P., Stille, J. K., Eds.; Springer Berlin Heidelberg: Berlin, Heidelberg, 1984; Vol. *58*, pp 1−53, DOI: 10.1007/3-540-12793-3_6.
(39) Brockway, C. E. Copolymerization of Methyl Methacrylate with Unsaturated Esters of Granular Starch. *J. Polym. Sci., Part A* **1965**, *3* (3), 1031−1036.
(40) Brockway, C. E.; Moser, K. B. Grafting of Poly (Methyl Methacrylate) to Granular Corn Starch. *J. Polym. Sci., Part A* **1963**, *1* (3), 1025−1039.
(41) Brockway, C. E.; Seaberg, P. A. Grafting of Polyacrylonitrile to Granular Corn Starch by Initiation with Cerium. *J. Polym. Sci. [A1]* **1967**, *5* (11), 2967−2971.
(42) Ezra, G.; Zilkha, A. Anionic Graft Polymerization of Propylene Oxide on Starch. *Eur. Polym. J.* **1970**, *6* (9), 1305−1311.
(43) Oster, G.; Oster, G. K.; Moroson, H. Ultraviolet Induced Crosslinking and Grafting of Solid High Polymers. *J. Polym. Sci.* **1959**, *34* (127), 671−684.
(44) Muthukrishnan, S.; Zhang, M.; Burkhardt, M.; Drechsler, M.; Mori, H.; Müller, A. H. E. Molecular Sugar Sticks: Cylindrical Glycopolymer Brushes. *Macromolecules* **2005**, *38* (19), 7926−7934.

(45) Schulz, G. O.; Milkovich, R. Graft Polymers with Macromonomers. I. Synthesis from Methacrylate-Terminated Polystyrene. *J. Appl. Polym. Sci.* **1982**, *27* (12), 4773−4786.
(46) Kobayashi, K.; Sumitomo, H.; Kobayashi, A.; Akaike, T. Oligosaccharide-Carrying Styrene-Type Macromers. Polymerization and Specific Interactions Between the Polymers and Liver Cells. *J. Macromol. Sci. Part - Chem.* **1988**, *25* (5−7), 655−667.
(47) Wataoka, I.; Urakawa, H.; Kobayashi, K.; Akaike, T.; Schmidt, M.; Kajiwara, K. Structural Characterization of Glycoconjugate Polystyrene in Aqueous Solution. *Macromolecules* **1999**, *32* (6), 1816−1821.
(48) Li, Z.; Tang, M.; Liang, S.; Zhang, M.; Biesold, G. M.; He, Y.; Hao, S. M.; Choi, W.; Liu, Y.; Peng, J.; Lin, Z. Bottlebrush Polymers: From Controlled Synthesis, Self-Assembly, Properties to Applications. *Prog. Polym. Sci.* **2021**, *116*, 101387.
(49) Sheiko, S. S.; Sumerlin, B. S.; Matyjaszewski, K. Cylindrical Molecular Brushes: Synthesis, Characterization, and Properties. *Prog. Polym. Sci. Oxf.* **2008**, *33* (7), 759−785.
(50) Gao, H.; Matyjaszewski, K. Synthesis of Molecular Brushes by "Grafting onto" Method: Combination of ATRP and Click Reactions. *J. Am. Chem. Soc.* **2007**, *129* (20), 6633−6639.
(51) Xiao, L.; Chen, Y.; Zhang, K. Efficient Metal-Free "Grafting onto" Method for Bottlebrush Polymers by Combining RAFT and Triazolinedione-Diene Click Reaction. *Macromolecules* **2016**, *49* (12), 4452−4461.
(52) Wu, Y.; Tang, Q.; Zhang, M.; Li, Z.; Zhu, W.; Liu, Z. Synthesis of Bottlebrush Polymers with V-Shaped Side Chains. *Polymer* **2018**, *143*, 190−199.
(53) Geng, Z.; Shin, J. J.; Xi, Y.; Hawker, C. J. Click Chemistry Strategies for the Accelerated Synthesis of Functional Macromolecules. *J. Polym. Sci.* **2021**, *59* (11), 963−1042.
(54) Becer, C. R.; Hoogenboom, R.; Schubert, U. S. Click Chemistry beyond Metal-Catalyzed Cycloaddition. *Angew. Chem., Int. Ed.* **2009**, *48* (27), 4900−4908.
(55) Schappacher, M.; Billaud, C.; Paulo, C.; Deffieux, A. Synthesis, Dimensions and Solution Properties of Linear and Macrocyclic Poly(Chloroethyl Vinyl Ether)-g-Polystyrene Comblike Polymers. *Macromol. Chem. Phys.* **1999**, *200* (10), 2377−2386.
(56) Selb, J.; Gallot, Y. Graft Copolymers: 1. Synthesis and Characterization of Poly(Styrene-g-2-Vinylpyridine). *Polym. Guildf* **1979**, *20* (10), 1259−1267.
(57) Gacal, B.; Durmaz, H.; Tasdelen, M. A.; Hizal, G.; Tunca, U.; Yagci, Y.; Demirel, A. L. Anthracene−Maleimide-Based Diels−Alder "Click Chemistry" as a Novel Route to Graft Copolymers. *Macromolecules* **2006**, *39* (16), 5330−5336.
(58) Cesana, S.; Kurek, A.; Baur, M. A.; Auernheimer, J.; Nuyken, O. Polymer-Bound Thiol Groups on Poly(2-Oxazoline)s. *Macromol. Rapid Commun.* **2007**, *28* (5), 608−615.
(59) Foster, J. C.; Varlas, S.; Couturaud, B.; Coe, Z.; O'Reilly, R. K. Getting into Shape: Reflections on a New Generation of Cylindrical Nanostructures' Self-Assembly Using Polymer Building Blocks. *J. Am. Chem. Soc.* **2019**, *141* (7), 2742−2753.
(60) Wang, Y.; Ren, R.; Ling, J.; Sun, W.; Shen, Z. One-Pot "Grafting-from" Synthesis of Amphiphilic Bottlebrush Block Copolymers Containing PLA and PVP Side Chains via Tandem ROP and RAFT Polymerization. *Polymer* **2018**, *138*, 378−386.
(61) Mukumoto, K.; Li, Y.; Nese, A.; Sheiko, S. S.; Matyjaszewski, K. Synthesis and Characterization of Molecular Bottlebrushes Prepared by Iron-Based ATRP. *Macromolecules* **2012**, *45* (23), 9243−9249.
(62) Martinez, M. R.; Sobieski, J.; Lorandi, F.; Fantin, M.; Dadashi-Silab, S.; Xie, G.; Olszewski, M.; Pan, X.; Ribelli, T. G.; Matyjaszewski, K. Understanding the Relationship between Catalytic Activity and Termination in PhotoATRP: Synthesis of Linear and Bottlebrush Polyacrylates. *Macromolecules* **2020**, *53* (1), 59−67.
(63) Cheng, G.; Böker, A.; Zhang, M.; Krausch, G.; Müller, A. H. E. Amphiphilic Cylindrical Core-Shell Brushes via a "Grafting from" Process Using ATRP. *Macromolecules* **2001**, *34* (20), 6883−6888.
(64) Burdyńska, J.; Li, Y.; Aggarwal, A. V.; Höger, S.; Sheiko, S. S.; Matyjaszewski, K. Synthesis and Arm Dissociation in Molecular Stars with a Spoked Wheel Core and Bottlebrush Arms. *J. Am. Chem. Soc.* **2014**, *136* (36), 12762−12770.
(65) Neugebauer, D. Two Decades of Molecular Brushes by ATRP. *Polymer* **2015**, *72*, 413−421.
(66) Matyjaszewski, K.; Tsarevsky, N. V. Nanostructured Functional Materials Prepared by Atom Transfer Radical Polymerization. *Nat. Chem.* **2009**, *1* (4), 276−288.
(67) Tanaka, J.; Häkkinen, S.; Boeck, P. T.; Cong, Y.; Perrier, S.; Sheiko, S. S.; You, W. Orthogonal Cationic and Radical RAFT Polymerizations to Prepare Bottlebrush Polymers. *Angew. Chem.* **2020**, *132* (18), 7270−7275.
(68) Shanmugam, S.; Cuthbert, J.; Kowalewski, T.; Boyer, C.; Matyjaszewski, K. Catalyst-Free Selective Photoactivation of RAFT Polymerization: A Facile Route for Preparation of Comblike and Bottlebrush Polymers. *Macromolecules* **2018**, *51* (19), 7776−7784.
(69) Sumerlin, B. S.; Neugebauer, D.; Matyjaszewski, K. Initiation Efficiency in the Synthesis of Molecular Brushes by Grafting from via Atom Transfer Radical Polymerization. *Macromolecules* **2005**, *38* (3), 702−708.
(70) Li, A.; Ma, J.; Sun, G.; Li, Z.; Cho, S.; Clark, C.; Wooley, K. L. One-Pot, Facile Synthesis of Well-Defined Molecular Brush Copolymers by a Tandem RAFT and ROMP, "Grafting-through" Strategy. *J. Polym. Sci. Part Polym. Chem.* **2012**, *50* (9), 1681−1688.
(71) Cho, H. Y.; Krys, P.; Szcześniak, K.; Schroeder, H.; Park, S.; Jurga, S.; Buback, M.; Matyjaszewski, K. Synthesis of Poly(OEOMA) Using Macromonomers via "Grafting-Through" ATRP. *Macromolecules* **2015**, *48* (18), 6385−6395.
(72) Yang, B.; Abel, B. A.; McCormick, C. L.; Storey, R. F. Synthesis of Polyisobutylene Bottlebrush Polymers via Ring-Opening Metathesis Polymerization. *Macromolecules* **2017**, *50* (19), 7458−7467.
(73) Radzinski, S. C.; Foster, J. C.; Matson, J. B. Synthesis of Bottlebrush Polymers via Transfer-to and Grafting-through Approaches Using a RAFT Chain Transfer Agent with a ROMP-Active Z-Group. *Polym. Chem.* **2015**, *6* (31), 5643−5652.
(74) Foster, J. C.; Radzinski, S. C.; Lewis, S. E.; Slutzker, M. B.; Matson, J. B. Norbornene-Containing Dithiocarbamates for Use in Reversible Addition-Fragmentation Chain Transfer (RAFT) Polymerization and Ring-Opening Metathesis Polymerization (ROMP). *Polymer* **2015**, *79*, 205−211.
(75) Sheiko, S. S.; Sumerlin, B. S.; Matyjaszewski, K. Cylindrical Molecular Brushes: Synthesis, Characterization, and Properties. *Prog. Polym. Sci.* **2008**, *33* (7), 759−785.
(76) Brocas, A.-L.; Mantzaridis, C.; Tunc, D.; Carlotti, S. Polyether Synthesis: From Activated or Metal-Free Anionic Ring-Opening Polymerization of Epoxides to Functionalization. *Prog. Polym. Sci.* **2013**, *38* (6), 845−873.
(77) Isono, T. Synthesis of Functional and Architectural Polyethers via the Anionic Ring-Opening Polymerization of Epoxide Monomers Using a Phosphazene Base Catalyst. *Polym. J.* **2021**, *53* (7), 753−764.
(78) Verkoyen, P.; Frey, H. Long-Chain Alkyl Epoxides and Glycidyl Ethers: An Underrated Class of Monomers. *Macromol. Rapid Commun.* **2020**, *41* (15), 2000225.
(79) Matyjaszewski, K. Macromolecular Engineering: From Rational Design through Precise Macromolecular Synthesis and Processing to Targeted Macroscopic Material Properties. *Prog. Polym. Sci.* **2005**, *30* (8−9), 858−875.
(80) Braunecker, W. A.; Matyjaszewski, K. Controlled/Living Radical Polymerization: Features, Developments, and Perspectives. *Prog. Polym. Sci.* **2007**, *32* (1), 93−146.
(81) Ouchi, M.; Terashima, T.; Sawamoto, M. Transition Metal-Catalyzed Living Radical Polymerization: Toward Perfection in Catalysis and Precision Polymer Synthesis. *Chem. Rev.* **2009**, *109* (11), 4963−5050.
(82) Walsh, D. J.; Hyatt, M. G.; Miller, S. A.; Guironnet, D. Recent Trends in Catalytic Polymerizations. *ACS Catal.* **2019**, *9* (12), 11153−11188.
(83) Wang, D.; Zhang, Z.; Hadjichristidis, N. C1 Polymerization: A Unique Tool towards Polyethylene-Based Complex Macromolecular Architectures. *Polym. Chem.* **2017**, *8* (28), 4062−4073.


https://doi.org/10.1021/acs.chemmater.1c04030
*Chem. Mater.* 2022, 34, 1990−2024

(84) Ihara, E.; Shimomoto, H. Polymerization of Diazoacetates: New Synthetic Strategy for C-C Main Chain Polymers. *Polymer* **2019**, *174*, 234−258.
(85) López-Barrón, C. R.; Tsou, A. H.; Hagadorn, J. R.; Throckmorton, J. A. Highly Entangled α-Olefin Molecular Bottlebrushes: Melt Structure, Linear Rheology, and Interchain Friction Mechanism. *Macromolecules* **2018**, *51* (17), 6958−6966.
(86) Aoshima, S.; Kanaoka, S. A Renaissance in Living Cationic Polymerization. *Chem. Rev.* **2009**, *109* (11), 5245−5287.
(87) López-Barrón, C. R.; Brant, P.; Eberle, A. P. R.; Crowther, D. J. Linear Rheology and Structure of Molecular Bottlebrushes with Short Side Chains. *J. Rheol.* **2015**, *59* (3), 865−883.
(88) López-Barrón, C. R.; Tsou, A. H.; Younker, J. M.; Norman, A. I.; Schaefer, J. J.; Hagadorn, J. R.; Throckmorton, J. A. Microstructure of Crystallizable α-Olefin Molecular Bottlebrushes: Isotactic and Atactic Poly(1-Octadecene). *Macromolecules* **2018**, *51* (3), 872−883.
(89) Choinopoulos, I. Grubbs' and Schrock's Catalysts, Ring Opening Metathesis Polymerization and Molecular Brushes-Synthesis, Characterization, Properties and Applications. *Polymers* **2019**, *11* (2), 298.
(90) Lin, T. P.; Chang, A. B.; Chen, H. Y.; Liberman-Martin, A. L.; Bates, C. M.; Voegtle, M. J.; Bauer, C. A.; Grubbs, R. H. Control of Grafting Density and Distribution in Graft Polymers by Living Ring-Opening Metathesis Copolymerization. *J. Am. Chem. Soc.* **2017**, *139* (10), 3896−3903.
(91) Hyatt, M. G.; Walsh, D. J.; Lord, R. L.; Andino Martinez, J. G.; Guironnet, D. Mechanistic and Kinetic Studies of the Ring Opening Metathesis Polymerization of Norbornenyl Monomers by a Grubbs Third Generation Catalyst. *J. Am. Chem. Soc.* **2019**, *141* (44), 17918−17925.
(92) Radzinski, S. C.; Foster, J. C.; Chapleski, R. C.; Troya, D.; Matson, J. B. Bottlebrush Polymer Synthesis by Ring-Opening Metathesis Polymerization: The Significance of the Anchor Group. *J. Am. Chem. Soc.* **2016**, *138* (22), 6998−7004.
(93) Birshtein, T. M.; Borisov, O. V.; Zhulina, Y. B.; Khokhlov, A. R.; Yurasova, T. A. Conformations of Comb-like Macromolecules. *Polym. Sci. USSR* **1987**, *29* (6), 1293−1300.
(94) Borisov, O. V.; Birshtein, T. M.; Zhulina, Y. B. The Temperature-Concentration Diagram of State for Solutions of Comb-like Macromolecules. *Polym. Sci. USSR* **1987**, *29* (7), 1552−1559.
(95) de Gennes, P.-G. *Scaling Concepts in Polymer Physics*; Cornell University Press: 1979.
(96) Fredrickson, G. H. Surfactant-Induced Lyotropic Behavior of Flexible Polymer Solutions. *Macromolecules* **1993**, *26* (11), 2825−2831.
(97) Yamakawa, H. *Modern Theory of Polymer Solutions*; Harper & Row: New York, 1971.
(98) Onsager, L. The Effects of Shape on the Interaction of Colloidal Particles. *Ann. N Acad. Sci.* **1949**, *51* (4), 627−659.
(99) Tsukahara, Y. Liquid Crystal Formation of Multibranched Polystyrene Induced by Molecular Anisotropy Associated with Its High Branch Density. *Polymer* **1995**, *36* (17), 3413−3416.
(100) Wintermantel, M.; Fischer, K.; Gerle, M.; Ries, R.; Schmidt, M.; Kajiwara, K.; Urakawa, H.; Wataoka, I. Lyotropic Phases Formed by "Molecular Bottlebrushes. *Angew. Chem., Int. Ed. Engl.* **1995**, *34* (1314), 1472−1474.
(101) Rathgeber, S.; Pakula, T.; Wilk, A.; Matyjaszewski, K.; Lee, H. il; Beers, K. L. Bottle-Brush Macromolecules in Solution: Comparison between Results Obtained from Scattering Experiments and Computer Simulations. *Polymer* **2006**, *47* (20), 7318−7327.
(102) Storm, I. M.; Kornreich, M.; Hernandez-Garcia, A.; Voets, I. K.; Beck, R.; Cohen Stuart, M. A.; Leermakers, F. A. M.; de Vries, R. Liquid Crystals of Self-Assembled DNA Bottlebrushes. *J. Phys. Chem. B* **2015**, *119* (10), 4084−4092.
(103) Nakamura, Y.; Norisuye, T. Brush-like Polymers. In *Soft Matter Characterization*; Springer Netherlands: Dordrecht, 2008; pp 235−286, DOI: 10.1007/978-1-4020-4465-6_5.
(104) Terao, K.; Nakamura, Y.; Norisuye, T. Solution Properties of Polymacromonomers Consisting of Polystyrene. 2. Chain Dimensions and Stiffness in Cyclohexane and Toluene. *Macromolecules* **1999**, *32* (3), 711−716.
(105) Hokajo, T.; Terao, K.; Nakamura, Y.; Norisuye, T. Solution Properties of Polymacromonomers Consisting of Polystyrene V. Effect of Side Chain Length on Chain Stiffness. *Polym. J.* **2001**, *33* (6), 481−485.
(106) Terao, K.; Hokajo, T.; Nakamura, Y.; Norisuye, T. Solution Properties of Polymacromonomers Consisting of Polystyrene. 3. Viscosity Behavior in Cyclohexane and Toluene. *Macromolecules* **1999**, *32* (11), 3690−3694.
(107) Shiokawa, K. Chain Dimensions of a Poly(Macromonomer) in a Good Solvent. *Polym. J.* **1995**, *27* (8), 871−874.
(108) Daoud, M.; Cotton, J. P. Star Shaped Polymers : A Model for the Conformation and Its Concentration Dependence. *J. Phys. (Paris)* **1982**, *43* (3), 531−538.
(109) Denesyuk, N. A. Conformational Properties of Bottle-Brush Polymers. *Phys. Rev. E* **2003**, *67* (5), 5201−5210.
(110) Denesyuk, N. A. Bottle-Brush Polymers as an Intermediate between Star and Cylindrical Polymers. *Phys. Rev. E* **2003**, *68* (3), 1293−11.
(111) Kawaguchi, S.; Akaike, K.; Zhang, Z.-M.; Matsumoto, H.; Ito, K. Water Soluble Bottlebrushes. *Polym. J.* **1998**, *30* (12), 1004−1007.
(112) Terao, K.; Takeo, Y.; Tazaki, M.; Nakamura, Y.; Norisuye, T. Polymacromonomer Consisting of Polystyrene. Light Scattering Characterization in Cyclohexane. *Polym. J.* **1999**, *31* (2), 193−198.
(113) Terao, K.; Hayashi, S.; Nakamura, Y.; Norisuye, T. Solution Properties of Polymacromonomers Consisting of Polystyrene. *Polym. Bull.* **2000**, *44* (3), 309−316.
(114) Amitani, K.; Terao, K.; Nakamura, Y.; Norisuye, T. Small-Angle X-Ray Scattering from Polystyrene Polymacromonomers in Cyclohexane. *Polym. J.* **2005**, *37* (4), 324−331.
(115) Hokajo, T.; Hanaoka, Y.; Nakamura, Y.; Norisuye, T. Translational Diffusion Coefficient of Polystyrene Polymacromonomers. Dependence on Side-Chain Length. *Polym. J.* **2005**, *37* (7), 529−534.
(116) Kikuchi, M.; Mihara, T.; Jinbo, Y.; Izumi, Y.; Nagai, K.; Kawaguchi, S. Characterization of Rodlike Poly(n-Hexyl Isocyanate) Macromonomers and Their Polymacromonomers by Light Scattering, SAXS, Intrinsic Viscosity, and Scanning Force Microscopy. *Polym. J.* **2007**, *39* (4), 330−341.
(117) Sugiyama, M.; Nakamura, Y.; Norisuye, T. Dilute-Solution Properties of Polystyrene Polymacromonomer Having Side Chains of over 100 Monomeric Units. *Polym. J.* **2008**, *40* (2), 109−115.
(118) Kikuchi, M.; Lien, L. T. N.; Narumi, A.; Jinbo, Y.; Izumi, Y.; Nagai, K.; Kawaguchi, S. Conformational Properties of Cylindrical Rod Brushes Consisting of a Polystyrene Main Chain and Poly(n-Hexyl Isocyanate) Side Chains. *Macromolecules* **2008**, *41* (17), 6564−6572.
(119) Kikuchi, M.; Takahara, A.; Kawaguchi, S. Dimensional Characterizations from Rod Stars to Brushes of Polymers with a Low Degree of Polymerization. *Macromolecules* **2017**, *50* (1), 324−331.
(120) Kratky, O.; Porod, G. Röntgenuntersuchung Gelöster Fadenmoleküle. *Recl. Trav. Chim. Pays-Bas* **1949**, *68* (12), 1106−1122.
(121) Yamakawa, H.; Yoshizaki, T. *Helical Wormlike Chains in Polymer Solutions*, 2nd ed.; Springer-Verlag: Berlin, Heidelberg, 2016.
(122) Wintermantel, M.; Schmidt, M.; Tsukahara, Y.; Kajiwara, K.; Kohjiya, S. Rodlike Combs. *Macromol. Rapid Commun.* **1994**, *15* (3), 279−284.
(123) Wintermantel, M.; Gerle, M.; Fischer, K.; Schmidt, M.; Wataoka, I.; Urakawa, H.; Kajiwara, K.; Tsukahara, Y. Molecular Bottlebrushes. *Macromolecules* **1996**, *29* (3), 978−983.
(124) Nemoto, N.; Nagai, M.; Koike, A.; Okada, S. Diffusion and Sedimentation Studies on Poly(Macromonomer) in Dilute Solution. *Macromolecules* **1995**, *28* (11), 3854−3859.
(125) Gerle, M.; Fischer, K.; Roos, S.; Müller, A. H. E.; Schmidt, M.; Sheiko, S. S.; Prokhorova, S.; Möller, M. Main Chain Conformation and Anomalous Elution Behavior of Cylindrical Brushes as Revealed by GPC/MALLS, Light Scattering, and SFM. *Macromolecules* **1999**, *32* (8), 2629−2637.
(126) Lecommandoux, S.; Chécot, F.; Borsali, R.; Schappacher, M.; Deffieux, A.; Brûlet, A.; Cotton, J. P. Effect of Dense Grafting on the Backbone Conformation of Bottlebrush Polymers: Determination of

the Persistence Length in Solution. *Macromolecules* **2002**, *35* (23), 8878−8881.
(127) Rathgeber, S.; Pakula, T.; Wilk, A.; Matyjaszewski, K.; Beers, K. L. On the Shape of Bottle-Brush Macromolecules: Systematic Variation of Architectural Parameters. *J. Chem. Phys.* **2005**, *122* (12), 124904−124914.
(128) Zhao, Y.; Jamieson, A. M.; Olson, B. G.; Yao, N.; Dong, S.; Nazarenko, S.; Hu, X.; Lal, J. Conformation of Comb-like Liquid Crystal Polymers in Isotropic Solution Probed by Small-Angle Neutron Scattering. *J. Polym. Sci. Part B Polym. Phys.* **2006**, *44* (17), 2412−2424.
(129) Nakamura, Y.; Norisuye, T. Backbone Stiffness of Comb-Branched Polymers. *Polym. J.* **2001**, *33* (11), 874−878.
(130) Subbotin, A.; Saariaho, M.; Ikkala, O.; ten Brinke, G. Elasticity of Comb Copolymer Cylindrical Brushes. *Macromolecules* **2000**, *33* (9), 3447−3452.
(131) Fischer, K.; Schmidt, M. Solvent-Induced Length Variation of Cylindrical Brushes. *Macromol. Rapid Commun.* **2001**, *22* (10), 787−791.
(132) Sheiko, S. S.; Borisov, O. V.; Prokhorova, S. A.; Möller, M. Cylindrical Molecular Brushes under Poor Solvent Conditions: Microscopic Observation and Scaling Analysis. *Eur. Phys. J. E* **2004**, *13* (2), 125−131.
(133) Prokhorova, S. A.; Sheiko, S. S.; Möller, M.; Ahn, C.-H.; Percec, V. Molecular Imaging of Monodendron Jacketed Linear Polymers by Scanning Force Microscopy. *Macromol. Rapid Commun.* **1998**, *19* (7), 359−366.
(134) Zhang, B.; Gröhn, F.; Pedersen, J. S.; Fischer, K.; Schmidt, M. Conformation of Cylindrical Brushes in Solution: Effect of Side Chain Length. *Macromolecules* **2006**, *39* (24), 8440−8450.
(135) Feuz, L.; Strunz, P.; Geue, T.; Textor, M.; Borisov, O. Conformation of Poly(L-Lysine)-Graft-Poly(Ethylene Glycol) Molecular Brushes in Aqueous Solution Studied by Small-Angle Neutron Scattering. *Eur. Phys. J. E* **2007**, *23* (3), 237−245.
(136) Yethiraj, A. A Monte Carlo Simulation Study of Branched Polymers. *J. Chem. Phys.* **2006**, *125* (20), 204901.
(137) Elli, S.; Ganazzoli, F.; Timoshenko, E. G.; Kuznetsov, Y. A.; Connolly, R. Size and Persistence Length of Molecular Bottle-Brushes by Monte Carlo Simulations. *J. Chem. Phys.* **2004**, *120* (13), 6257−6267.
(138) Saariaho, M.; Ikkala, O.; Szleifer, I.; Erukhimovich, I.; ten Brinke, G. On Lyotropic Behavior of Molecular Bottle-Brushes: A Monte Carlo Computer Simulation Study. *J. Chem. Phys.* **1997**, *107* (8), 3267−3276.
(139) Subbotin, A. V.; Semenov, A. N. Spatial Self-Organization of Comb Macromolecules. *Polym. Sci. Ser. A* **2007**, *49* (12), 1328−1357.
(140) Shiokawa, K.; Itoh, K.; Nemoto, N. Simulations of the Shape of a Regularly Branched Polymer as a Model of a Polymacromonomer. *J. Chem. Phys.* **1999**, *111* (17), 8165−8173.
(141) Khalatur, P. G.; Shirvanyanz, D. G.; Starovoitova, N. Y.; Khokhlov, A. R. Conformational Properties and Dynamics of Molecular Bottle-Brushes: A Cellular-Automaton-Based Simulation. *Macromol. Theory Simul* **2000**, *9* (3), 141−155.
(142) Vasilevskaya, V. V.; Klochkov, A. A.; Khalatur, P. G.; Khokhlov, A. R.; ten Brinke, G. Microphase Separation within a Comb Copolymer with Attractive Side Chains: A Computer Simulation Study. *Macromol. Theory Simul.* **2001**, *10*, 389−394.
(143) Pevnaya, O. S.; Kramarenko, E. Y.; Khokhlov, A. R. Comb Macromolecules with Attracting Functional Groups in Side Chains. *Polym. Sci. Ser. A* **2007**, *49* (11), 1233−1241.
(144) Stepanyan, R.; Subbotin, A.; ten Brinke, G. Comb Copolymer Brush with Chemically Different Side Chains. *Macromolecules* **2002**, *35* (14), 5640−5648.
(145) de Jong, J.; Ten Brinke, G. Conformational Aspects and Intramolecular Phase Separation of Alternating Copolymacromonomers: A Computer Simulation Study. *Macromol. Theory Simul.* **2004**, *13* (4), 318−327.
(146) Meissner, J. Basic Parameters, Melt Rheology, Processing and End-Use Properties of Three Similar Low Density Polyethylene Samples. *Pure Appl. Chem.* **1975**, *42*, 551−612.
(147) Billmeyer, H. W. The Molecular Structure of Polyethylene. III. Determination of Long Chain Branching. *J. Am. Chem. Soc.* **1953**, *75*, 6118−6122.
(148) Sperati, C. A.; Franta, W. A.; Starkweather, H. W. The Molecular Structure of Polythylene. V. The Effect of Chain Branching and Molecular Weight on Physical Properties. *J. Am. Chem. Soc.* **1953**, *75*, 6127−6133.
(149) Tian, J.; Yu, W.; Zhou, C. The Preparation and Rheology Characterization of Long Chain Branching Polypropylene. *Polymer* **2006**, *47* (23), 7962−7969.
(150) Yan, D.; Wang, W.-J.; Zhu, S. Effect of Long Chain Branching on Rheological Properties of Metallocene Polyethylene. *Polymer* **1999**, *40* (7), 1737−1744.
(151) Wagner, M. H.; Kheirandish, S.; Yamaguchi, M. Quantitative Analysis of Melt Elongational Behavior of LLDPE/LDPE Blends. *Rheol. Acta* **2004**, *44* (2), 198−218.
(152) McLeish, T. C. B. Molecular Rheology of H-Polymers. *Macromolecules* **1988**, *21* (4), 1062−1070.
(153) McLeish, T. C. Polymer Architecture Influence on Rheology. *Curr. Opin. Solid State Mater. Sci.* **1997**, *2* (6), 678−682.
(154) Vlassopoulos, D.; Fytas, G.; Pakula, T.; Roovers, J. Multiarm Star Polymers Dynamics. *J. Phys.: Condens. Matter* **2001**, *13* (41), R855−R876.
(155) Fetters, L. J.; Kiss, A. D.; Pearson, D. S.; Quack, G. F.; Vitus, F. J. Rheological Behavior of Star-Shaped Polymers. *Macromolecules* **1993**, *26* (4), 647−654.
(156) Yasuda, K.; Armstrong, R. C.; Cohen, R. E. Shear Flow Properties of Concentrated Solutions of Linear and Star Branched Polystyrenes. *Rheol. Acta* **1981**, *20* (2), 163−178.
(157) Doi, M.; Kuzuu, N. Y. Rheology of Star Polymers in Concentrated Solutions and Melts. *J. Polym. Sci. Polym. Lett. Ed.* **1980**, *18* (12), 775−780.
(158) Roovers, J.; Toporowski, P. M. Hydrodynamic Studies on Model Branched Polystyrenes. *J. Polym. Sci. Polym. Phys.* **1980**, *18* (9), 1907−1917.
(159) Kapnistos, M.; Kirkwood, K. M.; Ramirez, J.; Vlassopoulos, D.; Leal, L. G. Nonlinear Rheology of Model Comb Polymers. *J. Rheol.* **2009**, *53* (5), 1133−1153.
(160) Lentzakis, H.; Das, C.; Vlassopoulos, D.; Read, D. J. Pom-Pom-like Constitutive Equations for Comb Polymers. *J. Rheol.* **2014**, *58* (6), 1855−1875.
(161) Seo, S. E.; Hawker, C. J. The Beauty of Branching in Polymer Science. *Macromolecules* **2020**, *53*, 3257−3261.
(162) Hult, A.; Johansson, M.; Malmstrom, E. Hyperbranched Polymers. *Adv. Polym. Sci.* **1999**, *143*, 1−34.
(163) Chremos, A.; Douglas, J. F. Communication: When Does a Branched Polymer Become a Particle? *J. Chem. Phys.* **2015**, *143* (11), 111104.
(164) van Ruymbeke, E.; Lee, H.; Chang, T.; Nikopoulou, A.; Hadjichristidis, N.; Snijkers, F.; Vlassopoulos, D. Molecular Rheology of Branched Polymers: Decoding and Exploring the Role of Architectural Dispersity through a Synergy of Anionic Synthesis, Interaction Chromatography, Rheometry and Modeling. *Soft Matter* **2014**, *10* (27), 4762.
(165) La Mantia, F. P.; Valenza, A.; Acierno, D. Influence of the Structure of Linear Density Polyethylene on the Rheological and Mechanical Properties of Blends with Low Density Polyethylene. *Eur. Polym. J.* **1986**, *22* (8), 647−652.
(166) Tomalia, D. A.; Baker, H.; Dewald, J.; Hall, M.; Kallos, G.; Martin, S.; Roeck, J.; Ryder, J.; Smith, P. Dendritic Macromolecules: Synthesis of Starburst Dendrimers. *Macromolecules* **1986**, *19* (9), 2466−2468.
(167) Hsu, H.-P.; Paul, W.; Binder, K. One- and Two-Component Bottle-Brush Polymers: Simulations Compared to Theoretical Predictions. *Macromol. Theory Simul* **2007**, *16* (7), 660−689.
(168) Hsu, H.-P.; Paul, W.; Binder, K. Structure of Bottle-Brush Polymers in Solution: A Monte Carlo Test of Models for the Scattering Function. *J. Chem. Phys.* **2008**, *129* (20), 204904.


https://doi.org/10.1021/acs.chemmater.1c04030
*Chem. Mater.* 2022, 34, 1990−2024

(169) Hsu, H.-P.; Paul, W.; Binder, K. Polymer Chain Stiffness vs. Excluded Volume: A Monte Carlo Study of the Crossover towards the Worm-like Chain Model. *Eur. Lett.* **2010**, *92* (2), 28003.
(170) Hsu, H.-P.; Paul, W.; Binder, K. Understanding the Multiple Length Scales Describing the Structure of Bottle-Brush Polymers by Monte Carlo Simulation Methods. *Macromol. Theory Simul* **2011**, *20* (7), 510−525.
(171) Theodorakis, P. E.; Hsu, H.-P.; Paul, W.; Binder, K. Computer Simulation of Bottle-Brush Polymers with Flexible Backbone: Good Solvent versus Theta Solvent Conditions. *J. Chem. Phys.* **2011**, *135* (16), 164903−164914.
(172) Angelescu, D. G.; Linse, P. Monte Carlo Simulations of Multigraft Homopolymers in Good Solvent. *Macromolecules* **2014**, *47* (1), 415−426.
(173) Borisov, O. V.; Zhulina, E. B.; Birshtein, T. M. Persistence Length of Dendritic Molecular Brushes. *ACS Macro Lett.* **2012**, *1* (10), 1166−1169.
(174) Hsu, H.-P.; Paul, W.; Rathgeber, S.; Binder, K. Characteristic Length Scales and Radial Monomer Density Profiles of Molecular Bottle-Brushes: Simulation and Experiment. *Macromolecules* **2010**, *43* (3), 1592−1601.
(175) Dutta, S.; Wade, M. A.; Walsh, D. J.; Guironnet, D.; Rogers, S. A.; Sing, C. E. Dilute Solution Structure of Bottlebrush Polymers. *Soft Matter* **2019**, *15* (14), 2928−2941.
(176) Liang, H.; Wang, Z.; Sheiko, S. S.; Dobrynin, A. V. Comb and Bottlebrush Graft Copolymers in a Melt. *Macromolecules* **2019**, *52* (10), 3942−3950.
(177) Dutta, S.; Sing, C. E. Two Stretching Regimes in the Elasticity of Bottlebrush Polymers. *Macromolecules* **2020**, *53* (16), 6946−6955.
(178) Dutta, S.; Pan, T.; Sing, C. E. Bridging Simulation Length Scales of Bottlebrush Polymers Using a Wormlike Cylinder Model. *Macromolecules* **2019**, *52* (13), 4858−4874.
(179) Liang, H.; Sheiko, S. S.; Dobrynin, A. Supersoft and Hyperelastic Polymer Networks with Brushlike Strands. *Macromolecules* **2018**, *51* (2), 638−645.
(180) Liang, H.; Grest, G. S.; Dobrynin, A. V. Brush-Like Polymers and Entanglements: From Linear Chains to Filaments. *ACS Macro Lett.* **2019**, *8* (10), 1328−1333.
(181) Liang, H.; Wang, Z.; Dobrynin, A. V. Scattering from Melts of Combs and Bottlebrushes: Molecular Dynamics Simulations and Theoretical Study. *Macromolecules* **2019**, *52*, 5555.
(182) Jacobs, M.; Liang, H.; Pugnet, B.; Dobrynin, A. V. Molecular Dynamics Simulations of Surface and Interfacial Tension of Graft Polymer Melts. *Langmuir* **2018**, *34* (43), 12974−12981.
(183) Jacobs, M.; Liang, H.; Dashtimoghadam, E.; Morgan, B. J.; Sheiko, S. S.; Dobrynin, A. V. Nonlinear Elasticity and Swelling of Comb and Bottlebrush Networks. *Macromolecules* **2019**, *52*, 5095−5101.
(184) Daniel, W. F. M.; Burdyńska, J.; Vatankhah-Varnoosfaderani, M.; Matyjaszewski, K.; Paturej, J.; Rubinstein, M.; Dobrynin, A. V.; Sheiko, S. S. Solvent-Free, Supersoft and Superelastic Bottlebrush Melts and Networks. *Nat. Mater.* **2016**, *15* (2), 183−189.
(185) Cao, Z.; Carrillo, J.-M. Y.; Sheiko, S. S.; Dobrynin, A. V. Computer Simulations of Bottle Brushes: From Melts to Soft Networks. *Macromolecules* **2015**, *48* (14), 5006−5015.
(186) Cao, Z.; Daniel, W. F. M.; Vatankhah-Varnosfaderani, M.; Sheiko, S. S.; Dobrynin, A. V. Dynamics of Bottlebrush Networks. *Macromolecules* **2016**, *49* (20), 8009−8017.
(187) Mitra, I.; Li, X.; Pesek, S. L.; Makarenko, B.; Lokitz, B. S.; Uhrig, D.; Ankner, J. F.; Verduzco, R.; Stein, G. E. Thin Film Phase Behavior of Bottlebrush/Linear Polymer Blends. *Macromolecules* **2014**, *47* (15), 5269−5276.
(188) Miyagi, K.; Mei, H.; Terlier, T.; Stein, G. E.; Verduzco, R. Analysis of Surface Segregation of Bottlebrush Polymer Additives in Thin Film Blends with Attractive Intermolecular Interactions. *Macromolecules* **2020**, *53* (15), 6720−6730.
(189) Mah, A. H.; Laws, T.; Li, W.; Mei, H.; Brown, C. C.; Ievlev, A.; Kumar, R.; Verduzco, R.; Stein, G. E. Entropic and Enthalpic Effects in Thin Film Blends of Homopolymers and Bottlebrush Polymers. *Macromolecules* **2019**, *52* (4), 1526−1535.
(190) Mei, H.; Laws, T. S.; Mahalik, J. P.; Li, J.; Mah, A. H.; Terlier, T.; Bonnesen, P.; Uhrig, D.; Kumar, R.; Stein, G. E.; Verduzco, R. Entropy and Enthalpy Mediated Segregation of Bottlebrush Copolymers to Interfaces. *Macromolecules* **2019**, *52* (22), 8910−8922.
(191) Saleh, O. A. Perspective: Single Polymer Mechanics across the Force Regimes. *J. Chem. Phys.* **2015**, *142* (19), 194902.
(192) Rocha, M. S.; Storm, I. M.; Bazoni, R. F.; Ramos, É. B.; Hernandez-Garcia, A.; Cohen Stuart, M. A.; Leermakers, F.; de Vries, R. Force and Scale Dependence of the Elasticity of Self-Assembled DNA Bottle Brushes. *Macromolecules* **2018**, *51* (1), 204−212.
(193) Marko, J. F.; Siggia, E. D. Stretching DNA. *Macromolecules* **1995**, *28* (26), 8759−8770.
(194) Berezney, J. P.; Marciel, A. B.; Schroeder, C. M.; Saleh, O. A. Scale-Dependent Stiffness and Internal Tension of a Model Brush Polymer. *Phys. Rev. Lett.* **2017**, *119* (12), 127801−127810.
(195) Zhulina, E. B.; Sheiko, S. S.; Borisov, O. Solution and Melts of Barbwire Bottlebrushes : Hierarchical Structure and Scale-Dependent Elasticity. *Macromolecules* **2019**, *52*, 1671−1684.
(196) Pincus, P. Excluded Volume Effects and Stretched Polymer Chains. *Macromolecules* **1976**, *9* (3), 386−388.
(197) Dalsin, S. J.; Hillmyer, M. A.; Bates, F. S. Molecular Weight Dependence of Zero-Shear Viscosity in Atactic Polypropylene Bottlebrush Polymers. *ACS Macro Lett.* **2014**, *3* (5), 423−427.
(198) Pesek, S. L.; Xiang, Q.; Hammouda, B.; Verduzco, R. Small-Angle Neutron Scattering Analysis of Bottlebrush Backbone and Side Chain Flexibility. *J. Polym. Sci., Part B: Polym. Phys.* **2017**, *55* (1), 104−111.
(199) Dalsin, S. J.; Hillmyer, M. A.; Bates, F. S. Linear Rheology of Polyolefin-Based Bottlebrush Polymers. *Macromolecules* **2015**, *48* (13), 4680−4691.
(200) Hu, M.; Xia, Y.; McKenna, G. B.; Kornfield, J. A.; Grubbs, R. H. Linear Rheological Response of a Series of Densely Branched Brush Polymers. *Macromolecules* **2011**, *44* (17), 6935−6943.
(201) Haugan, I. N.; Maher, M. J.; Chang, A. B.; Lin, T. P.; Grubbs, R. H.; Hillmyer, M. A.; Bates, F. S. Consequences of Grafting Density on the Linear Viscoelastic Behavior of Graft Polymers. *ACS Macro Lett.* **2018**, *7* (5), 525−530.
(202) López-Barrón, C. R.; Shivokhin, M. E.; Hagadorn, J. R. Extensional Rheology of Highly-Entangled $\alpha$-Olefin Molecular Bottlebrushes. *J. Rheol.* **2019**, *63* (6), 917−926.
(203) Abbasi, M.; Faust, L.; Wilhelm, M. Comb and Bottlebrush Polymers with Superior Rheological and Mechanical Properties. *Adv. Mater.* **2019**, *31* (26), 1806484.
(204) Iwawaki, H.; Inoue, T.; Nakamura, Y. Rheo-Optical Study on Dynamics of Bottlebrush-like Polymacromonomer Consisting of Polystyrene. *Macromolecules* **2011**, *44* (13), 5414−5419.
(205) Iwawaki, H.; Urakawa, O.; Inoue, T.; Nakamura, Y. Rheo-Optical Study on Dynamics of Bottlebrush-like Polymacromonomer Consisting of Polystyrene. II. Side Chain Length Dependence on Dynamical Stiffness of Main Chain. *Macromolecules* **2012**, *45* (11), 4801−4808.
(206) Maleki, H.; Theodorakis, P. E. Structure of Bottle-Brush Brushes under Good Solvent Conditions: A Molecular Dynamics Study. *J. Phys.: Condens. Matter* **2011**, *23* (50), 505104−505109.
(207) Zhang, Z.; Carrillo, J.-M. Y.; Ahn, S. K.; Wu, B.; Hong, K.; Smith, G. S.; Do, C. Atomistic Structure of Bottlebrush Polymers: Simulations and Neutron Scattering Studies. *Macromolecules* **2014**, *47* (16), 5808−5814.
(208) Fytas, N. G.; Theodorakis, P. E. Molecular Dynamics Simulations of Single-Component Bottle-Brush Polymers with Flexible Backbones under Poor Solvent Conditions. *J. Phys.: Condens. Matter* **2013**, *25* (28), 285105−285111.
(209) Lyubimov, I.; Wessels, M. G.; Jayaraman, A. Molecular Dynamics Simulation and PRISM Theory Study of Assembly in Solutions of Amphiphilic Bottlebrush Block Copolymers. *Macromolecules* **2018**, *51* (19), 7586−7599.


https://doi.org/10.1021/acs.chemmater.1c04030
*Chem. Mater.* 2022, 34, 1990−2024

(210) Paturej, J.; Kreer, T. Hierarchical Excluded Volume Screening in Solutions of Bottlebrush Polymers. *Soft Matter* **2017**, *13* (45), 8534−8541.
(211) Carrillo, J.-M. Y.; Sheiko, S. S.; Dobrynin, A. V. Molecular Dynamics Simulations of Bottlebrush Macromolecules in Two Dimensional Polymeric Melts under Flow Conditions. *Soft Matter* **2011**, *7* (6), 2805−2807.
(212) Wessels, M. G.; Jayaraman, A. Molecular Dynamics Simulation Study of Linear, Bottlebrush, and Star-like Amphiphilic Block Polymer Assembly in Solution. *Soft Matter* **2019**, *15* (19), 3987−3998.
(213) Wessels, M. G.; Jayaraman, A. Self-Assembly of Amphiphilic Polymers of Varying Architectures near Attractive Surfaces. *Soft Matter* **2020**, *16* (3), 623−633.
(214) Alaboalirat, M.; Qi, L.; Arrington, K. J.; Qian, S.; Keum, J. K.; Mei, H.; Littrell, K. C.; Sumpter, B. G.; Carrillo, J. M. Y.; Verduzco, R.; Matson, J. B. Amphiphilic Bottlebrush Block Copolymers: Analysis of Aqueous Self-Assembly by Small-Angle Neutron Scattering and Surface Tension Measurements. *Macromolecules* **2019**, *52* (2), 465−476.
(215) Wang, Z.; Safran, S. A. Size Distribution for Aggregates of Associating Polymers. II. Linear Packing. *J. Chem. Phys.* **1988**, *89* (8), 5323−5328.
(216) Witten, T. A.; Pincus, P. A. Colloid Stabilization by Long Grafted Polymers. *Macromolecules* **1986**, *19* (10), 2509−2513.
(217) Dalsin, S. J.; Rions-Maehren, T. G.; Beam, M. D.; Bates, F. S.; Hillmyer, M. A.; Matsen, M. W. Bottlebrush Block Polymers: Quantitative Theory and Experiments. *ACS Nano* **2015**, *9* (12), 12233−12245.
(218) Spencer, R. K. W.; Matsen, M. W. Field-Theoretic Simulations of Bottlebrush Copolymers. *J. Chem. Phys.* **2018**, *149* (18), 184901.
(219) Fredrickson, G. *The Equilibrium Theory of Inhomogeneous Polymers*; Oxford University Press: 2013.
(220) Levi, A. E.; Lequieu, J.; Horne, J. D.; Bates, M. W.; Ren, J. M.; Delaney, K. T.; Fredrickson, G. H.; Bates, C. M. Miktoarm Stars via Grafting-Through Copolymerization: Self-Assembly and the Star-to-Bottlebrush Transition. *Macromolecules* **2019**, *52* (4), 1794−1802.
(221) Panagiotou, E.; Delaney, K. T.; Fredrickson, G. H. Theoretical Prediction of an Isotropic to Nematic Phase Transition in Bottlebrush Homopolymer Melts. *J. Chem. Phys.* **2019**, *151* (9), 094901.
(222) Lequieu, J.; Quah, T.; Delaney, K. T.; Fredrickson, G. H. Complete Photonic Band Gaps with Nonfrustrated ABC Bottlebrush Block Polymers. *ACS Macro Lett.* **2020**, *9* (7), 1074−1080.
(223) Schweizer, K. S.; Curro, J. G. *Phys. Rev. Lett.* **1987**, *58*, 246−249.
(224) Nair, N.; Jayaraman, A. Self-Consistent PRISM Theory−Monte Carlo Simulation Studies of Copolymer Grafted Nanoparticles in a Homopolymer Matrix. *Macromolecules* **2010**, *43*, 8251−8263.
(225) Hansen, J. P.; McDonald, I. R. *Theory of Simple Liquids*; Elsevier: Boston, 2006.
(226) Charvet, R.; Novak, B. M. One-Pot, One-Catalyst Synthesis of Graft Copolymers by Controlled ROMP and ATRP Polymerizations. *Macromolecules* **2004**, *37*, 8808−8811.
(227) Cheng, C.; Khoshdel, E.; Wooley, K. L. Facile One-Pot Synthesis of Brush Polymers through Tandem Catalysis Using Grubbs' Catalyst for Both Ring-Opening Metathesis and Atom Transfer Radical Polymerizations. *Nano Lett.* **2006**, *6* (8), 1741−1746.
(228) Radzinski, S. C.; Foster, J. C.; Matson, J. B. Preparation of Bottlebrush Polymers via a One-Pot Ring-Opening Polymerization (ROP) and Ring-Opening Metathesis Polymerization (ROMP) Grafting-Through Strategy. *Macromol. Rapid Commun.* **2016**, *37* (7), 616−621.
(229) Walsh, D. J.; Guironnet, D. Macromolecules with Programmable Shape, Size, and Chemistry. *Proc. Natl. Acad. Sci. U. S. A.* **2019**, *116* (5), 1538−1542.
(230) Kluthe, K. E. I.; Wagner, M.; Klapper, M. Simultaneous Bottlebrush Polymerization. *Macromolecules* **2021**, *54* (3), 1465−1477.
(231) Walsh, D. J.; Dutta, S.; Sing, C. E.; Guironnet, D. Engineering of Molecular Geometry in Bottlebrush Polymers. *Macromolecules* **2019**, *52* (13), 4847−4857.
(232) Liu, W.-B.; Xu, X. H.; Kang, S. M.; Song, X.; Zhou, L.; Liu, N.; Wu, Z. Q. Bottlebrush Polymers Carrying Side Chains on Every Backbone Atom: Controlled Synthesis, Polymerization-Induced Emission, and Circularly Polarized Luminescence. *Macromolecules* **2021**, *54* (7), 3158−3168.
(233) Su, Y. X.; Xu, L.; Xu, X. H.; Hou, X. H.; Liu, N.; Wu, Z. Q. Controlled Synthesis of Densely Grafted Bottlebrushes That Bear Helical Polyisocyanide Side Chains on Polyisocyanide Backbones and Exhibit Greatly Increased Viscosity. *Macromolecules* **2020**, *53*, 3224.
(234) Chang, A. B.; Lin, T. P.; Thompson, N. B.; Luo, S. X.; Liberman-Martin, A. L.; Chen, H. Y.; Lee, B.; Grubbs, R. H. Design, Synthesis, and Self-Assembly of Polymers with Tailored Graft Distributions. *J. Am. Chem. Soc.* **2017**, *139* (48), 17683−17693.
(235) Lin, T. P.; Chang, A. B.; Luo, S. X.; Chen, H. Y.; Lee, B.; Grubbs, R. H. Effects of Grafting Density on Block Polymer Self-Assembly: From Linear to Bottlebrush. *ACS Nano* **2017**, *11* (11), 11632−11641.
(236) Ma, H.; Wang, Q.; Sang, W.; Han, L.; Liu, P.; Chen, J.; Li, Y.; Wang, Y. Synthesis of Bottlebrush Polystyrenes with Uniform, Alternating, and Gradient Distributions of Brushes via Living Anionic Polymerization and Hydrosilylation. *Macromol. Rapid Commun.* **2015**, *36* (8), 726−732.
(237) Jiang, L.; Nykypanchuk, D.; Pastore, V. J.; Rzayev, J. Morphological Behavior of Compositionally Gradient Polystyrene-Polylactide Bottlebrush Copolymers. *Macromolecules* **2019**, *52* (21), 8217−8226.
(238) Jiang, L.; Nykypanchuk, D.; Ribbe, A. E.; Rzayev, J. One-Shot Synthesis and Melt Self-Assembly of Bottlebrush Copolymers with a Gradient Compositional Profile. *ACS Macro Lett.* **2018**, *7* (6), 619−623.
(239) Li, A.; Li, Z.; Zhang, S.; Sun, G.; Policarpio, D. M.; Wooley, K. L. Synthesis and Direct Visualization of Dumbbell-Shaped Molecular Brushes. *ACS Macro Lett.* **2012**, *1* (1), 241−245.
(240) Radzinski, S. C.; Foster, J. C.; Scannelli, S. J.; Weaver, J. R.; Arrington, K. J.; Matson, J. B. Tapered Bottlebrush Polymers: Cone-Shaped Nanostructures by Sequential Addition of Macromonomers. *ACS Macro Lett.* **2017**, *6* (10), 1175−1179.
(241) Yavitt, B. M.; Fei, H. F.; Kopanati, G. N.; Winter, H. H.; Watkins, J. J. Power Law Relaxations in Lamellae Forming Brush Block Copolymers with Asymmetric Molecular Shape. *Macromolecules* **2019**, *52* (4), 1557−1566.
(242) Gao, A. X.; Liao, L.; Johnson, J. A. Synthesis of Acid-Labile PEG and PEG-Doxorubicin-Conjugate Nanoparticles via Brush-First ROMP. *ACS Macro Lett.* **2014**, *3* (9), 854−857.
(243) Johnson, J. A.; Lu, Y. Y.; Burts, A. O.; Lim, Y. H.; Finn, M. G.; Koberstein, J. T.; Turro, N. J.; Tirrell, D. A.; Grubbs, R. H. Core-Clickable PEG-Branch-Azide Bivalent-Bottle-Brush Polymers by ROMP: Grafting-through and Clicking-To. *J. Am. Chem. Soc.* **2011**, *133* (3), 559−566.
(244) Lv, F.; Liu, D.; Cong, H.; Shen, Y.; Yu, B. Synthesis, Self-Assembly and Drug Release Behaviors of a Bottlebrush Polymer-HCPT Prodrug for Tumor Chemotherapy. *Colloids Surf. B Biointerfaces* **2019**, *181* (April), 278−284.
(245) Ohnsorg, M. L.; Prendergast, P. C.; Robinson, L. L.; Bockman, M. R.; Bates, F. S.; Reineke, T. M. Bottlebrush Polymer Excipients Enhance Drug Solubility: Influence of End-Group Hydrophilicity and Thermoresponsiveness. *ACS Macro Lett.* **2021**, *10* (3), 375−381.
(246) Yu, Y.; Chen, C. K.; Law, W. C.; Mok, J.; Zou, J.; Prasad, P. N.; Cheng, C. Well-Defined Degradable Brush Polymer-Drug Conjugates for Sustained Delivery of Paclitaxel. *Mol. Pharmaceutics* **2013**, *10* (3), 867−874.
(247) Sowers, M. A.; Mccombs, J. R.; Wang, Y.; Paletta, J. T.; Morton, S. W.; Dreaden, E. C.; Boska, M. D.; Ottaviani, M. F.; Hammond, P. T.; Rajca, A.; Johnson, J. A. Redox-Responsive Branched-Bottlebrush Polymers for in Vivo MRI and Fluorescence Imaging. *Nat. Commun.* **2014**, *5*, 5460.
(248) Fouz, M. F.; Mukumoto, K.; Averick, S.; Molinar, O.; McCartney, B. M.; Matyjaszewski, K.; Armitage, B. A.; Das, S. R. Bright Fluorescent Nanotags from Bottlebrush Polymers with DNATipped Bristles. *ACS Cent. Sci.* **2015**, *1* (8), 431−438.
(249) Senkum, H.; Gramlich, W. M. Cationic Bottlebrush Polymers from Quaternary Ammonium Macromonomers by Grafting-Through


https://doi.org/10.1021/acs.chemmater.1c04030
*Chem. Mater.* 2022, 34, 1990−2024

Ring-Opening Metathesis Polymerization. *Macromol. Chem. Phys.* **2020**, *221* (5), 1900476.
(250) Müllner, M. Molecular Polymer Brushes in Nanomedicine. *Macromol. Chem. Phys.* **2016**, *217* (20), 2209−2222.
(251) Alvaradejo, G. G.; Nguyen, H. V. T.; Harvey, P.; Gallagher, N. M.; Le, D.; Ottaviani, M. F.; Jasanoff, A.; Delaittre, G.; Johnson, J. A. Polyoxazoline-Based Bottlebrush and Brush-Arm Star Polymers via ROMP: Syntheses and Applications as Organic Radical Contrast Agents. *ACS Macro Lett.* **2019**, *8* (4), 473−478.
(252) Rzayev, J. Molecular Bottlebrushes: New Opportunities in Nanomaterials Fabrication. *ACS Macro Letters.* **2012**, *1*, 1146−1149.
(253) Teo, Y. C.; Xia, Y. Facile Synthesis of Macromonomers via ATRP-Nitroxide Radical Coupling and Well-Controlled Brush Block Copolymers. *Macromolecules* **2019**, *52* (1), 81−87.
(254) Verduzco, R.; Li, X.; Pesek, S. L.; Stein, G. E. Structure, Function, Self-Assembly, and Applications of Bottlebrush Copolymers. *Chem. Soc. Rev.* **2015**, *44* (8), 2405−2420.
(255) Nam, J.; Kim, Y. J.; Kim, J. G.; Seo, M. Self-Assembly of Monolayer Vesicles via Backbone-Shiftable Synthesis of Janus Core-Shell Bottlebrush Polymer. *Macromolecules* **2019**, *52* (24), 9484−9494.
(256) Fang, A.; Lin, S.; Ng, F. T. T.; Pan, Q. Synthesis of Core-Shell Bottlebrush Polymers of Poly(Polycaprolactone-b-Polyethylene Glycol) via Ring-Opening Metathesis Polymerization. *J. Macromol. Sci. Part A* **2021**, *0* (0), 1−11.
(257) Varlas, S.; Hua, Z.; Jones, J. R.; Thomas, M.; Foster, J. C.; O'Reilly, R. K. Complementary Nucleobase Interactions Drive the Hierarchical Self-Assembly of Core-Shell Bottlebrush Block Copolymers toward Cylindrical Supramolecules. *Macromolecules* **2020**, *53* (22), 9747−9757.
(258) Nese, A.; Li, Y.; Averick, S.; Kwak, Y.; Konkolewicz, D.; Sheiko, S. S.; Matyjaszewski, K. Synthesis of Amphiphilic Poly(*N*-Vinylpyrrolidone)-*b*-Poly(Vinyl Acetate) Molecular Bottlebrushes. *ACS Macro Lett.* **2012**, *1* (1), 227−231.
(259) Yamauchi, Y.; Yamada, K.; Ishida, Y. Synthesis of Water-Soluble Bottlebrush Polymer with Hydrophobic Core and Hydrophilic Shell as Cylindrical Host for Guest Uptake. *Chem. Lett.* **2019**, *48* (11), 1410−1413.
(260) Karavolias, M. G.; Elder, J. B.; Ness, E. M.; Mahanthappa, M. K. Order-to-Disorder Transitions in Lamellar Melt Self-Assembled Core-Shell Bottlebrush Polymers. *ACS Macro Lett.* **2019**, *8* (12), 1617−1622.
(261) Bolton, J.; Rzayev, J. Synthesis and Melt Self-Assembly of PS-PMMA-PLA Triblock Bottlebrush Copolymers. *Macromolecules* **2014**, *47* (9), 2864−2874.
(262) Bolton, J.; Rzayev, J. Tandem RAFT-ATRP Synthesis of Polystyrene - Poly(Methyl Methacrylate) Bottlebrush Block Copolymers and Their Self-Assembly into Cylindrical Nanostructures. *ACS Macro Lett.* **2012**, *1* (1), 15−18.
(263) Rzayev, J. Synthesis of Polystyrene-Polylactide Bottlebrush Block Copolymers and Their Melt Self-Assembly into Large Domain Nanostructures. *Macromolecules* **2009**, *42* (6), 2135−2141.
(264) Yu, Y. G.; Chae, C. G.; Kim, M. J.; Seo, H.-B.; Grubbs, R. H.; Lee, J. S. Precise Synthesis of Bottlebrush Block Copolymers from $\omega$-End-Norbornyl Polystyrene and Poly(4-Tert-Butoxystyrene) via Living Anionic Polymerization and Ring-Opening Metathesis Polymerization. *Macromolecules* **2018**, *51* (2), 447−455.
(265) Ahmed, E.; Womble, C. T.; Weck, M. Synthesis and Aqueous Self-Assembly of ABCD Bottlebrush Block Copolymers. *Macromolecules* **2020**, *53* (20), 9018−9025.
(266) Seo, H.-B.; Yu, Y. G.; Chae, C. G.; Kim, M. J.; Lee, J. S. Synthesis of Ultrahigh Molecular Weight Bottlebrush Block Copolymers of $\omega$-End-Norbornyl Polystyrene and Polymethacrylate Macromonomers. *Polymer* **2019**, *177* (May), 241−249.
(267) Su, L.; Heo, G. S.; Lin, Y. N.; Dong, M.; Zhang, S.; Chen, Y.; Sun, G.; Wooley, K. L. Syntheses of Triblock Bottlebrush Polymers through Sequential ROMPs: Expanding the Functionalities of Molecular Brushes. *J. Polym. Sci. Part Polym. Chem.* **2017**, *55* (18), 2966−2970.
(268) Chen, K.; Hu, X.; Zhu, N.; Guo, K. Design, Synthesis, and Self-Assembly of Janus Bottlebrush Polymers. *Macromol. Rapid Commun.* **2020**, *41* (20), 2000357.
(269) Kawamoto, K.; Zhong, M.; Gadelrab, K. R.; Cheng, L. C.; Ross, C. A.; Alexander-Katz, A.; Johnson, J. A. Graft-through Synthesis and Assembly of Janus Bottlebrush Polymers from A-Branch-B Diblock Macromonomers. *J. Am. Chem. Soc.* **2016**, *138* (36), 11501−11504.
(270) Nguyen, H. V. T.; Gallagher, N. M.; Vohidov, F.; Jiang, Y.; Kawamoto, K.; Zhang, H.; Park, J. V.; Huang, Z.; Ottaviani, M. F.; Rajca, A.; Johnson, J. A. Scalable Synthesis of Multivalent Macromonomers for ROMP. *ACS Macro Lett.* **2018**, *7* (4), 472−476.
(271) Rokhlenko, Y.; Kawamoto, K.; Johnson, J. A.; Osuji, C. O. Sub-10 Nm Self-Assembly of Mesogen-Containing Grafted Macromonomers and Their Bottlebrush Polymers. *Macromolecules* **2018**, *51* (10), 3680−3690.
(272) Xu, B.; Feng, C.; Huang, X. A Versatile Platform for Precise Synthesis of Asymmetric Molecular Brush in One Shot. *Nat. Commun.* **2017**, *8* (1), 333 DOI: 10.1038/s41467-017-00365-2.
(273) Choi, C.; Self, L.; Okayama, Y.; Levi, A. E.; Gerst, M.; Speros, J. C.; Hawker, C. J.; Read de Alaniz, J.; Bates, C. M. Light-Mediated Synthesis and Reprocessing of Dynamic Bottlebrush Elastomers under Ambient Conditions. *J. Am. Chem. Soc.* **2021**, *143*, 9866.
(274) Mahajan, L. H.; Ndaya, D.; Deshmukh, P.; Peng, X.; Gopinadhan, M.; Osuji, C. O.; Kasi, R. M. Optically Active Elastomers from Liquid Crystalline Comb Copolymers with Dual Physical and Chemical Cross-Links. *Macromolecules* **2017**, *50*, 5929.
(275) Vatankhah-varnosfaderani, M.; Daniel, W. F. M.; Everhart, M. H.; Pandya, A. A.; Liang, H.; Sheiko, S. S.; Matyjaszewski, K.; Dobrynin, A. V. Mimicking biological stress−strain behaviour with synthetic elastomers. *Nature* **2017**, *549* (7673), 497−501.
(276) Dashtimoghadam, E.; Fahimipour, F.; Keith, A. N.; Vashahi, F.; Popryadukhin, P.; Vatankhah-varnosfaderani, M.; Sheiko, S. S. Reconstructive Surgery. *Nat. Commun. No.* **2021**, *12*, 1−11.
(277) Cai, L.; Kodger, T. E.; Guerra, R. E.; Pegoraro, A. F.; Rubinstein, M.; Weitz, D. A. *Soft Poly (Dimethylsiloxane) Elastomers from Architecture- Driven Entanglement Free Design* **2015**, *27*, 5132−5140.
(278) Sarapas, J. M.; Chan, E. P.; Rettner, E. M.; Beers, K. L. *Compressing and Swelling To Study the Structure of Extremely Soft Bottlebrush Networks Prepared by ROMP* **2018**, *51*, 2359.
(279) Cai, L. Molecular Understanding for Large Deformations of Soft Bottlebrush Polymer Networks. *Soft Matter* **2020**, *16*, 6259−6264.
(280) Slegeris, R.; Ondrusek, B. A.; Chung, H. *Polym. Chem.* **2017**, *8*, 4707−4715.
(281) Reynolds, V. G.; Mukherjee, S.; Xie, R.; Levi, A. E.; Atassi, A.; Uchiyama, T.; Wang, H.; Chabinyc, L.; Bates, C. M. Super-soft solvent-free bottlebrush elastomers for touch sensing. *Materials Horizons* **2020**, *7*, 181−187.
(282) Mukherjee, S.; Xie, R.; Reynolds, V. G.; Uchiyama, T.; Levi, A. E.; Valois, E.; Wang, H.; Chabinyc, M. L.; Bates, C. M. *Universal Approach to Photo-Crosslink Bottlebrush Polymers* **2020**, *53*, 1090.
(283) Mei, H.; Mah, A. H.; Hu, Z.; Li, Y.; Terlier, T.; Stein, G. E.; Verduzco, R. *Rapid Processing of Bottlebrush Coatings through UV-Induced Cross-Linking* **2020**, *9*, 1135.
(284) Mukumoto, K.; Averick, S. E.; Park, S.; Nese, A.; Mpoukouvalas, A.; Zeng, Y.; Koynov, K.; Leduc, P. R.; Matyjaszewski, K. Phototunable Supersoft Elastomers Using Coumarin Functionalized Molecular Bottlebrushes for Cell-Surface Interactions Study. *Macromolecules* **2014**, *47* (22), 7852−7857.
(285) Mah, A. H.; Mei, H.; Basu, P.; Laws, T. S.; Ruchhoeft, P.; Stein, G. E.; Verduzco, R. Swelling Responses of Surface-Attached Bottlebrush Polymer Networks. *Soft Matter* **2018**, *14*, 6728−6736.
(286) Xiong, H.; Zhang, L.; Wu, Q.; Zhang, H.; Peng, Y.; Zhao, L.; Huang, G.; Wu, J. A strain-adaptive, self-healing, breathable and perceptive bottle-brush material inspired by skin. *Materials Chemistry A* **2020**, *8*, 24645−24654.
(287) Self, L.; Sample, C. S.; Levi, A. E.; Li, K.; Xie, R.; de Alaniz, J. R.; Bates, C. M. Dynamic Bottlebrush Polymer Networks: Self-Healing in Super-Soft Materials. *J. Am. Chem. Soc.* **2020**, *142*, 7567−7573.

(288) Li, M.; Zhou, B.; Lyu, Q.; Jia, L.; Tan, H.; Xie, Z.; Xiong, B.; Xue, Z.; Zhang, L.; Zhu, J. Self-healing and recyclable photonic elastomers based on a water soluble supramolecular polymer. *Mater. Chem. Front.* **2019**, *3*, 2707−2715.
(289) Daniel, W. F. M.; Burdyńska, J.; Vatankhah-Varnoosfaderani, M.; Matyjaszewski, K.; Paturej, J.; Rubinstein, M.; Dobrynin, A. V.; Sheiko, S. S. Solvent-Free, Supersoft and Superelastic Bottlebrush Melts and Networks. *Nat. Mater.* **2016**, *15* (2), 183−189.
(290) Vatankhah-Varnosfaderani, M.; Daniel, W. F. M.; Everhart, M. H.; Pandya, A. A.; Liang, H.; Matyjaszewski, K.; Dobrynin, A. V.; Sheiko, S. S. Mimicking Biological Stress−Strain Behaviour with Synthetic Elastomers. *Nature* **2017**, *549* (7673), 497−501.
(291) Vatankhah-Varnoosfaderani, M.; Daniel, W. F. M.; Zhushma, A. P.; Li, Q.; Morgan, B. J.; Matyjaszewski, K.; Armstrong, D. P.; Spontak, R. J.; Dobrynin, A. V.; Sheiko, S. S. Bottlebrush Elastomers: A New Platform for Freestanding Electroactuation. *Adv. Mater.* **2017**, *29* (2), 1604209.
(292) Pakula, T.; Zhang, Y.; Matyjaszewski, K.; Lee, H. il; Boerner, H.; Qin, S.; Berry, G. C. Molecular Brushes as Super-Soft Elastomers. *Polymer* **2006**, *47* (20), 7198−7206.
(293) Karimkhani, V.; Vatankhah-Varnosfaderani, M.; Keith, A. N.; Dashtimoghadam, E.; Morgan, B. J.; Jacobs, M.; Dobrynin, A. V.; Sheiko, S. S. Tissue-Mimetic Dielectric Actuators: Free-Standing, Stable, and Solvent-Free. *ACS Appl. Polym. Mater.* **2020**, *2* (5), 1741−1745.
(294) Keith, A. N.; Vatankhah-Varnosfaderani, M.; Clair, C.; Fahimipour, F.; Dashtimoghadam, E.; Lallam, A.; Sztucki, M.; Ivanov, D. A.; Liang, H.; Dobrynin, A. V.; Sheiko, S. S. Bottlebrush Bridge between Soft Gels and Firm Tissues. *ACS Cent. Sci.* **2020**, *6* (3), 413−419.
(295) Vatankhah-Varnosfaderani, M.; Keith, A. N.; Cong, Y.; Liang, H.; Rosenthal, M.; Sztucki, M.; Clair, C.; Magonov, S.; Ivanov, D. A.; Dobrynin, A. V.; Sheiko, S. S. Chameleon-like Elastomers with Molecularly Encoded Strain-Adaptive Stiffening and Coloration. *Science* **2018**, *359* (6383), 1509−1513.
(296) Sheiko, S. S.; Dobrynin, A. V. Architectural Code for Rubber Elasticity: From Supersoft to Superfirm Materials. *Macromolecules* **2019**, *52* (20), 7531−7546.
(297) Chen, Y.; Guan, Z. Self-Healing Thermoplastic Elastomer Brush Copolymers Having a Glassy Polymethylmethacrylate Backbone and Rubbery Polyacrylate-Amide Brushes. *Polymer* **2015**, *69*, 249−254.
(298) Tang, M.; Zheng, P.; Wang, K.; Qin, Y.; Jiang, Y.; Cheng, Y.; Li, Z.; Wu, L. Autonomous Self-Healing, Self-Adhesive, Highly Conductive Composites Based on a Silver-Filled Polyborosiloxane/Polydimethylsiloxane Double-Network Elastomer. *J. Mater. Chem. A* **2019**, *7* (48), 27278−27288.
(299) Self, J. L.; Sample, C. S.; Levi, A. E.; Li, K.; Xie, R.; De Alaniz, J. R.; Bates, C. M. Dynamic Bottlebrush Polymer Networks: Self-Healing in Super-Soft Materials. *J. Am. Chem. Soc.* **2020**, *142* (16), 7567−7573.
(300) Choi, C.; Self, J. L.; Okayama, Y.; Levi, A. E.; Gerst, M.; Speros, J. C.; Hawker, C. J.; Read De Alaniz, J.; Bates, C. M. Light-Mediated Synthesis and Reprocessing of Dynamic Bottlebrush Elastomers under Ambient Conditions. *J. Am. Chem. Soc.* **2021**, *143* (26), 9866−9871.
(301) Xie, R.; Mukherjee, S.; Levi, A. E.; Reynolds, V. G.; Wang, H.; Chabinyc, M. L.; Bates, C. M. Room Temperature 3D Printing of Super-Soft and Solvent-Free Elastomers. *Sci. Adv.* **2020**, *6* (46), eabc6900.
(302) Xie, R.; Mukherjee, S.; Levi, A. E.; Self, J. L.; Wang, H.; Chabinyc, M. L.; Bates, C. M. Yielding Behavior of Bottlebrush and Linear Block Copolymers. *Macromolecules* **2021**, *54* (12), 5636−5647.
(303) Daniel, W. F. M.; Xie, G.; Vatankhah Varnoosfaderani, M.; Burdyńska, J.; Li, Q.; Nykypanchuk, D.; Gang, O.; Matyjaszewski, K.; Sheiko, S. S. Bottlebrush-Guided Polymer Crystallization Resulting in Supersoft and Reversibly Moldable Physical Networks. *Macromolecules* **2017**, *50* (5), 2103−2111.
(304) Nian, S.; Lian, H.; Gong, Z.; Zhernenkov, M.; Qin, J.; Cai, L. H. Molecular Architecture Directs Linear-Bottlebrush-Linear Triblock Copolymers to Self-Assemble to Soft Reprocessable Elastomers. *ACS Macro Lett.* **2019**, *8* (11), 1528−1534.
(305) Joannopoulos, J. D.; Johnson, S. G.; Winn, J. N.; Meade, R. D. *Photonic Crystals: Molding the Flow of Light*; Princeton University Press: Princeton, NJ, 2008.
(306) Edrington, A. C.; Urbas, A. M.; DeRege, P.; Chen, C. X.; Swager, T. M.; Hadjichristidis, N.; Xenidou, M.; Fetters, L. J.; Joannopoulos, J. D.; Fink, Y.; Thomas, E. L. Polymer-Based Photonic Crystals. *Adv. Mater.* **2001**, *13* (6), 421−425.
(307) Fink, Y.; Winn, J. N.; Fan, S.; Chen, C.; Michel, J.; Joannopoulos, J. D.; Thomas, E. L. A Dielectric Omnidirectional Reflector. *Science* **1998**, *282* (5394), 1679−1682.
(308) Boyle, B. M.; Collins, J. L.; Mensch, T. E.; Ryan, M. D.; Newell, B. S.; Miyake, G. M. Impact of Backbone Composition on Homopolymer Dynamics and Brush Block Copolymer Self-Assembly. *Polym. Chem.* **2020**, *11* (45), 7147−7158.
(309) Alfrey, T.; Gurnee, E. F.; Schrenk, W. J. Physical Optics of Iridescent Multilayered Plastic Films. *Polym. Eng. Sci.* **1969**, *9* (6), 400−404.
(310) Liberman-Martin, A. L.; Chu, C. K.; Grubbs, R. H. Application of Bottlebrush Block Copolymers as Photonic Crystals. *Macromol. Rapid Commun.* **2017**, *38* (13), 1700058.
(311) Boyle, B. M.; French, T. A.; Pearson, R. M.; McCarthy, B. G.; Miyake, G. M. Structural Color for Additive Manufacturing: 3D-Printed Photonic Crystals from Block Copolymers. *ACS Nano* **2017**, *11* (3), 3052−3058.
(312) Chae, C. G.; Yu, Y. G.; Seo, H. B.; Kim, M. J.; Grubbs, R. H.; Lee, J. S. Experimental Formulation of Photonic Crystal Properties for Hierarchically Self-Assembled POSS-Bottlebrush Block Copolymers. *Macromolecules* **2018**, *51* (9), 3458−3466.
(313) Miyake, G. M.; Weitekamp, R. A.; Piunova, V. A.; Grubbs, R. H. Synthesis of Isocyanate-Based Brush Block Copolymers and Their Rapid Self-Assembly to Infrared-Reflecting Photonic Crystals. *J. Am. Chem. Soc.* **2012**, *134* (34), 14249−14254.
(314) Runge, M. B.; Bowden, N. B. *Synthesis of High Molecular Weight Comb Block Copolymers and Their Assembly into Ordered Morphologies in the Solid State* **2007**, *129*, 10551.
(315) Sveinbjörnsson, B. R.; Weitekamp, R. A.; Miyake, G. M.; Xia, Y.; Atwater, H. A.; Grubbs, R. H. Rapid Self-Assembly of Brush Block Copolymers to Photonic Crystals. *Proc. Natl. Acad. Sci. U. S. A.* **2012**, *109* (36), 14332−14336.
(316) Guo, T.; Wang, Y.; Qiao, Y.; Yuan, X.; Zhao, Y.; Ren, L. Thermal Property of Photonic Crystals (PCs) Prepared by Solvent Annealing Self-Assembly of Bottlebrush PS-b-PtBA. *Polymer* **2020**, *194*, 122389.
(317) Patel, B. B.; Walsh, D. J.; Kim, D. H.; Kwok, J.; Lee, B.; Guironnet, D.; Diao, Y. Tunable Structural Color of Bottlebrush Block Copolymers through Direct-Write 3D Printing from Solution. *Sci. Adv.* **2020**, *6* (24), eaaz7202 DOI: 10.1126/sciadv.aaz7202.
(318) Song, D.-P.; Zhao, T. H.; Guidetti, G.; Vignolini, S.; Parker, R. M. *Hierarchical Photonic Pigments via the Confined Self-Assembly of Bottlebrush Block Copolymers* **2019**, DOI: 10.1021/acsnano.8b07845.
(319) Wade, M. A.; Walsh, D.; Lee, J. C.-W.; Kelley, E. G.; Weigandt, K. M.; Guironnet, D.; Rogers, S. A. Color, Structure, and Rheology of a Diblock Bottlebrush Copolymer Solution. *Soft Matter* **2020**, *16*, 4919−4931.
(320) Song, D.-P.; Li, C.; Colella, N. S.; Lu, X.; Lee, J.-H.; Watkins, J. J. Thermally Tunable Metallodielectric Photonic Crystals from the Self-Assembly of Brush Block Copolymers and Gold Nanoparticles. *Adv. Opt. Mater.* **2015**, *3*, 1169−1175.
(321) Song, D.-P.; Li, C.; Li, W.; Watkins, J. J. Block Copolymer Nanocomposites with High Refractive Index Contrast for One-Step Photonics. *ACS Nano* **2016**, *10*, 1216−1223.
(322) Song, D.-P.; Shahin, S.; Xie, W.; Mehravar, S.; Liu, X.; Li, C.; Norwood, R. A.; Lee, J.-H.; Watkins, J. J. Directed Assembly of Quantum Dots Using Brush Block Copolymers for Well-Ordered Nonlinear Optical Nanocomposites. *Macromolecules* **2016**, *49*, 5068−5075.
(323) Song, D.-P.; Li, C.; Colella, N. S.; Xie, W.; Li, S.; Lu, X.; Gido, S.; Lee, J.-H.; Watkins, J. J. Large-Volume Self-Organization of Polymer/Nanoparticle Hybrids with Millimeter-Scale Grain Sizes Using Brush Block Copolymers. *J. Am. Chem. Soc.* **2015**, *137*, 12510−12513.

(324) Angelescu, D. E.; Waller, J. H.; Register, R. A.; Chaikin, P. M. Shear-Induced Alignment in Thin Films of Spherical Nanodomains. *Adv. Mater.* **2005**, *17* (15), 1878−1881.
(325) Winey, K. I.; Patel, S. S.; Larson, R. G.; Watanabe, H. Interdependence of Shear Deformations and Block Copolymer Morphology. *Macromolecules* **1993**, *26* (10), 2542−2549.
(326) Nikoubashman, A.; Register, R. A.; Panagiotopoulos, A. Z. Sequential Domain Realignment Driven by Conformational Asymmetry in Block Copolymer Thin Films. *Macromolecules* **2014**, *47* (3), 1193−1198.
(327) Marencic, A. P.; Register, R. A. Controlling Order in Block Copolymer Thin Films for Nanopatterning Applications. *Annu. Rev. Chem. Biomol. Eng.* **2010**, *1* (1), 277−297.
(328) Wunenburger, A. S.; Colin, A.; Colin, T.; Roux, D. Undulation Instability under Shear: A Model to Explain the Different Orientations of a Lamellar Phase under Shear? *Eur. Phys. J. E* **2000**, *2* (3), 277−283.
(329) Diat, O.; Roux, D.; Nallet, F. Effect of Shear on a Lyotropic Lamellar Phase. *J. Phys. II* **1993**, *3* (9), 1427−1452.
(330) Patel, B. B.; Walsh, D. J.; Kim, D. H.; Kwok, J.; Lee, B.; Guironnet, D.; Diao, Y. Tunable Structural Color of Bottlebrush Block Copolymers through Direct-Write 3D Printing from Solution. *Sci. Adv.* **2020**, *6* (24), eaaz7202.
(331) Patel, B. B.; Chang, Y.; Park, S. K.; Wang, S.; Rosheck, J.; Patel, K.; Walsh, D.; Guironnet, D.; Diao, Y. PolyChemPrint: A Hardware and Software Framework for Benchtop Additive Manufacturing of Functional Polymeric Materials. *J. Polym. Sci.* **2021**, *59* (21), 2468−2478.
(332) Sunday, D. F.; Dolejsi, M.; Chang, A. B.; Richter, L. J.; Li, R.; Kline, R. J.; Nealey, P. F.; Grubbs, R. H. Confinement and Processing Can Alter the Morphology and Periodicity of Bottlebrush Block Copolymers in Thin Films. *ACS Nano* **2020**, *14* (12), 17476−17486.
(333) Nian, S.; Zhu, J.; Zhang, H.; Gong, Z.; Freychet, G.; Zhernenkov, M.; Xu, B.; Cai, L.-H. Three-Dimensional Printable, Extremely Soft, Stretchable, and Reversible Elastomers from Molecular Architecture-Directed Assembly. *Chem. Mater.* **2021**, *33* (7), 2436−2445.
(334) Albert, J. N. L.; Epps, T. H. Self-Assembly of Block Copolymer Thin Films. *Mater. Today* **2010**, *13* (6), 24−33.
(335) Daniel, W. F. M.; Burdyńska, J.; Vatankhah-Varnoosfaderani, M.; Matyjaszewski, K.; Paturej, J.; Rubinstein, M.; Dobrynin, A. V.; Sheiko, S. S. Solvent-Free, Supersoft and Superelastic Bottlebrush Melts and Networks. *Nat. Mater.* **2016**, *15* (2), 183−189.
(336) Levental, I.; Georges, P. C.; Janmey, P. A. Soft Biological Materials and Their Impact on Cell Function. *Soft Matter* **2007**, *3* (3), 299−306.
(337) Xie, R.; Mukherjee, S.; Levi, A. E.; Reynolds, V. G.; Wang, H.; Chabinyc, M. L.; Bates, C. M. Room Temperature 3D Printing of Super-Soft and Solvent-Free Elastomers. *Sci. Adv.* **2020**, *6* (46), eabc6900.
(338) Breen, C. P.; Nambiar, A. M. K.; Jamison, T. F.; Jensen, K. F. Ready, Set, Flow! Automated Continuous Synthesis and Optimization. *Trends Chem.* **2021**, *3* (5), 373−386.
(339) Zaquen, N.; Rubens, M.; Corrigan, N.; Xu, J.; Zetterlund, P. B.; Boyer, C.; Junkers, T. Polymer Synthesis in Continuous Flow Reactors. *Prog. Polym. Sci.* **2020**, *107*, 101256.
(340) Reis, M. H.; Leibfarth, F. A.; Pitet, L. M. Polymerizations in Continuous Flow: Recent Advances in the Synthesis of Diverse Polymeric Materials. *ACS Macro Lett.* **2020**, *9* (1), 123−133.
(341) Hoogenboom, R.; Meier, M. A. R.; Schubert, U. S. Combinatorial Methods, Automated Synthesis and High-Throughput Screening in Polymer Research: Past and Present. *Macromol. Rapid Commun.* **2003**, *24* (1), 15−32.
(342) Chen, Y.; Wang, Q.; Mills, C. E.; Kann, J. G.; Shull, K. R.; Tullman-Ercek, D.; Wang, M. High-Throughput Screening Test for Adhesion in Soft Materials Using Centrifugation. *ACS Cent. Sci.* **2021**, *7* (7), 1135−1143.
(343) Chan, J. M.; Kordon, A. C.; Zhang, R.; Wang, M. Direct Visualization of Bottlebrush Polymer Conformations in the Solid State. *Proc. Natl. Acad. Sci. U. S. A.* **2021**, *118* (40), e2109534118.
(344) Walsh, D. J.; Wade, M. A.; Rogers, S. A.; Guironnet, D. Challenges of Size-Exclusion Chromatography for the Analysis of Bottlebrush Polymers. *Macromolecules* **2020**, *53* (19), 8610−8620.
(345) Ferguson, A. L. Machine Learning and Data Science in Soft Materials Engineering. *J. Phys.: Condens. Matter* **2018**, *30* (4), 043002.
(346) Sunday, D. F.; Martin, T. B.; Chang, A. B.; Burns, A. B.; Grubbs, R. H. Addressing the Challenges of Modeling the Scattering from Bottlebrush Polymers in Solution. *J. Polym. Sci.* **2020**, *58* (7), 988−996.
(347) Lodge, T. P.; Hiemenz, P. C. *Polymer Chemistry*, 3rd ed.; CRC Press: Boca Raton, FL, 2020.
(348) Ewoldt, R. H. Defining Nonlinear Rheological Material Functions for Oscillatory Shear. *J. Rheol.* **2013**, *57* (1), 177−195.
(349) Ewoldt, R. H.; Hosoi, A. E.; McKinley, G. H. New Measures for Characterizing Nonlinear Viscoelasticity in Large Amplitude Oscillatory Shear. *J. Rheol.* **2008**, *52* (6), 1427−1458.
(350) Hyun, K.; Wilhelm, M.; Klein, C. O.; Cho, K. S.; Nam, J. G.; Ahn, K. H.; Lee, S. J.; Ewoldt, R. H.; McKinley, G. H. A Review of Nonlinear Oscillatory Shear Tests: Analysis and Application of Large Amplitude Oscillatory Shear (LAOS). *Prog. Polym. Sci.* **2011**, *36* (12), 1697−1753.
(351) Lee, J. C.-W.; Hong, Y.-T.; Weigandt, K. M.; Kelley, E. G.; Kong, H.; Rogers, S. A. Strain Shifts under Stress-Controlled Oscillatory Shearing in Theoretical, Experimental, and Structural Perspectives: Application to Probing Zero-Shear Viscosity. *J. Rheol.* **2019**, *63* (6), 863−881.
(352) Lee, J. C.-W.; Weigandt, K. M.; Kelley, E. G.; Rogers, S. A. Structure-Property Relationships via Recovery Rheology in Viscoelastic Materials. *Phys. Rev. Lett.* **2019**, *122* (24), 248003.
(353) Lee, J. C. -W.; Porcar, L.; Rogers, S. A. Recovery Rheology via Rheo-SANS: Application to Step Strains under Out-of-equilibrium Conditions. *AIChE J.* **2019**, *65* (12), e16797 DOI: 10.1002/aic.16797.
(354) Singh, P. K.; Lee, J. C.-W.; Patankar, K. A.; Rogers, S. A. Revisiting the Basis of Transient Rheological Material Functions: Insights from Recoverable Strain Measurements. *J. Rheol.* **2021**, *65* (2), 129−144.
(355) Donley, G. J.; Singh, P. K.; Shetty, A.; Rogers, S. A. Elucidating the G″ Overshoot in Soft Materials with a Yield Transition via a Time-Resolved Experimental Strain Decomposition. *Proc. Natl. Acad. Sci. U. S. A.* **2020**, *117* (36), 21945−21952.
(356) Rogers, S. A. In Search of Physical Meaning: Defining Transient Parameters for Nonlinear Viscoelasticity. *Rheol. Acta* **2017**, *56* (5), 501−525.
(357) Rogers, S. A.; Lettinga, M. P. A Sequence of Physical Processes Determined and Quantified in Large-Amplitude Oscillatory Shear (LAOS): Application to Theoretical Nonlinear Models. *J. Rheol.* **2012**, *56* (1), 1−25.
(358) Rogers, S. A.; Erwin, B. M.; Vlassopoulos, D.; Cloitre, M. A Sequence of Physical Processes Determined and Quantified in LAOS: Application to a Yield Stress Fluid. *J. Rheol.* **2011**, *55* (2), 435−458.
(359) Park, J. D.; Rogers, S. A. Rheological Manifestation of Microstructural Change of Colloidal Gel under Oscillatory Shear Flow. *Phys. Fluids* **2020**, *32* (6), 063102.
(360) Huang, S.; Kong, X.; Xiong, Y.; Zhang, X.; Chen, H.; Jiang, W.; Niu, Y.; Xu, W.; Ren, C. An Overview of Dynamic Covalent Bonds in Polymer Material and Their Applications. *Eur. Polym. J.* **2020**, *141*, 110094.
(361) Yu, K.; Xin, A.; Wang, Q. Mechanics of Self-Healing Polymer Networks Crosslinked by Dynamic Bonds. *J. Mech. Phys. Solids* **2018**, *121*, 409−431.
(362) Bowman, C. N.; Kloxin, C. J. Covalent Adaptable Networks: Reversible Bond Structures Incorporated in Polymer Networks. *Angew. Chem., Int. Ed.* **2012**, *51* (18), 4272−4274.
(363) Chremos, A.; Theodorakis, P. E. Morphologies of Bottle-Brush Block Copolymers. *ACS Macro Lett.* **2014**, *3* (10), 1096−1100.
(364) Bejagam, K. K.; Singh, S. K.; Ahn, R.; Deshmukh, S. A. Unraveling the Conformations of Backbone and Side Chains in Thermosensitive Bottlebrush Polymers. *Macromolecules* **2019**, *52* (23), 9398−9408.


https://doi.org/10.1021/acs.chemmater.1c04030
*Chem. Mater.* 2022, 34, 1990−2024

(365) Cahn, J. W.; Hilliard, J. E. Free Energy of a Nonuniform System. I. Interfacial Free Energy. *J. Chem. Phys.* **1958**, *28*, 258−267.
(366) Inguva, P. K.; Walker, P. J.; Yew, H. W.; Zhu, K.; Haslam, A. J.; Matar, O. K. Continuum-Scale Modelling of Polymer Blends Using the Cahn−Hilliard Equation: Transport and Thermodynamics. *Soft Matter* **2021**, *17* (23), 5645−5665.
(367) Sato, T.; Han, C. C. Dynamics of Concentration Fluctuation in a Polymer Blend on Both Sides of the Phase Boundary. *J. Chem. Phys.* **1988**, *88* (3), 2057−2065.
(368) Huang, C.; Olvera de la Cruz, M. The Early Stages of the Phase Separation Dynamics in Polydisperse Polymer Blends. *Macromolecules* **1994**, *27* (15), 4231−4241.
(369) Strobl, G. R. Structure Evolution during Spinodal Decomposition of Polymer Blends. *Macromolecules* **1985**, *18* (3), 558−563.
(370) Tree, D. R.; Dos Santos, L. F.; Wilson, C. B.; Scott, T. R.; Garcia, J. U.; Fredrickson, G. H. Mass-Transfer Driven Spinodal Decomposition in a Ternary Polymer Solution. *Soft Matter* **2019**, *15* (23), 4614−4628.
(371) Tree, D. R.; Delaney, K. T.; Ceniceros, H. D.; Iwama, T.; Fredrickson, G. H. A Multi-Fluid Model for Microstructure Formation in Polymer Membranes. *Soft Matter* **2017**, *13* (16), 3013−3030.
(372) Müller, M. Process-Directed Self-Assembly of Copolymers: Results of and Challenges for Simulation Studies. *Prog. Polym. Sci.* **2020**, *101*, 101198.
(373) Pike, D. Q.; Detcheverry, F. A.; Müller, M.; de Pablo, J. J. Theoretically Informed Coarse Grain Simulations of Polymeric Systems. *J. Chem. Phys.* **2009**, *131* (8), 084903.
(374) Detcheverry, F. A.; Pike, D. Q.; Nealey, P. F.; Müller, M.; de Pablo, J. J. Monte Carlo Simulation of Coarse Grain Polymeric Systems. *Phys. Rev. Lett.* **2009**, *102* (19), 197801.
(375) Liu, H.; Qian, H.-J.; Zhao, Y.; Lu, Z.-Y. Dissipative Particle Dynamics Simulation Study on the Binary Mixture Phase Separation Coupled with Polymerization. *J. Chem. Phys.* **2007**, *127* (14), 144903.
(376) Muller, M.; Smith, G. D. Phase Separation in Binary Mixtures Containing Polymers: A Quantitative Comparison of Single-Chain-in-Mean-Field Simulations and Computer Simulations of the Corresponding Multichain Systems. *J. Poly Sci. Part B Poly Phys.* **2005**, *43*, 934−958.
(377) Rouse, P. E. A Theory of the Linear Viscoelastic Properties of Dilute Solutions of Coiling Polymers. *J. Chem. Phys.* **1953**, *21* (7), 1272−1280.
(378) Mai, D. J.; Marciel, A. B.; Sing, C. E.; Schroeder, C. M. Topology-Controlled Relaxation Dynamics of Single Branched Polymers. *ACS Macro Lett.* **2015**, *4* (4), 446−452.
(379) Patel, S. F.; Young, C. D.; Sing, C. E.; Schroeder, C. M. Nonmonotonic Dependence of Comb Polymer Relaxation on Branch Density in Semidilute Solutions of Linear Polymers. *Phys. Rev. Fluids* **2020**, *5* (12), 121301.
(380) Mai, D. J.; Saadat, A.; Khomami, B.; Schroeder, C. M. Stretching Dynamics of Single Comb Polymers in Extensional Flow. *Macromolecules* **2018**, *51* (4), 1507−1517.
(381) Hsiao, K.-W.; Schroeder, C. M.; Sing, C. E. Ring Polymer Dynamics Are Governed by a Coupling between Architecture and Hydrodynamic Interactions. *Macromolecules* **2016**, *49* (5), 1961−1971.
(382) Zhou, Y.; Hsiao, K.-W.; Regan, K. E.; Kong, D.; McKenna, G. B.; Robertson-Anderson, R. M.; Schroeder, C. M. Effect of Molecular Architecture on Ring Polymer Dynamics in Semidilute Linear Polymer Solutions. *Nat. Commun.* **2019**, *10* (1), 1753.
(383) Zhou, Y.; Young, C. D.; Lee, M.; Banik, S.; Kong, D.; McKenna, G. B.; Robertson-Anderson, R. M.; Sing, C. E.; Schroeder, C. M. Dynamics and Rheology of Ring-Linear Blend Semidilute Solutions in Extensional Flow: Single Molecule Experiments. *J. Rheol.* **2021**, *65* (4), 729−744.
(384) Young, C. D.; Zhou, Y.; Schroeder, C. M.; Sing, C. E. Dynamics and Rheology of Ring-Linear Blend Semidilute Solutions in Extensional Flow. Part I: Modeling and Molecular Simulations. *J. Rheol.* **2021**, *65* (4), 757−777.
(385) Tu, M. Q.; Lee, M.; Robertson-Anderson, R. M.; Schroeder, C. M. Direct Observation of Ring Polymer Dynamics in the Flow-Gradient Plane of Shear Flow. *Macromolecules* **2020**, *53* (21), 9406−9419.
(386) Young, C. D.; Qian, J. R.; Marvin, M.; Sing, C. E. Ring Polymer Dynamics and Tumbling-Stretch Transitions in Planar Mixed Flows. *Phys. Rev. E* **2019**, *99* (6), 062502.
(387) Chen, W.; Zhang, K.; Liu, L.; Chen, J.; Li, Y.; An, L. Conformation and Dynamics of Individual Star in Shear Flow and Comparison with Linear and Ring Polymers. *Macromolecules* **2017**, *50* (3), 1236−1244.
(388) Liebetreu, M.; Ripoll, M.; Likos, C. N. Trefoil Knot Hydrodynamic Delocalization on Sheared Ring Polymers. *ACS Macro Lett.* **2018**, *7* (4), 447−452.
(389) Liebetreu, M.; Likos, C. N. Hydrodynamic Inflation of Ring Polymers under Shear. *Commun. Mater.* **2020**, *1* (1), 4.
(390) Young, C. D.; Sing, C. E. Simulation of Semidilute Polymer Solutions in Planar Extensional Flow via Conformationally Averaged Brownian Noise. *J. Chem. Phys.* **2019**, *151* (12), 124907.
(391) Ermak, D. L.; McCammon, J. A. Brownian Dynamics with Hydrodynamic Interactions. *J. Chem. Phys.* **1978**, *69* (4), 1352−1360.
(392) Ahlrichs, P.; Dünweg, B. Lattice-Boltzmann Simulation of Polymer-Solvent Systems. *Int. J. Mod. Phys. C* **1998**, *09* (08), 1429−1438.
(393) Gompper, G.; Ihle, T.; Kroll, D. M.; Winkler, R. G. Multi-Particle Collision Dynamics: A Particle-Based Mesoscale Simulation Approach to the Hydrodynamics of Complex Fluids. *Adv. Polym. Sci.*; Vol. *221*, DOI: 10.1007/978-3-540-87706-6_1.
(394) Ando, T.; Chow, E.; Saad, Y.; Skolnick, J. Krylov Subspace Methods for Computing Hydrodynamic Interactions in Brownian Dynamics Simulations. *J. Chem. Phys.* **2012**, *137* (6), 064106.
(395) Fiore, A. M.; Balboa Usabiaga, F.; Donev, A.; Swan, J. W. Rapid Sampling of Stochastic Displacements in Brownian Dynamics Simulations. *J. Chem. Phys.* **2017**, *146* (12), 124116.
(396) Miao, L.; Young, C. D.; Sing, C. E. An Iterative Method for Hydrodynamic Interactions in Brownian Dynamics Simulations of Polymer Dynamics. *J. Chem. Phys.* **2017**, *147* (2), 024904.
(397) Sasmal, C.; Hsiao, K.-W.; Schroeder, C. M.; Ravi Prakash, J. Parameter-Free Prediction of DNA Dynamics in Planar Extensional Flow of Semidilute Solutions. *J. Rheol.* **2017**, *61* (1), 169−186.
(398) Statt, A.; Howard, M. P.; Panagiotopoulos, A. Z. Influence of Hydrodynamic Interactions on Stratification in Drying Mixtures. *J. Chem. Phys.* **2018**, *149* (2), 024902.
(399) Bird, R. B.; Armstrong, R. C.; Hassager, O. *Dynamics of Polymeric Liquids, Vol. 1: Fluid Mechanics*, 2nd ed.; Wiley: New York, NY, 1987; Vol. *1*.
(400) Bird, R. B.; Curtiss, C. F.; Armstrong, R. C.; Hassager, O. *Dynamics of Polymeric Liquids, Vol. 2: Kinetic Theory*, 2nd ed.; Wiley: New York, NY, 1987; Vol. *2*.
(401) Larson, R. G. *Constitutive Equations for Polymer Melts and Solutions*; Butterworths: Stoneham, MA, 1988.
(402) Milner, S. T.; McLeish, T. C. B. Reptation and Contour-Length Fluctuations in Melts of Linear Polymers. *Phys. Rev. Lett.* **1998**, *81* (3), 725−728.
(403) Giesekus, H. A Simple Constitutive Equation for Polymer Fluids Based on the Concept of Deformation-Dependent Tensorial Mobility. *J. Non-Newton. Fluid Mech.* **1982**, *11* (1−2), 69−109.
(404) Dutta, S.; Graham, M. D. Mechanistic Constitutive Model for Wormlike Micelle Solutions with Flow-Induced Structure Formation. *J. Non-Newton. Fluid Mech.* **2018**, *251*, 97−106.
(405) Cates, M. E. Nonlinear Viscoelasticity of Wormlike Micelles (and Other Reversibly Breakable Polymers). *J. Phys. Chem.* **1990**, *94* (1), 371−375.